NANOCRYSTALLINE CELLULOSE (NCC) FROM OIL PALM FIBER VIA ULTRASOUND ASSISTED HYDROLYSIS AND IT'S REINFORCEMENT IN POLY VINYL ALCOHOL (PVA) HYDROGEL

ZIANOR AZRINA BTE ZIANON ABDIN

DOCTOR OF PHILOSOPHY

(CHEMICAL ENGINEERING)

UNIVERSITI MALAYSIA PAHANG

UNIVERSITI MALAYSIA PAHANG

DECLARATION OF THESIS AND COPYRIGHT	

Author's Full Name　: ZIANOR AZRINA BTE ZIANON ABDIN

Date of Birth　　　: 16 DECEMBER 1988

Title　　　　　　: NANOCRYSTALLINE CELLULOSE FROM OIL PALM
FIBER VIA ULTRASOUND ASSISTED HYDROLYSIS AND
IT'S REINFORCEMENT IN POLY VINYL ALCOHOL
(PVA) HYDROGEL

Academic Session　: SEMESTER II 2020/2021

I declare that this thesis is classified as:

☐　CONFIDENTIAL　　　(Contains confidential information under the Official
　　　　　　　　　　　　Secret Act 1997)*

☐　RESTRICTED　　　　(Contains restricted information as specified by the
　　　　　　　　　　　　organization where research was done)*

☑　OPEN ACCESS　　　　I agree that my thesis to be published as online open access
　　　　　　　　　　　　(Full Text)

I acknowledge that Universiti Malaysia Pahang reserves the following rights:

1. The Thesis is the Property of Universiti Malaysia Pahang
2. The Library of Universiti Malaysia Pahang has the right to make copies of the thesis for
   the purpose of research only.
3. The Library has the right to make copies of the thesis for academic exchange.

Certified by:

_____　　　　　　_____
(Student's Signature)　　　　　　　　　(Supervisor's Signature)

881216-06-5544　　　　　　　　　　PROF DR. MUHAMMAD
　　　　　　　　　　　　　　　　　　DALOUR HOSSEIN BEG
_____　　　　　　_____
New IC　　　　　　　　　　　　　Name of Supervisor
Date: 16 APRIL 2021　　　　　　　　Date: 16 APRIL 2021

NOTE : * If the thesis is CONFIDENTIAL or RESTRICTED, please attach a thesis declaration letter.

SUPERVISOR'S DECLARATION

We hereby declare that we have checked this thesis and in our opinion, this thesis is adequate in terms of scope and quality for the award of the degree of Doctor of Philosophy (Chemical Engineering).

_____

(Supervisor's Signature)

Full Name   : PROFESSOR DR. MUHAMMAD DALOUR HOSSEIN BEG

Position   : PROFESSOR

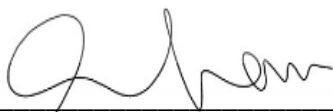Date   : 16 APRIL 2021

_____

(Co-supervisor's Signature)

Full Name   : PROFESSOR DATO' TS. DR. ROSLI BIN MOHD YUNUS

Position   : PROFESSOR

Date   : 16 APRIL 2021
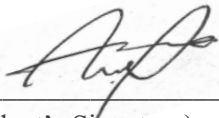
_____

(Co-supervisor's Signature)

Full Name   : DR. RIDZUAN BIN RAMLI

Position   : RESEARCH OFFICER

Date   : 16 APRIL 2021

STUDENT'S DECLARATION

I hereby declare that the work in this thesis is based on my original work except for quotations and citations which have been duly acknowledged. I also declare that it has not been previously or concurrently submitted for any other degree at Universiti Malaysia Pahang or any other institutions.

_____
(Student's Signature)

Full Name   : ZIANOR AZRINA BTE ZIANON ABDIN
ID Number   : PKC13003
Date   : 16 APRIL 2021

NANOCRYSTALLINE CELLULOSE FROM OIL PALM FIBER VIA
ULTRASOUND ASSISTED HYDROLYSIS AND IT'S REINFORCEMENT IN
POLY VINYL ALCOHOL (PVA) HYDROGEL

ZIANOR AZRINA BTE ZIANON ABDIN

Thesis submitted in fulfillment of the requirements

for the award of the degree of

Doctor of Philosophy (Chemical Engineering)

Faculty of Chemical and Process Engineering Technology

UNIVERSITI MALAYSIA PAHANG

APRIL 2021

Dedicated to my husband (Mohd Aiman), our triplets (Oumar, Yusouff and A'isyah) and my parent (Zianon Abdin Ali and Nora'in Mustapa).

ACKNOWLEDGEMENTS

ABSTRAK

Perkembangan dalam nanoteknologi membawa ke arah penggunaan nanopartikel bagi kepelbagaian aplikasi. Nanokristal selulosa (NCC) adalah salah satu bahan nanofiber yang baru sebagai penguat pengisi nanofil. Pada masa ini, kaedah hidrolisis banyak dilaksanakan bagi proses penghasilan NCC. Walau bagaimanapun, terdapat beberapa kelemahan yang perlu dititikberatkan akan penggunaan kaedah ini seperti mengambil masa yang lama dan pengurangan selulosa yang sering mempengaruhi hasil NCC. Oleh itu, dalam kajian ini, NCC dihasilkan dari tandan buah kelapa sawit (REFB) menggunakan kaedah hidrolisis asid dengan bantuan ultrasonik.Hasil NCC dioptimumkan melalui Respon permukaan Methodogi (RSM). Selain itu, NCC dimodifikasikan menggunakan *polyester hyperbranched* (HBPE) dan gabungan NCC dan Modifikasi NCC (MNCC) ke dalam PVA hidrogel nanokomposit juga dikaji. Kajian eksperimen dimulakan dengan REFB sebagai bahan permulaan untuk menghasilkan NCC. NCC dihasilkan dari pulpa selulosa yang dirawat (TEFBP) yang diperoleh dari REFB menggunakan kaedah kombinasi ultrasound dan hidrolisis. Pengeluaran optimum NCC dari kaedah ini dilakukan dengan menggunakan RSM menggunakan *Central Composite Design*(CCD). HBPE dengan Kumpulan terminal–OH kemudiannya digunakan untuk memodifikasikan NCC yang dioptimumkan. Selepas itu, 3%NCC dan 3%MNCC dimasukkan ke dalam hidrogel PVA untuk menghasilkan nanokomposit hidrogel dan sifat nanokomposit ini dikaji dengan sewajarnya.Hasil daripada FESEM mendedahkan morfologi NCC berbentuk sfera. Analisis XRD menunjukkan bahawa kristaliniti NCC ialah 80% lebih tinggi daripada bahan permulaan kajian, REFB iaitu 42%. Selain itu, NCC juga menunjukkan kestabilan terma yang tinggi pada suhu 362,17°C berbanding REFBpada suhu 289,82°C. Didapati bahawa kepekatan asid (64%) dan suhu hidrolisis (63 °C)adalah keadaan optimum untuk penghasilan NCC yang maksimum iaitu sebanyak 75%. Pngubahsuaian NCC oleh HBPE disahkan melalui spektrum FTIR yang menunjukkan peningkatan pada kumpulan -OH, serta kewujudan kumpulan baru (C = O) yang dikaitkan dengan kehadiran HBPE pada NCC. Selain itu, keputusan MNCC bagi XRD dan TGA adalah 84% dan 388 °C, iaitu sedikit tinggi berbanding NCC yang dihasilkan sebelumnya. kadar penyerapan air oleh PVA/NCC dan PVA/MNCChidrogel nanokomposit menunjukkan bahawa tahap keseimbangan nisbah penyerapan air adalah sebanyak 450% dan 480% iaitu lebih tinggi daripada PVA hidrogel dengan hanya 230% sahaja. Analisis FESEM menunjukkan bahawa kemasukan NCC dan MNCC ke dalam PVA hidrogel menghasilkan struktur pori yang lebih kecil. Secara khusus, PVA/MNCC hidrogel nanokomposit menawarkan sifat yang lebih baik disebabkan oleh pengubahsuaian NCC menggunakan HBPE yang dilihat sebagai berkesan. Hal ini menunjukkan peningkatan ketara dalam kestabilan terma hidrogel pada PVA/MNCC. Berdasarkan penemuan kajian ini dapat disimpulkan bahawa penggunaan ultrasonik semasa hidrolisis bagi penghasilan NCC dapat meningkatkan kuantiti NCC yang dihasilkan, yang mana NCC dilihat sangat berpotensi aplikasi bertahap tinggi dengan kepelbagaian penguat untuk pengembangan nanokomposit.

ABSTRACT

Developments in nanotechnology have lead to the usage of nanoparticles for various applications. Nanocrsytalline cellulose (NCC) is one of the nanofibers materials represent a new emerging natural source of reinforcing nanofillers. Currently, hydrolysis method is implemented for the NCC production. However, a certain number of drawbacks were addressed using this method such as time-consuming and cellulose degradation which often affects the yield of NCC. Therefore, in this study, the NCC, was produced from oil palm empty fruit bunch(REFB) using ultrasound assisted acid hydrolysis method. The NCC yield was optimized through Response Surface Methodology (RSM). Other than that, the NCC was functionalized using hyperbranched polyester (HBPE) and the incorporation of NCC and Modified NCC(MNCC) into PVA hydrogel nanocomposites were also studied. The NCC was produce from treated cellulose pulp(TEFBP) obtained from REFB using combination of ultrasound and hydrolysis method. The optimization of the NCC production from this method was conducted by employing RSM using Central Composite Design(CCD). A HBPE was then used to functionalize the optimized NCC. Subsequently, the 3% NCC and 3% modified MNCC were separately incorporated into PVA hydrogel and the properties of the nanocomposites were investigated accordingly. The result from Field Emission Scanning Electron Microscope(FESEM) revealed a spherical morphology of the produced NCC. X-ray Diffraction (XRD) analysis for NCC shows the crystallinity of 80% which is higher than starting material, REFB by 42%. The obtained NCC also exhibits high thermal stability of 362.17°C compared to REFB with 289.82°C. The acid concentration of 64% and hydrolysis temperature of 60°C were found to be the optimum condition for maximum NCC yield of 75%. The functionalization of NCC by HBPE was confirmed with Fourier Transform Infrared Spectroscopy (FITR) spectra with increasing –OH groups and new form of group (C=O) which is attributed to the presence of HBPE on the NCC. On the other hand, the XRD and Thermogravimetric Analysis (TGA) results for MNCC are 84% and 388°C respectively, which is slightly higher compared to the produced NCC with 82% and 378°C respectively. The adsorption property of the PVA/NCC and PVA/MNCC nanocomposites was shows that the equilibrium degree of swelling ratio for PVA/NCC and PVA/MNCC hydrogels is higher than the PVA neat by 450% and 480% respectively. FESEM analysis revealed that the incorporation of NCC and MNCC into the PVA hydrogel reduced pore structure of PVA hydrogel. Particulaly, PVA/MNCC nanocomposite offers better properties which are attributed to the effective modification of the NCC using HBPE. This was further reflected in the notable improvement in thermal stability of the PVA/MNCC hydrogel. Based on the findings of this study, the usage of ultrasound during hydrolysis of NCC could improve the quantity of NCC, which are greatly potential for high-end applications with versatile reinforcement for the development of nanocomposite.

TABLE OF CONTENT

LIST OF TABLES

اونيـۏرسيتي مليـسيا قهڠ

UNIVERSITI MALAYSIA PAHANG

LIST OF FIGURES

xiii

UMP

اونيـۆرسيتي مليسيا قهڠ

UNIVERSITI MALAYSIA PAHANG

LIST OF SYMBOLS

°C	Degree Celsius
λ	Weight length
g	Gram
hr	Hour
°	Degree
%	Percentage
cm	Centimeter
ml	Mililiter
mm	Milimeter
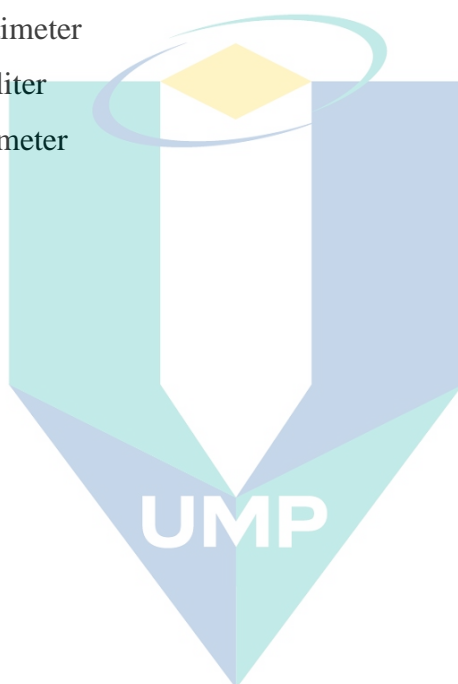
LIST OF ABBREVIATIONS

DSC	Differential Scanning Calorimetry
EFBP	Empty Fruit Bunch Pulp
FESEM	Field Emission Scanning Electron Microscope
FTIR	Fourier Transform Infrared Spectroscopy
GF	Gel Fraction
HBPE	Hyperbranched Polymer
MCC	Microcrystalline Cellulose
MNCC	Modified Nanocrystalline Cellulose
NCC	Nanocrystalline Cellulose
NCs	Nanocellulose
PVA	Polyvinyl Alcohol
REFB	Oil Palm Empty Fruit Bunch
SR	Swelling Ratio
TEFBP	Treated Empty Fruit Bunch Pulp
TGA	Thermogravimetric Analysis
XRD	X-ray Diffraction

CHAPTER 1

INTRODUCTION

1.1   Introduction

Nowadays, there are huge concerns on the use of petroleum-based plastics, particularly considering their potential negative effects on the environment. Specifically, this plastics are traditionally produced from petroleum oil and are not sustainable (Polman, Gruter, Parsons, & Tietema, 2021). Therefore, there is a drastic exhaustion of fossil resources due to overdependence on petroleum products, which are most times not recyclable. In order to overcome this challenge and to circumvent the negative environmental impacts, there is a growing interest in alternatives to petroleum resources. Notably, research interests are growing on the development of biopolymer materials such as natural biopolymers (starches and proteins) and synthetic biopolymers (PVA, PLA, and others) which can replace the petroleum-based materials. Interestingly, these biopolymer materials are low-cost, high mechanical strength, and easy to process. However, these biopolymers are far behind when compare to the fossil based plastic in term of strength, stability and other mechanical attributes (A. George, Sanjay, Srisuk, Parameswaranpillai, & Siengchin, 2020).

To overcome these shortcomings, the fillers was added to the biopolymer matrix to enhance the properties such as lower the coefficient of linear expansion, decrease shrinkage, and reduce molding cycles, increase thermal conductivity and lower resistivity(Youssef & El-sayed, 2018). Different reinforcing fillers have been used to improve the properties of the biopolymers such as carbon nanotubes (A.K.M et al., 2016), clay (Boujemaoui, Mazières, Malmström, Destarac, & Carlmark, 2016), silver nanoparticle (Kamoun, Chen, Mohy, & Kenawy, 2015), graphene (X.-N. Yang et al., 2016), cellulose (W. Li et al., 2014) and several others. However, among these potential fillers, Nanocelluloses (NCs) which produced from cellulosic materials has attracted great attention. These NCs include nanocrystalline cellulose (NCC), microfiblated

cellulose(MFC), and bacterial cellulose(BC). Among the various derivatives of NCs, there has recently been an increased interest in the production of NCC. This is basically due to its abundance, renewability, biodegradability, high aspect ratio and crystallinity, excellent optical properties and excellent mechanical properties(Liu et al., 2014b). Therefore, NCC has many potential applications, particularly for the production of value-added materials. NCC can be described as a needle or rod-shaped crystalline material with a width of about 1-10 nm and hundreds of nanometers in length. NCC is well known for its diverse applications such as additives for pharmaceuticals and drug delivery, bone replacement and tooth repair, improved paper and packaging products, reinforcement in polymer composite, food and cosmetics additives, and hydrogels.

Several raw materials have been utilized to produce NCC, such as softwood pulp, cotton, rice straw, bamboo fiber, tunicate and oil palm empty fruit bunch (REFB).For the most part of raw materials, REFB is considered as a potential material for sustainable large scale production of NCC. This is due to a large amount of cellulosic waste, which often generated on a yearly in the oil palm industry. Malaysia is the world second largest producer of palm oil (32.14%) after Indonesia (53.04%) (Amran, Zakaria, Chia, Fang, & Masli, 2017). Malaysia produced approximately 83 million dry tonnes of oil palm biomass in 2012 and is expected to increase the production to 85–110 million tonnes by 2020 worldwide(Liu et al., 2014b). Notable among these wastes, REFB are constitutes a significant proportion of the residues from the oil palm industry. Interestingly, the 73% fiber content of REFB obtained from waste in oil palm industry makes it as a good candidate for the production of NCC. In addition to the large abundance of REFB, it is considered as a low cost material, which makes it highly desirable for production of NCC. Furthermore, the high cellulose content of REFB which is about 42.7 to 65% (Shinoj, Visvanathan, Panigrahi, & Kochubabu, 2011) also contributes to its potential as starting material for NCC production.

Previously, NCC has been generally extracted by using strong acid hydrolysis (C.S., George, & Narayanankutty, 2016; Kumar, Negi, Choudhary, & Bhardwaj, 2014; Martínez-Sanz, Lopez-Rubio, & Lagaron, 2011; N. Wang, Ding, & Cheng, 2008). However, certain drawbacks are associated with acid hydrolysis method such as time-consumption and cellulose degradation which often affects the yield of NCC, as well reduces its commercial availability (Y. Wang et al., 2017). Therefore, the mechanical

treatments such as ultrasound(Rohaizu & Wanrosli, 2017a), microwave (S. Li et al., 2013) and homogenization(Cao, Ding, Yu, & Al-Deyab, 2012) have been adopted as assistance for hydrolysis method. The use of mechanical treatment is the most well-known and widely used to improved the efficiency in virtue of the intensification of the heat and mass transfer(Lu, Z., Fan, L., Zheng, H., Lu, Q., Liao, Y., Huang, 2013).

To alleviate this problem, ultrasound treatment was employed during acid hydrolysis where it can help to facilitate proper mixing and enhance the chemical reaction of the liquid. To date, the previous report on the ultrasound treatment only focused on the usage after hydrolysis process for dispersion of NCC (Filson & Dawson-Andoh, 2009).However, there have been no significant reports on the application of ultrasound during hydrolysis of REFB for the production of NCC. Therefore, it is believed that the application of ultrasound during acid hydrolysis can serve as a promising approach to extract NCC from REFB.

It is well known that the NCC is hydrophilic in nature. Therefore, numerous reports on nanocomposites containing NCC and hydrophilic polymers such as polyvinyl alcohol (PVA) have been done(H. Bai, Li, Zhang, Wang, & Dong, 2018; Butylina, Geng, & Oksman, 2016; Jimena S Gonzalez, Ludueña, Ponce, & Alvarez, 2014; Jayaramudu et al., 2018; H.-Z. Li, Chen, & Wang, 2015; Qiao et al., 2015a; Rescignano et al., 2014; Y. M. Zhou, Fu, Zheng, & Zhan, 2012). Due to the hydrophilic properties of PVA dispersion of hydrophilic NCC into the PVA matrix can be easily achieved by blending an aqueous PVA solution with NCC. Interestingly, PVA has many excellent characteristics, such as high hydrophilic properties, sufficient mechanical strength, and low cost(Qiao et al., 2015a). Therefore, PVA has been widely applied as a hydrogel, membrane material for separations processes, barrier membrane for food packaging, as pharmaceutical component, as materials for artificial human organs and as a biomaterial. Furthermore, the recent developments in the application of PVA majorly focus on its use as hydrogel materials.

Hydrogel is a three-dimensional network material, which consists of a hydrophilic polymer that swells and retains moisture without being dissolved. There have been various reported studies on PVA based hydrogels (Kamoun, Kenawy, Tamer, El-meligy, & Mohy, 2015; Nafo & Al-Mayah, 2020; Wu et al., 2019).Generally, hydrogels can prepare by either using physical or chemical cross-linking methods.

3

Physical method can obtain by the repeated cycles of freezing and thawing, which result in the formation of crystallites and gelation. Comparing to chemically method, physical method offer advantages in term of better biocompatibility and mechanical properties as well required no additional chemical cross-linker(Qiao et al., 2015b).PVA hydrogels contains over 50% water, are brittle and have a poor microstructure and mechanical properties(Bian et al., 2018). In addition, PVA hydrogel produce by physical approach can exhibit poor stability to absorbed moisture due to repetition of freeze thaw cycles. The repetition of this cycle is believed to improved the mechanical properties of PVA hydrogel but resulted in lowering the swelling of water through the PVA polymer, which often disrupts its barrier properties. It is however worthy of note that the absorption of water by a hydrogel is one of the most critical factors that determine its properties and applications. This is because swollen hydrogels usually contain liquid-filled cavities which able to absorb a significant amount of the electrolyte. One way to improve the properties of PVA hydrogel is by incorporating fillers into the PVA hydrogel. Despite the improved of the mechanical properties of PVA hydrogel by physical method, but still, the PVA hydrogel are not strong enough to serve for various application of hydrogel. Therefore, that incorporation of NCC can improve the compressive and absorption properties of the PVA hydrogels. So far, there has been little research on the incorporation of NCC into PVA hydrogel. Interestingly, NCC has good water stability and mechanical stability. Thus, it is suitable for incorporation as fillers in PVA polymeric matrix.

Although NCC is considered as a promising nano-filler in the nanocomposite applications, its wider use to improve the thermal and mechanical properties of PVA hydrogel but limited in the adsorption capability(H. Bai et al., 2018). In addition, NCC also tends to agglomerate during the drying process due to the formation of inter- and intra-molecule hydrogen bonds, which affects its performance in the composites. The numerous active hydroxyl groups on the reactive surface of NCC, it is potential for further modification. This could be via physical or chemical reactions. In fact, most of the surface modification of NCC went through the chemical modification. In this study, the NCC was physically modified by non-covalent attachment via Hyperbranched Polyester (HBPE). Interestingly, water-soluble hyperbranched Polyester (HBPE) with terminal –OH group has a big potential especially for the improvement in the adsorption capability of NCC into PVA hydrogel.

1.2   Problem Statement

Palm oil empty fruit bunch is one of the major wastes in the Malaysia palm oil industries. These by-products of oil palm are not resourcefully utilized, and the explosive expansion of oil palm plantation has generated huge amounts of vegetable waste, creating problems in replanting operations and tremendous environmental concerns. This issue derive the researchers to find the ideas on transforming the waste (EFB) into the most valuable product. With high cellulose content of EFB, this wastes has the potential to be exploited to produce high value products, particularly in the form of Nanocrystalline Cellulose (NCC). The specific problems regarding to NCC from EFB are stated below:

i.   The preparation of NCC using the acid hydrolysis method for EFB has been studied extensively in past few decades. Significant attention has not been concerted on the incorporation of ultrasound treatment to assist the hydrolysis process. Moreover, no study was conducted on the preparation of NCC from EFBusing the combination of ultrasound and hydrolysis processes. Therefore, there is need to explore this approach.

ii.   Mostly, chemical methods were employed for the purpose of functionalization of NCC. However, using chemical functionalization of NCC often involves repetitive and complicated reaction chemistry, which is, not convenient. Likewise, the surface modification using physical approaches seems to be more promising due to the simplicity of the method and preserves the properties of the filler compared to chemical modification (Kaboorani & Riedl, 2015). This is highly controllable and it is an easily operated process compared to other delicate chemical modifications (Lin and Dufresne, 2015).As far as concern, limited studies have been focus on the modification of NCC using physical approach. So far, the physical modification of NCC using hyperbranched polyester (HBPE) with numerous terminal hydroxyl groups has not been reported elsewhere.

iii.   The incorporation of NCC with PVA hydrogels only improved the thermal stability, without enhancing the adsorption properties of the hydrogel which limits the application of NCC. Interestingly, the large number of hydroxyl

groups presences in the HBPE are capable for used as a cross-linking agent with NCC in order to improve the water adsorption of the resulting hydrogel. Up until now, none of the literatures has reported on the application of modified NCC with HBPE in PVA hydrogel. Therefore, there is need for detailed study to investigate and understand how the functionalized NCC using HBPE will influence the NCC properties, as well as the incorporated with PVA hydrogels in order to ensure improvement in adsorption capability of hydrophilic polymer matrices.

1.3   Research Objective

The objectives of this research are as follow:

i.   To isolate, optimize, characterize and compare Nanocrystalline cellulose (NCC) from Oil Palm Empty Fruit Bunch Fiber via ultrasound-assisted acid hydrolysis with REFB, PEFB, and TPEFB.

ii.   To functionalize the surface of NCC with Hyperbranched Polyester(HBPE) via non covalent interaction and to investigate the effect of HBPE concentration on NCC.

iii.   To compare the characteristic and mechanical performance of NCC and Modified (NCC) with REFB, EPB pulp incorporated into PVA hydrogels.

1.4   Scope of the Study

To achieve the research objectives, the following scopes are outlined:

i.   Characterization of REFB, PEFB, TPEFB, and NCC by FESEM, FTIR, TGA, and XRD.

ii.   Screening the effects of acid hydrolysis concentration(50%-64%), hydrolysis time(90min-180min), ultrasound time(30min-90min), and temperature(45°C-60°C) on the yield of NCC using full factorial design(FFD) by Design expert software V8.06.

iii.   Optimization of NCC production parameter to obtain a high yield of NCC using Centra Composite Design (CCD) from Design expert software V8.06.

iv.   To analyse the functionalization of the HBPE on the surface of NCC at different concentration such as, 0.1mmol/g, 0.3mmol/g and 0.5mmol/g using non covalent interaction.

v.   Characterization of NCC and Modified (NCC) by TGA, XRD, FTIR, XPS, and DSC analysis.

vi.   To find the best condition of NCC into PVA hydrogel using different concentration such 1%, 3%, 5% and 7%wt via freeze thawing method (F-T).

vii.   Characterization of PVA hydrogel and PVA/NCC hydrogel using morphology (FeSEM), Thermal stability (TGA), Crystallinity (DSC), swelling ratio (SR), Gel Content (GC), chemical structure (FTIR) and mechanical properties (Compression test).

vi.   Characterization of PVA hydrogel, PVA/NCC, and PVA/MNCC hydrogel using FESEM, TGA, swelling ratio (SR), Gel Content (GC), FTIR, and compression test.

1.5   Significance of Study

This research explored the use of oil palm empty fruit bunch fiber as one of the alternative sources to produce NCC. The notable significance of this study are as follows:

i.   Production of NCC using the ultrasound-assisted hydrolysis process provides a new alternative approach to NCC production which is a significant contribution to knowledge in this field. On the other hand, the use of oil palm empty fruit bunch for NCC production is a good way of deriving economic value from agricultural wastes due to the large mass of wastes emanating from the oil palm industry.

ii. The functionalization of the surface of NCC is one of the crucial parts to diversify its application. The use of physical approach in this research via non-covalent interaction is a notable alternative to the conventional chemical approach used to functionalize NCC. Notably, this approach combines features such as simplicity, environmental friendliness, and time-saving. This could be of immense benefit to the development of similar approaches for subsequent studies.

iii. Also, the hydrophilic nature of NCC makes it suitable for the water-based polymer such as PVA. Notably, NCC is very rich in surface polar hydroxyl group (-OH) which provides excellent means for bonding with water molecules. Interestingly, the highly reactive surface of NCC has been further modified in this study to increase its water uptake. Significantly, incorporation of the modified NCC into PVA helped to improve the properties of the PVA hydrogel by providing high swelling ratio, which is highly desirable for hydrogel applications. This is a notable step forward in the application of PVA hydrogel applications and it is a good foundation for subsequent studies with similar objectives.

1.6   Thesis outline

The main aim of the research presented in this thesis was to prepare NCC via ultrasound-assisted hydrolysis of cellulose obtained from oil palm empty fruit bunch fibers and to demonstrate the potential application of the NCC in PVA hydrogels. This thesis consists of five main chapters as summarized below:

Chapter 1:

This chapter provides an overview of the NCC background, the techniques used to prepare and modified NCC, the availability of REFB in Malaysia, and the application of NCC in PVA hydrogel. Furthermore, the objectives and scopes of this study are presented in this chapter. In addition, the significance of this study is presented in this chapter.

Chapter 2:

This chapter provides a comprehensive review of the preparation method and optimization of NCC from previous and recent studies. This section also summarizes the surface modification of NCC by physical and chemical methods. Nevertheless, the application of NCC in PVA hydrogel wasbriefly addressed. Furthermore, the notable gap that needs to be filled is presented in this chapter.

Chapter 3:

Chapter 3 provides a detailed description of the experimental procedures of the preparation, optimization, modification, and nanocomposite of PVA/NCC hydrogel. In addition, information about the chemicals and materials used in the research are presented in this chapter. Furthermore, the different characterization techniques such as morphology, thermal studies, crystallinity, mechanical strength, and adsorption study are further described.

Chapter 4:

This chapter presents the results obtained from the experimental procedures, as well as the different characterization and optimization processes. The discussion of the results obtained were presented in this chapter with good comparisons with previous studies. Relevant articles are cited to support the claims made based on the results obtained.

Chapter 5:

Chapter 5 presents a conclusion of the research. The conclusion was drawn based on the objectives of the study and the results presented in Chapter 4. In addition, recommendations for further studies are presented in this chapter.

CHAPTER 2

LITERATURE REVIEW

2.1 Introduction

This chapter presents a review of previous studies on the preparation of nanocrystalline cellulose (NCC). Specifically, a brief overview of the nanocellulose background and the starting materials used for the production of NCC. Moreover, an overview of other possible approaches for the preparation of NCC other than acid hydrolysis using sulphuric acid are presented. Furthermore, the modification approaches of NCC such as physical approaches and chemical approaches are also highlighted with emphasis on optimum parameters, using optimizations tools for production and modification. Then, the incorporation of NCC into PVA hydrogel in order to meet different requirements is discussed.

2.2 Background and Classification of Nanocellulose (NCs)

The term "nanocellulose" is widely used to describe a range of quite different cellulose-based nanomaterials that have one dimension in the nanometer range (Gómez H. et al., 2016). Generally, either length or diameter of the cellulose particles should be in the nano size (1-100 nm) in order for it to be called as Nanocellulose. Nanocelluloses are typically classified into three main groups, such as Nanocrystalline Cellulose(NCC), Microfibrillated Cellulose(MFC), and Bacterial cellulose(BC). Table 2.1 shows the classification of nanocellulose.

Table 2.1   Classification of nanocellulose.

Classification of Nanocellulose	Size	Another term
Nanocrystalline Cellulose (NCC)	1–100 nm in diameter and tens to hundreds of nanometers in length	Cellulose nanocrystals (CNC), and cellulose nanowhiskers.
Microfibrillated Cellulose (MFC)	1 µm and diameters ranging from 10 to 100 nm	Cellulose Nanofibrills, Nanofibrillated Cellulose (NFC), Nanofibrillar Cellulose, and Microfibirls
Bacterial Cellulose (BC)	less than 100 nm wide and 2 to 4 nm in diameter	Microbial cellulose (MC), biocellulose, or bacterial cellulose (BC).

2.2.1   Nanocrystalline Cellulose(NCC)

NCC is a highly crystalline rod-shaped monocrystalline cellulose domain (whisker) with a diameter range between 1–100 nm, and tens to hundreds of nanometers in length (W. Bai, Holbery, & Li, 2009; De Souza Lima MM, 2004; Grishkewich, Mohammed, Tang, & Tam, 2017; Ruiz et al, 2000). As such, NCC can also be referred by other terms such as Cellulose Nanocrystals (CNC), and Cellulose Nanowhiskers (CNW).Generally, cellulose contains both crystalline and amorphous regions. Acid hydrolysis is often used to remove the amorphous region, leaving behind the crystalline particles namely as NCC which is illustrated in Figure 2.1. The amorphous regions present in the cellulose chain are more easily accessible to the acid for the hydrolytic action due to kinetic force and steric hindrance, whereas the crystalline regions are generally resistant to the hydrolysis.

11
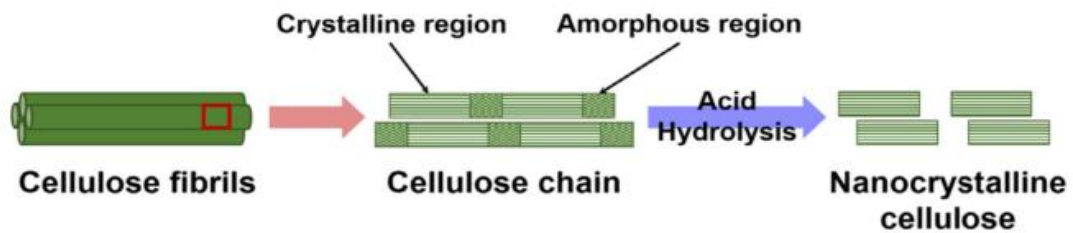
Figure 2.1   Isolation of NCC from cellulose by sulphuric acid hydrolysis

Source: Phanthong et al., (2018)

2.2.2   Microfibrillated cellulose (MFC)

MFC is a long-shaped cellulose derivative with length higher than 1µm and diameters ranging from 10 to 100nm (Grishkewich et al., 2017). MFC can also be referred by other terms such as Cellulose Nanofibrills, Nanofibrillated Cellulose (NFC), Nanofibrillar Cellulose, and Microfibirls. Compared to NCC, MFC often possesses lower crystallinity as MFC contains both amorphous and crystalline cellulose chains. Usually, MFC can produce through either mechanical treatment or chemical treatment. Commonly, MFC may produce via mechanical treatments such as homogenization, grinding, steam explosion, cryocrushing, and many others. Among these, homogenizing and grinding is considered as the most common and effective method for the scaling production of MFCin present.

Moreover, MFC is mainly commercially produced and used in various applications including composites, coatings, personal care, constructions, and others (Rajinipriya et al., 2018). However, the major disadvantage of MFC, for example, its properties of highly hydrophilic often restricts its application especially corporate in hydrophobic polymers. Furthermore, the production process for MFC using mechanical treatment often consumes high-energy. Interestingly, these shortcomings can be addressed through the use of different pre-treatment and surface modifications.

2.2.3   Bacterial Cellulose (BC)

Bacterial cellulose (BC) is a cellulose derivative with cellulosic network structure in the form of a pellicle of randomly assembled ribbon-shaped fibrils less than 100 nm wide and 2 to 4 nm in diameter. BC is generally produced involving enzymatic

polymerization of glucose by the cultivation of Gluconobacter genera bacteria such as Acetobacter xylinum species for days(Jasmani and Adnan, 2017). This BC is also often referred to as microbial cellulose(MC). Although the diameters of MFC and BC are similar (<100 nm), the main difference between these two types of nanocellulose is their purity and crystal structure. Specifically, BC is essentially pure cellulose without any other components such as lignin, hemicellulose, pectin, and others(Mahfoudhi and Boufi, 2017).Whereas MFC mainly consists of both cellulose and hemicelluloses.

2.3   Sources of Nanocrystalline cellulose (NCC)

Nanocrystalline cellulose (NCC) is primarily obtained from naturally occurring cellulose fibers which are biodegradable and renewable. Therefore, it is often considered as a sustainable and environmentally friendly material for most applications. Previous research has been reported on the preparation of NCC from different sources (starting materials) including softwood, bamboo cellulose, palm oil tress, bacterial cellulose bagasse, rice straw, sugar beet primary cell wall cellulose, cotton, and others. Generally, the possible starting materials of NCC can be broadly classified into five main categories such as wood plant fibers, non-wood plant fibers, agricultural residue, microcrystalline cellulose (MCC), and processed waste. Although these types of cellulose sources are properly classified, the huge variety in their structure and composition are the main determinants of the dimension, properties, and yield of NCC produced. Table 2.2 presents a summary of the classes of starting materials for nanocrystalline cellulose (NCC), and their main compositions (cellulose, hemicelluloses, and lignin). As presented in Table 2.3, there are many of cellulose-based raw materials used to produce NCC.

However, in the cell walls, cellulose is surrounded by hemicellulose and lignin. Therefore, the preparation of NCC generally involves the removal of these non-cellulosic components to make it suitable for different applications (Abraham et al., 2011)

13

Table 2.2   The starting materials for nanocrystalline cellulose (NCC) and main composition (cellulose, hemicelluloses, and lignin)

Raw Materials	Source	Composition (%)			References
		Cellulose	**Hemicellulose**	**Lignin**	
Wood fiber	Angelim vermelho	47.6	19.4	33.0	(Abushammala et al., 2015)
	kenaf	36	-	18	(Brinchi et al., 2013)
	Wood sawdust	61.2	9.3	25.6	(Shaheen and Emam, 2018)
	pine wood	-	-	21.5	(Bui et al., 2015)
	eucalyptus	44.3	26.9	26.1	(Kunaver et al., 2016)
Non wood plant fiber	Corncob	47.4	30.3	16.5	(Ditzel et al., 2017)
	Acacia mangium	47.1	31.1	23.0	(Jasmani and Adnan, 2017)
	Elephant grass (Pennisetum purpureum)	41.8	24.7	28.0	(Nascimento and Rezende, 2018)
Agricultural residue	Coir fibre	39.3	2	49.2	(Eldho Abraham et al., 2013)
	Sweet Potato Residue	83.57	12.81	2.27	(H. Lu et al., 2013a)
	Mengkuang leaves	37.3	34.4	24	(Sheltami et al., 2012)
	Sugarcane Bagasse	40–50	25–35	18–24	(Mandal and Chakrabarty, 2011)
	Rice straw	38.3	31.6	11.8	(Musa et al., 2017)
	rice husk	35	30	18	(Islam et al., 2017)
	sugar palm fibres (Arenga pinnata)	43.88	7.24	33.24	(Ilyas et al., 2018)
	Roselle fiber (Hibiscus sabdariffa)	58.63–64.50			(Kia et al., 2018)
	Oil Palm Empty Fruit Bunch (EFB)	59.14	12.07	25.33	(Zianor Azrina et al., 2017a)
	Oil Palm Trunk (OPT)	50.74		11.68	(Lamaming et al., 2015)
	kelp (Laminaria japonica) waste	42	-	-	(Z. Liu et al., 2017)
	de-pectinated sugar beet pulp	44.96	25.40	11.23	(Meng Li, Li-jun Wang, Dong Li, Yan-Ling Cheng, 2014)
	pistachio shells	60.62	-	12.80	(Marett et al., 2017)
	Sago (Cycas circinalis) seed shells	36.5	22.5	23.6	(Naduparambath and Purushothaman, 2016)
Microcrystalline cellulose (MCC)	Microcrystalline cellulose	85.02	11.65	2.05	(H. Lu et al., 2013a)
Processed waste	office waste paper	-	-	-	(Lei et al., 2018)
	discarded cigarette filters (DCF)	-	-	-	(Ogundare et al., 2017)
	waste cotton cloth	90	-	-	(Z. Wang et al., 2017)

14

2.3.1 Wood plant fibers (Forest residue)

Wood is the most commercially used cellulose-containing natural resource. Some of the previous studies have confirmed the preparation of NCC from wood plant sources such as Angelim Vermelho (Dinizia excelsa) wood, sawdust, kenaf, pinewood, eucalyptus, and others. There are two classification of woods such as softwood and hardwood. The distinguish between the hardwoods and softwoods is based on its anatomy, where the structure of hardwood being more complex and heterogeneous than softwood. Due to these diverse in structure, the mechanical treatment required for the softwood cellulose fibers is more easily compared to the hardwood cellulose fibers. The sources from wood plant fibers are widely used to prepare NCC mainly because of their abundance and cheaper nature. It can be efficiently produced in large quantities, following a series of well-established procedures. However, despite of it's advantages, it might not suitable for long term as it will bring to the destruction of the forestry. Due to this disadvantage, the non-wood plants were much more preferable as it is sustainable resources.

2.3.2 Non-wood plant fibers

Cellulose from non-wood plant fibers is also a well-known source for NCC production. The production of NCC from various non-wood cellulose sources has been reported in the literature. A wide variety of non-wood materials such as corncob(Ditzel et al., 2017), Acacia mangium(Jasmani and Adnan, 2017), elephant grass(Nascimento and Rezende, 2018), and others have been used as cellulose sources as reported in the literature. However, despite the use of this cellulose from non-wood plant fibers as a major source of NCC production, there are certain limitations of these sources including requiring large storage capacity, high silica content, and pollution problem. These drawbacks may lead to an increasing interest in cellulose from agricultural residues and municipal solid waste materials (MSW). Interest in these agricultural residue materials is mainly associated with their salient advantages. This includes large abundance, lightweight, low cost, and biodegradability.

2.3.3 Agricultural waste

Despite wood plant fibers and non-wood plant fibers materials, agricultural wastes have recently been investigated as one of the starting materials for the

production of NCC. Various sources of agricultural wastes such as coir fibre(Eldho Abraham et al., 2013), sweet potato residue(H. Lu et al., 2013), mengkuang leaves(Sheltami et al., 2012), sugarcane bagasse(Mandal and Chakrabarty, 2011), rice straw(Musa et al., 2017), rice husk(Islam et al., 2017), sugar palm fibres (arenga pinnata)(Ilyas et al., 2018), roselle fiber (hibiscus sabdariffa)(Kia et al., 2018), oil palm empty fruit bunch (EFB) (Zianor Azrina et al., 2017), oil palm trunk (OPT) (Lamaming et al., 2017), kelp (laminaria japonica) waste(Z. Liu et al., 2017), de-pectinated sugar beet pulp (Meng Li, Li-jun Wang, Dong Li, Yan-Ling Cheng, 2014), pistachio shells (Marett et al., 2017), sago seed shells (cycas circinalis) (Naduparambath et al., 2018), ground nut (Arachis hypogeal) (Bano and Negi, 2017) and others have been reported as viable cellulose resources for the production of NCC. The abundance of these materials as well as being cost-effective agricultural residues are particularly the most attractive reasons for their use especially considering the fact that they support the sustainability of NCC production. On the other hand, from the environment viewpoint, the use of agricultural residues would substantially help to reduce pollution, conserve energy, as well as reduce production costs. Therefore, it is envisaged that several other materials in this category will still be explored in the future studies. Likewise, subsequent studies would search for alternatives to these materials, but with superior properties.

2.3.4 Microcrystalline cellulose

Microcrystalline cellulose (MCC) has recently gained more interest as one of the starting materials for NCC production due to its renewability, non-toxicity, biodegradability, high mechanical properties, high surface area, and biocompatibility. Microcrystalline cellulose is identified as a high crystalline structure of cellulose-containing multi-sized cellulose microfibril (Mishra et al., 2018). Microcrystalline cellulose (MCC) can be identified as a fine, white, odorless, crystalline powder, which is a biodegradable material. Generally, MCC is often obtained through the hydrolysis of other cellulose materials by using dilute mineral acids. Therefore, MCC is typically characterized by a high degree of crystallinity, even though there are variations between grades. The crystallinity values typically range from 55 to 80% as determined by X-ray diffraction (XRD). Literature review shows that several researchers have used MCC as a starting material for the production of NCC(Capadona et al., 2009; Krishnamachari et al., 2012; W. Li et al., 2012; H. Liu et al., 2010).

Generally, the choice of using MCC may be considered by many researchers, as a simple pathway to NCC production as it does not necessarily require any further cellulose pre-treatment. However, the use of MCC for NCC production often results in low NCC yield. In a particular study by Xiong et al., (2012), it was reported that the NCC yield obtained using MCC from cotton waste decreased compare to the starting material of cotton from 78.1% to 21.5%. The reason for the decreasing yield was attributed to the limited crystalline region. Therefore, in order to obtain high yield of NCC, the use of waste raw material based pulp is being considered as a suitable and cost-effective approach compared to MCC (Jin shi Fan, 2012). Actually, material based pulps normally contain very insignificant amounts of hemicellulose and lignin. This particularly makes it more appropriate for NCC productions. Notably, the absence of the amorphous and non-cellulosic components from the pulp would help to increase the crystallinity of NCC (Khatoon et al., 2012). Overall, it has been observed that the use of NCC is not economical on a large scale especially due to the expensive cost of the MCC.

2.3.5 Processed Wastes

In order to minimize the production cost of NCC, it has been observed that material based wastes can be highly effective. A considerable amount of literature has been published on the use of processed wastes for NCC production. Some of the notable studies on this include studies on the use of the waste materials such as office waste paper (Lei et al., 2018), discarded cigarette filters (DCF) (Ogundare et al., 2017), waste cotton cloth (Fattahi Meyabadi et al., 2014) and others as the starting materials in the production of NCC. Although these materials can be a viable alternative source of NCC, there have been no sufficient reports on the cellulose content of most of these materials. As such, it is difficult to ascertain the possible yield of NCC that may be obtained from these materials. On the other hand, rigorous treatment processes are often required prior to the suitability of these materials for NCC production. Unfortunately, this can reduce the quality of the NCC produced, as well as undoubtedly raise the production cost.

2.3.6 The potential of oil palm empty fruit bunch (EFB) as starting material for NCC production

As presented in the previous section, it is evident that cellulose from agricultural-based materials has a huge potential, for large-scale production of NCC. Notably, agricultural wastes could pose a serious environmental problem during disposal as these wastes are often either burnt or accumulated in the soil. Therefore, utilizing this waste for the value-added product can help to overcome possible environmental issues, while creating a new form of economy for these materials. Notably, agriculture waste is the richest form of natural fiber and it is a more promising and sustainable material (Rajinipriya et al., 2018).Therefore, there is an increasing interest in sustainable materials produced using agriculture. Compared to other classes of materials such as wood, which contains cellulose in its secondary cell wall, it is more facile to isolate cellulose from agriculture fibers wherein the cellulose is found in the primary cell wall. This helps to reduce the energy consumed during fibrillation.

Oil palm is the highest yielding edible oil crop in the world. Interestingly, lignocellulosic fibers can be extracted from different parts of the oil palm tree such as the trunk, frond, fruit mesocarp, and empty fruit bunch (EFB). Among these, the empty fruit bunch is of particular interest. An empty fruit bunch is a fibrous mass that is left behind after separating the fruits from sterilized fresh fruit bunches (FFB).The management of the waste of oil palm industry has attracted the interest among the researchers, and the value-added products obtained from empty fruit bunch (EFB) have proven the suitability of this raw material as a lignocellulosic source (García et al., 2016).

Malaysia is known as one of the largest producers of palm oil (32.14%) after Indonesia (53.04%)(Amran et al., 2017). This is because oil palm is one of the major industrial crops in Malaysia. As such, a large proportion of 23.98 million tons of EFB were produced in Asia(Amran et al., 2017). About 104.28 million tons of oil palm was produced from Malaysian oil palm industry in 2015. The oil palm in Malaysia is from the species of Elaeis *guineensis* Jacq which originates from West Africa and was introduced into Malaysia in the 1860s. With the growing worldwide demand for palm

oils sector, the annual production of oil palm is expected to increase from 85 million tonnes to 110 million tonnes by 2020 (Rohaizu and Wanrosli, 2017b)

Considering the vast plantation area, it has been reported that 24 million tons of oil palm empty fruit bunch is being generated annually and only a small amount of this is being used as fuel for electricity and steam production. The remaining vast majority is mostly dumped as waste. Notably, about 70% of the crop yield is the residue, and this makes the potential use of this waste as a source of cellulosic fibers become more interesting. Significantly, the oil palm empty fruit bunch (REFB) contains up to about 73% fiber with components such as cellulose, lignin, and hemicelluloses. Therefore, REFB has great potential to be used as a raw material for the production of nanocrystalline cellulose.

2.4   Preparation of NCC

The isolation of NCC can be achieved through acid hydrolysis, directly after purification of cellulose from biomass. The preparation of NCC consists of three main stages. The first stage is the delignification process to obtain the purified cellulose as the starting material for NCC production. In this process, the non-cellulosic components such as lignin, hemicellulose, and other impurities such as wax, silica, and others are removed in order to obtain pure cellulose. After the delignification process, the cellulose will then be subjected to the second stages of chemical treatment where cellulose is hydrolyzed to produce highly crystalline regions. After this stage, the NCC can be isolated using a mechanical treatment in order to reduce the size as well to disperse the NCC. A summary of these processes is presented in Figure 2.2.

```
┌─────────────────────────────┐
│        Raw materials        │
└─────────────────────────────┘
              │
              ▼
┌─────────────────────────────┐
│    Delignification process   │
└─────────────────────────────┘
              │
              ▼
┌─────────────────────────────┐
│      Chemical hydrolysis     │
└─────────────────────────────┘
              │
              ▼
┌─────────────────────────────┐
│     Mechanical treatment     │
└─────────────────────────────┘
```
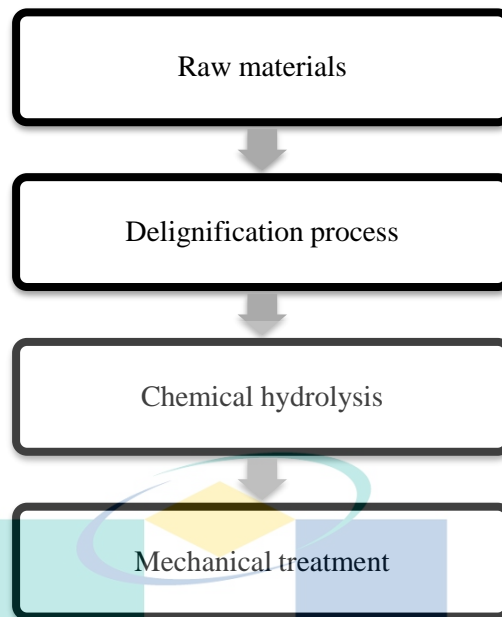
Figure 2.2   Summary of the main stages involved in the preparation of NCC

2.4.1   Delignification process (Removal of Lignin)

The production of nanocrystalline cellulose requires initial treatment processes such as the delignification of the lignocellulosic feedstock materials. The delignification process is used to remove all the impurities including lignin, hemicelluloses, ashes, waxes, as well as other non-cellulosic compounds in order to enhance the quality of cellulose. This will help to facilitate the hydrolysis of cellulose during chemical hydrolysis for the preparation of the NCC. There are three main approaches for the delignification process such as physical, enzymatic, and chemical. The physical approach involves the use of mechanical processes such as chipping, grinding, milling, and other thermal methods. However, these approach of the physical method has a number of limitations such as being less efficient, and large energy consumption. On the other hand, these mechanical treatments are not suitable for lignin removal. In fact, several impurities might still be retained in the treated sample. Another approach involves the use of enzymes which is often considered a more suitable approach, particularly due to its environmental friendliness. However, this approach also has several drawbacks such as being less efficient and consumes large energy. Another limitation of this approach is that the treatment process often takes a longer time. These drawbacks make it unsuitable for application in large-scale production processes. Therefore, the chemical approach is often preferred due to the low energy consumption, easy handling, high yield of cellulose content as well as low cost of production.

Generally, the notable methods that have been reported in the literature for the production of NCC include pulping, and steam explosion.

2.4.1.1   Steam explosion

The steam explosion has been observed to be an efficient delignification method used to remove the lignin from lignocellulose materials. The steam explosion has been explored for different researches for the past two decades, especially due to the amenability of the resulting feedstock to enzymatic hydrolysis. Some of the major advantages of the steam explosion include significantly low environmental impact, low energy consumption, lower capital investment, and less hazardous process chemicals (Kaushik and Singh, 2011). Generally, the steam explosion is a treatment process where the woody biomass is treated with hot steam under pressure, which disintegrates the biomass matrix structure, opens up the fibers, as well breaks up the fiber structure(Kaushik and Singh, 2011). Steam explosion decomposes the hemicelluloses and lignin in the starting materials and converts it into low molecular weight fractions which can be recovered through extraction. Due to this, most of the water-soluble fractions such as hemicellulose can be removed by water extraction. In addition, a part of the low molecular weight fraction of lignin is also extracted. However, other chemical treatments are required to remove all the lignin content. The effectiveness of the steam explosion is dependent on the biomass feedstock and, for instance, the process is less effective for softwood than for hardwood (Brinchi et al., 2013). Notwithstanding, this approach increases the ease of grinding of the cellulose, making it more accessible for further steps of fermentation, hydrolysis, or densification.

2.4.1.2   Pulping technique

Pulping is another one of the delignification processes use for converting wood into pulp (wood fibers) by removing as much as possible, the non-cellulosic components such as lignin and hemicelluloses using a chemical or mechanical process. The pulping process by mechanical approach is seldom used due to the expensive process and high energy requirements. Therefore, instead of mechanical pulping, most of the recent researches makes use of chemical pulping. During the chemical pulping process, the lignin and hemicelluloses are removed by extraction with an appropriate medium such as mineral acids and sodium or potassium hydroxides. There are five major types of chemical pulping methods namely bisulfate, sulfite, neutral sulfite, kraft,and soda pulping. A considerable amount of literature has been published on the

use of the pulping method for the production of NCC using various types of cellulose sources. This includes Organosolv delignification treatment(Robles et al., 2018), and soda pulping (Augusto et al., 2015; Jasmani and Adnan, 2017; Y. Liu et al., 2014a) among others. Among all these pulping methods, soda pulping with concentrated sodium hydroxide has been broadly used in the pulp industry due to its efficiency in microfibril separation as well as lignin and hemicellulose removal. In fact, it has been well reported that the cellulose resource obtained from the pulping method could be easily converted into nanocellulose products due to less process cost as well as low energy and chemical consumption. Generally, it has been reported that pulps with almost no lignin content are more desirable for cellulose materials in NCC production(Phanthong et al., 2018).

2.4.2 Chemical treatment

The chemical treatment is mainly used to obtain nanocrystalline cellulose from cellulose fibers after the delignification process. The chemical treatment namely acid hydrolysis is a well-known method and has been widely used for various types of cellulose fiber. During this treatment, the cellulose fibers are initially hydrolyzed by removing the amorphous regions of the cellulose and then inducing the fragmentation of the crystalline segments as a single crystal of NCC. Figure 2.3 shows the schematic process involved in the hydrolysis of cellulose fiber in the nanocrystalline cellulose production.
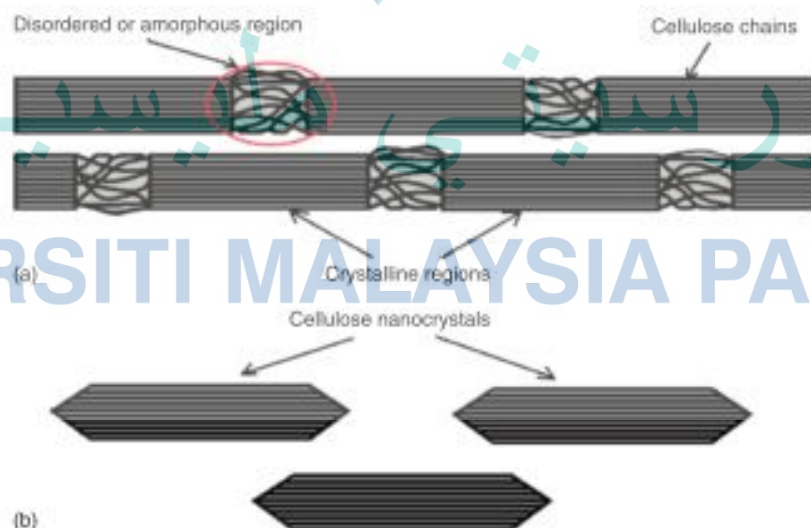
Figure 2.3 a) The arrangement of crystalline and amorphous domains in cellulose and (b) preparation of Nanocrystalline Cellulose (NCC)

Source: Kargarzadeh et al., (2017)

2.4.2.1 Acid Hydrolysis

Acid hydrolysis treatment is well known for the preparation of nanocrystalline cellulose (NCC). The controlled acid hydrolysis reacts with cellulose (both crystalline and amorphous region) and reduces the amorphous regions of the cellulose, leaving the whole crystalline part and leading to the formation of single crystals(Brito et al., 2012). Several studies have been published on the acid hydrolysis method (L. Chen & Fu, 2013; Krishnamachari et al., 2012; Pasquini et al., 2010; Siqueira et al., 2009; Wang et al., 2008).Based on these studies, it has been observed that there are various parameters which can influence the cellulose hydrolysis during the production of NCC. Some of these parameters include hydrolysis time, temperature, choice of a suitable acid, acid concentration, and acid to cellulose ratio (Kasyapi et al., 2013).

In a particular study, the effect of sulfuric acid concentration, reaction temperature, and hydrolysis time on the nanocrystalline cellulose yield have been studied by Fan & Li, 2012. Based on the study, it was concluded that the sulfuric acid concentration presents the highest influence on the yield of NCC, followed by the reaction time, then reaction temperature. This observation aligns with the report of Ioelovich, 2012 who suggested that the required acid concentration for acid hydrolysis is between 50wt% to 63 wt% where at low concentration (<50 wt. %), could not facilitate the production of NCC. This is due to the nanocrystalline blends remained together, making it difficult for nanocrystalline cellulose (NCC) to be formed. On the other hand, when the concentration is much high (>63 wt. %), the cellulose tends to undergo the dissolving process accompanied by depolymerization of cellulose.

Besides acid concentration, hydrolysis time also plays important role in the yield NCC. In a particular study, Chen et al., 2009 investigated the effects of hydrolysis time on pea hull fibre by using sulphuric acid and found that the thermal stability of NCC decreased as the hydrolysis time increased as a result of the longer contact time between pea hull fibre and sulfuric acid during the hydrolysis period. Therefore, it can be inferred that the acid concentration and hydrolysis time are related to each other in their influence on the yield of NCC. In another vein, the temperature can also influence the acid hydrolysis. This is evident from a previous study where it was reported that the crystallinity increased until 60 °C due to the removal of impurities and amorphous regions(Khatoon et al., 2012).

23

As stated, the acid concentration, hydrolysis time, and hydrolysis temperature could affect the yield of NCC. However, it is worthy of note that the choice of acid also plays a significant role in the preparation of NCC. So far, sulphuric acid and hydrochloride acid are widely used. However, other acids such as hydrobromic acid, formic acid, phosphoric acid, and combination of acid have also been reportedly used. Among these potential acids, sulfuric acid is a well-known acid used to prepare NCC mainly due to its ability to disintegrate the amorphous regions and introduce negative charges to the nanoparticle surfaces (H. Lu et al., 2013). On the other hand, sulfate-triggered negative charges which are introduced onto the surface of NCC facilitate its dispersion in water compared to the NCC produce by hydrochloric acid and hydrobromic acid which often present low dispersibility in water and tend to flocculate. Although the presence of negative charges helps to facilitate the dispersion of sulfate charged NCC in water, the major problem with the use of this acid is that the presence of acid sulfate groups would decrease the thermal stability of cellulose. This is basically due to the dehydration reaction and consequently, the thermal disintegration temperature of cellulose nanowhiskers prepared by sulfuric acid would be low as reported in the literature (Y. Chen et al., 2009). In order to overcome the possible low thermal stability of NCC, phosphoric acid has been proposed as a promising solution. In a particular study, Camarero et al., 2013 studied the isolation of thermally stable cellulose nanocrystals by phosphoric acid hydrolysis and found that the phosphoric acid in acid hydrolysis gives the higher thermal stability as well as dispersibility of NCC compared to hydrochloric acid and sulphuric acid. In another study, formic acid was used instead of sulphuric acid (Kasyapi et al., 2013). It was reported that formic acid does not break the intermolecular H-bonds in jute cellulose and thus not an effective choice for acid hydrolysis treatment. On the other hand, mixed acid containing hydrochloric acid and water in an organic acid has been observed to be a potential alternative. Notably, this approach has been identified as a viable method for surface modification of cellulose, and it can also help to improve its dispersion in organic solvents and prevents the formation of strong hydrogen bonding upon drying (Braun and Dorgan, 2009).

2.4.2.2   Enzyme assisted hydrolysis

The other method of chemical treatment for NCC is the enzyme assisted hydrolysis. Enzymatic hydrolysis, which is an eco-friendly approach, is particularly suitable for health care applications such as personal hygiene products, biomedicines, cosmetics, pharmaceutical, and others. During the enzymatic hydrolysis, the reaction rate gradually decreases until the reaction stops. Several factors related both to the enzymes and the substrate itself have been proposed to be responsible for this phenomenon (Penttilä et al., 2013). However, hydrolysis rate and temperature have been reported to give a high impact on the properties of NCC, rather than the effect of enzyme loading. Specifically, faster rates of hydrolysis were observed at higher temperatures which have been estimated and compared to the effect of enzyme load. On the other hand, the incubation temperature was found to be less important as far as the total hydrolysis rate is concerned (Ahola et al., 2008).

Some of the notable reports on this approach is the study conducted by Y. Zhang et al., 2012. They successfully prepared NCC from MCC by using the microbial hydrolysis of *Trichoderma reesei*. The results of the study indicated that the NCC yield was about 18% after 5 days of fermentation. The obtained NCC however exhibits lower crystallinity compared to the conventional acid hydrolysis method. This was associated with the use of MCC as the raw material in the fermentation process. This led to the issue of nutrient availability due to its insolubility as well as difficulties in penetration of the fungi into its amorphous regions (P.Satyamurthy et al., 2011).

2.4.3   Mechanical Treatments

Mechanical treatments are often used to isolate the NCC after hydrolysis. Usually, the mechanical treatment is used to reduce the size of the obtained cellulose crystal into the nanometer scale. The most notable used mechanical treatments in the preparation of NCC are homogenization and ultrasound. These are generally incorporated into the final stages of the NCC preparations in order to reduce the size of the hydrolyzed cellulose thereby increasing its dispersion.

2.4.3.1 High-pressure homogenization

High-pressure homogenization has been applied in the production of nanocrystalline cellulose (NCC) in order to further disperse, and reduce the size of the NCC. Usually, the fibrillar structure of the cellulose fibers will be broken down by the homogenizer in order to release NCC in form of a stable suspension in the medium(H. Lu et al., 2013; T. Wang and Drzal, 2012). After the homogenization process, obtained NCC suspension normally will not precipitate or flocculate and will exhibit a plastic rheological property (Bendahou et al., 2010; H. Lu et al., 2012).

One major advantage of using the homogenizing method is it's to reduce the mean particle size of cellulose, decreased the particle size distribution, break down the disulfide linkage and hydrophobic group, as well as increasing the thermal stability. On the other hand, the shear forces applied by the homogenizer mainly focuses on the amorphous regions of cellulose fibers, resulting in the production of NCC, a higher crystallinity derivative (Zhao et al., 2013). However, this method has a number of limitations which makes it unsuitable industrial applications. For example, high cost is required to solve the problems with fibers clogging in the homogenizer and it is also known for high energy consumption (R. Charani et al., 2013).

2.4.3.2 Ultrasonication

The other mechanical method that has drawn large research attention is ultrasonication. Ultrasonication applies shear forces on cellulosic chains causing the partial separation of the swelled regions due to acid and temperature treatments. This will help to increase the crystalline value and yield increase (Khatoon et al., 2012). It is however worthy of note that the length of NCC obtained from ultrasonication might depend on the ultrasonic treatment time (W. Li et al., 2012). It has been observed from the literature that the ultrasonication of NCC is very effective in reducing the size of the natural cellulose particles and it also assists in the clumping of the compact particle structure to a more open fibrous structure (D.V. Pinjari, 2010). This phenomenon can be explained by the effect of acoustic cavitation which leads to the creation, growth, and collapse of a bubble that is formed in a liquid as shown by Figure 2.4.

The violent collapse induces micro jets and gives shock waves on the surface of the cellulose fibers, causing erosion which leads to a split along the axial direction(W. Li et al., 2013).

In a particular study on the rheological properties and structure of NCC suspensions by Shafiei et al., 2012, it was found that increasing the applied ultrasound energy significantly decreases the viscosity of the NCC, as it influences the structure of ordered chiral nematic domains. In a separate study, it was suggested that the yield of NCC can be improved by increasing the processing time (K.Oksman et al., 2011).On the other hand, it has also been reported that the NCC isolated using ultrasonication or high-pressure homogenization exhibits better thermal stability than nanowhiskers isolated with acid hydrolysis (K.Oksman et al., 2011).
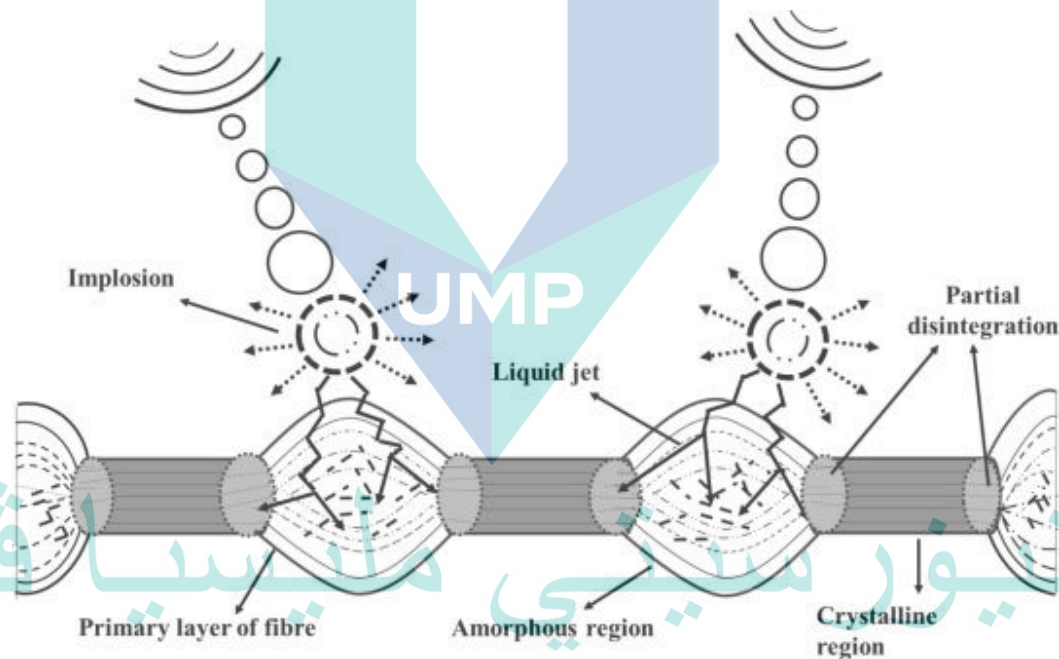
Figure 2.4   Schematic diagram of the ultrasonication process.
Source: Sayyed, Mohite, Deshmukh, & Pinjari, (2018)

2.4.4   Alternative to chemical treatment

2.4.4.1   Combination of chemical and mechanical treatment

Although the preparation of nanocrystalline cellulose (NCC) by acid hydrolysis has been done by many researchers, however, this approach sometimes creates another problem. Specifically, the acid hydrolysis requires higher energy, and it is considered

environmentally hazardous due to the use of highly concentrated acid which potentially modified the surface of the NCC. Owing to these drawbacks, several alternative methods have been recently explored in order to minimize the negative effects of conventional acid hydrolysis. Notable among these is the use of ultrasound-assisted hydrolysis using weak or strong organic acid, microwave-assisted hydrolysis, and homogenization assisted hydrolysis.

a)Ultrasound-Assisted Acid hydrolysis

Sonication or otherwise known as ultrasonication is the application of sound energy to physical and chemical systems. The mechanism of sonication involves the production of bubbles in a liquid. This causes acoustic cavitations, formation, growth, and implosive collapse of bubbles to produce hot spots that help to disperse NCC. In a particular study, ultrasonication was used to disperse NCC after the acid hydrolysis process Kim et al., 2013.It was reported that the ultrasonic treatment during acid hydrolysis was effective in producing smaller nanoparticles. Actually, the energy dissipated during the cavitation directly affects crystalline nature because of the generation of hot spots.

Generally, the mechanical effect of ultrasound treatment improves the dispersion of fibers and could be one reason for the higher NCC yield as reported in the literature (Rattaz et al., 2011). Notably, strong acid hydrolysis of amorphous cellulose combined with ultrasound treatment could result in highly crystalline cellulose nanofibers that are often termed whiskers (Stelte and Sanadi, 2009). On the overall, ultrasonication give an additional potential in the processing of liquids, by improving the mixing and chemical reactions in various applications (Li, Wang and Liu 2011). This is one reason for its suitability in NCC production in liquid medium.

b)Combination of acid hydrolysis and homogenization

Homogenization is being combined with a chemical treatment to fabricate highly uniform NCC particles. In a particular study, these two approaches were combined and the result was reportedly highly desirable (H. Liu et al., 2010). However, it was reported afterward that the rheology was dependent on the structure and concentration of NCC(D. Liu et al., 2011).The major differences between these approaches are summarized in Table 2.3

Table 2.3   The major differences ofmechanical treatment and combine chemical and mechanical approaches.

Mechanical Treatment	Ultrasonic	**Rod-shaped**	**50 to 250 nm**	**10 to20 nm**	**-**	**(W. Li et al., 2012)**
Combination of Chemical and mechanical treatment	Combination of acid hydrolysis and ultrasonic	Rod-shaped	96 nm	10 to 20 nm	-	(W.Li & R.Wang 2011)
	Combination of acid hydrolysis, ultrasonication & homogenization	spherical or ellipic granules	20-60nm	-	-	(H. Lu et al, 2012)
	Combination of acid hydrolysis and homogenization	spherical	-	30-120 nm	-	(Purkait et al., 2011)
	Combination of Acid hydrolysis and high-pressure homogenizer	Needle shape	90±50nm	10±4nm	10-15	(D. Chen et al., 2012)

2.5   Characterization of NCC

The characterization of NCC has generated significant interest in the scientific and industrial fields. Generally, the characteristics of the NCC often depend on the properties of the raw materials, and methods used for production. The analysis used to characterize the NCC generally involves a few analytical instruments such as microscopy, spectroscopy, rheological and thermal instruments.

2.5.1   The microstructure of nanocrystalline cellulose (NCC)

As stated, NCC is commonly produced via acid hydrolysis and the NCC obtained will normally be in nanometer size. However, the dimension and morphology of the NCC might vary depending on the source, the condition for preparations used such as time, temperature, purity, as well as the experimental techniques. The dimensions of NCC obtained from different sources and preparation methods are summarized in Figure 2.5.Generally, the ratio of length to diameter (L/D)of NCC, which is known as the geometrical aspect ratio, is very important to the reinforcing capability of NCC. Usually, NCC with a high aspect ratio shows better reinforcing ability. This is because the aspect ratio of NCC is very important in the formation of percolated networks, which helps to improve the mechanical performances in polymer nanocomposites.

As presented in Figure 2.5, it is evident that the NCC formed mostly exhibits rod-like particles. Nevertheless, other morphologies of NCC are also obtained in different shapes such as needle shape and spherical shape as presented in Figure 2.5.The morphological characteristics of NCC are usually studied by using a few types of microscopy such as transmission electron microscopy (TEM) scanning electron microscopy (SEM), and atomic force microscopy (AFM). The most conventional and most commonly used for observing the morphology of NCC is TEM.
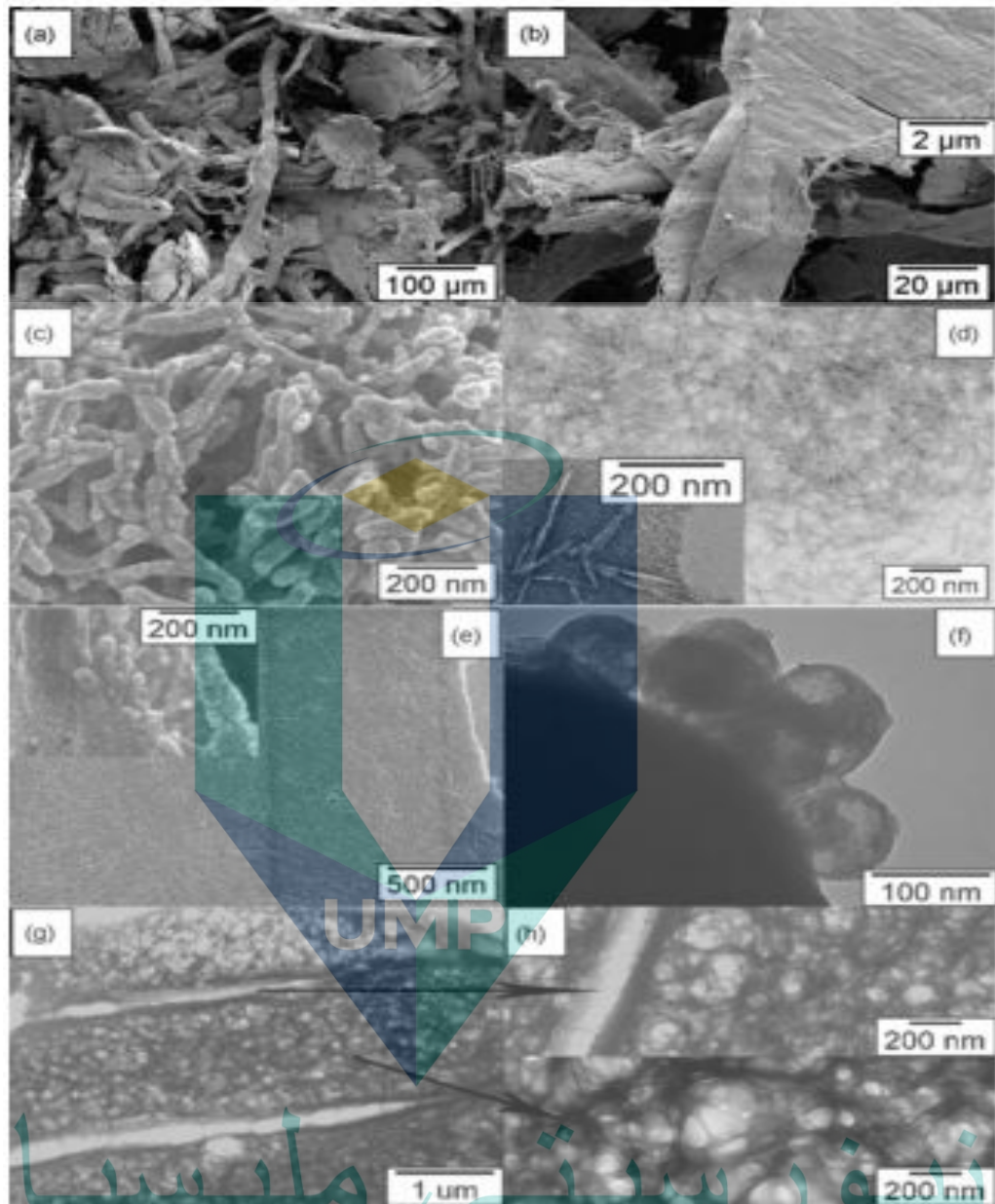
Figure 2.5 SEM images of cellulose (a and b) powder and SEM (left, except (g) which is TEM) and TEM (right) images of nanocrystals in the forms of (c and d) rods, (e and f) spheres, (g and h) porous network.

Source: P. Lu and Hsieh, (2010)

Table 2.4   The dimensions of NCC obtained from different sources through different preparation methods.

Preparation Technique	Method	Cross Section	L(nm)	D(nm)	Aspect Ratio	References
Chemical treatment	Acid hydrolysis	Rod-shaped	100 ± 28	8 ± 3	22	(Brito, Pereira, Putaux, & Jean, 2012)
	Acid hydrolysis	Rod-shaped	135.1nm	30nm	-	(Fan & Li, 2012)
	acid hydrolysis	Rod-shaped	80-500nm	6nm	20-60	(Rosa et al., 2010)
	acid hydrolysis	needle-shaped	210.8 ± 44.2 nm	4.15 ± 1.08 nm	53.4 ± 15.8	(Silvério et al.,2013)
	Acid hydrolysis	Rod-shaped	177 nm	12 nm	19	(J. P. S. Morais et al., 2013)
	Acid hydrolysis		200 nm	5–25 nm	10–20	(Sheltami et al., 2012)
	Acid hydrolysis	Rod shape	400–500 nm	25 to 30 nm	_	(R. Li et al., 2009)
	Acid hydrolysis	Needle shaped	255 ± 55nm	4 ± 2nm,	64	(Khatoon et al,. 2012; E. D. Morais et al., 2011)
	Acid hydrolysis	cylindrical shaped	270 nm	30.7 nm	_	(P. Lu and Hsieh, 2012)

2.5.2 Thermal properties of nanocellulose

Thermal stability is important for filler materials. NCC possesses good thermal stability compared to several other fillers. Mostly, the thermal stability of NCC is often analyzed by using Thermogravimetric Analysis (TGA). The TGA consist of two elements of analysis such as TGA analysis, which represents the study of thermal stability of the NCC, and the derivative thermogravimetric analysis (DTG) that provides information about the maximum weight loss of the components in NCC. Usually, TGA curves show two stages such as the weight loss due to moisture content mainly below 100°C as the first stage, and the second stage composes of the decomposition of cellulose materials between 200-400°C such as dehydration, decarboxylation, depolymerization, and decomposition of glycosyl units(Trache, Donnot, Khimeche, Benelmir, & Brosse, 2014). Generally, NCC exhibits higher decomposition temperature compared to its raw materials due to the high crystallinity index that acts as a barrier for heat transfer such that the decomposition temperature would be shifted to the higher temperature range(Lamaming, Hashim, Leh, & Sulaiman, 2017).

As for the raw materials used for NCC production, the TGA curve will exhibit 4 stages which are the moisture content at low temperature of below 220°C, hemicelluloses decomposition from 220-315°C,cellulose decomposition around 315°C and lignin decomposition above 400°C. However, in some cases, another peak might appear above 600°C.This often indicates that only inorganic compound remains in the sample. Other than that, the activation energy for thermal degradation also reveals information about the nature of thermal degradation and their crystalline packing. It has been reported that the activation energies of the degradation of cellulose nanocrystals can be significantly lowered by introducing sulphate groups via sulphuric acid hydrolysis(Naduparambath et al., 2018).

2.5.3 Crystallinity of nanocellulose

After hydrolysis, NCC generally exhibitsa higher crystallinity index compared to the raw material due to the dissolution of the amorphous region during the hydrolysis treatment. However, the crystallinity depends on the lignocellulosic sources. Usually, the crystallinity degree of NCC is often around 70-90%. Mostly the degree of crystallinity index of NCC depends on the cellulose content of the raw materials. The

crystallinity index is mainly measured by using X-ray powder diffraction (XRD). Other than that, other tools may also be used. Notably, the NCC produced via by sulfuric acid hydrolysis usually possesses less crystallinity compared to the NCC produced by hydrochloric acid hydrolysis. However, the crystallinity of NCC can be improved by increasing the hydrolysis period due to the removal of more amorphous region from the cellulose material.

2.6   Optimization of NCC

Optimization is mainly used to improve the performance of a product, a process, or a system in order to achieve the best possible benefit. Therefore, optimization is mainly used in engineering to describe a means of identifying the optimum conditions to apply a procedure, or operate a system so as to produce the best possible output. Conventional optimization procedures require the monitor of one factor at a time on a particular response, while other factors are kept constant. This approach is called one-factor-at-a-time or one-variable-at-a-time. However, the main disadvantage of this approach is that it does not take consider the interactive effects of combined variables. As such, the effect of parameters on the response is not fully depicted. On the other hand, this approach requires more experimental runs to conduct particular research which generally consumes more time and it is more expensive.

Alternatively, optimization of the experimental process or variable may be carried out using multivariate techniques. The most commonly used and relevant multivariate approach used in engineering is the response surface methodology (RSM). Response surface methodology is a collection of mathematical and statistical procedures that may be used to develop, optimize, and improve laboratory and industrial processes. It is more appropriate in cases where several factors influence the outcome or result of an experiment or reaction. Specifically, it can help to reduce the number of experimental runs required for the process, and at the same time help to maximize the output based on the data generated. The obtained data can then be used to develop an empirical model that correlates the response to the experimental factors.

2.6.1   Response surface methodology

It is well known that the efficiency of any particular process may be influenced by various parameters or factors. Most of the time, there is significant interaction

among these factors which makes it difficult to accurately assess the influence or effect of any particular factor. This necessitates the need for optimization tools in order to determine the optimum conditions to combine various factors, or to run an experiment. Over the past decade, response surface methodology (RSM) has recently attracted large attention as a viable optimization technique. Most often RSM is used to map a response surface over a particular region of concern or to select optimum conditions to achieve desirable outputs. Invariably, it can help to decrease the number of experimental runs required for a process. In addition, it helps to provide surface contours which make it easy to clearly visualize the interaction of factors. The principle and definition of terms involved in optimization using RSM are well reported in the literature.

Generally, the RSM technique has been observed to be very efficient especially considering the fact that the amount of data required is less compared to convention manual approaches. The first notable report on the use of RSM as an optimization technique in the production of cellulose nanocrystals (CNC) from MCC was in 2006 by Bonderson and his team. In their study, RSM was combined with the Fractional Factorial Resolution technique to optimize factors such as hydrolysis time, hydrolysis temperature, MCC concentration, acid concentration, and sonication time. However, it was observed that the optimum conditions used resulted in an undesirably low yield (30%) of CNC. On the other hand, a three-factor, the three-level orthogonal design was used in another study under a similar process and a yield of over 82% was reportedly obtained at the optimum conditions. Other notable studies have also been reported from different cellulose sources with varying yield such as cotton pulp fibers where a yield of 64% was reported, filter paper which produced a yield of 86%, and bleached kraft eucalyptus pulp which produced a yield of 64%. It is noteworthy that most of these reported studies used different designs in combination with RSM. Interestingly, based on recent studies, it has been observed that that the yield of NCC may be improved through optimization of factors in order to attain the best interactions using RSM through factorial and central composite design. Therefore, this makes this approach worthy of further investigation, using different cellulose sources for the production of NCC.

2.6.2   Factorial and central composite design

A factorial experiment is otherwise called a fractional factorial design and it is a facile method to which can be used to determine the significant factors or variables that present significant influence on the desired output. In other words, it is mainly used to screen the number of factors in order to identify the significant few. This would help to avoid complexity and reduction in the number of experimental runs during the optimization process.

With respect to RSM, either of two efficient designs may be used namely central composite design (CCD) and Box-Behnken design (BBD). However, the most commonly used among these two is the CCD. In a particular study, the Box-Wilson CCD was used to optimize the hydrolysis of bleached kraft eucalyptus pulp and a CNC yield of 64% was reported. More recently, the CCD was used to study the acid hydrolysis of wood pulp for the production of cellulose nanocrystals and a yield of between 66-69% was reported. Likewise, the CCD was used in another study to optimize the parameters involved in the hydrolysis process for the isolation of MCC from OPEFB fiber. It was reported that the optimum conditions obtained from the optimization process helped to produce MCC with highly desirable thermochemical properties. These studies indicate that CCD is a viable tool for the optimization of acid hydrolysis processes for the production of highly crystalline cellulose derivatives such as CNC or NCC.

2.7   Functionalization of NCC

It is well known that Nanocrystalline Cellulose (NCC) has the potential to be used as reinforcement in composite applications. However, blending the unmodified NCC with other polymer matrix materials rarely works out due to the lack of interaction of the NCC surface with the polymer matrix. In other words, the NCC surfaces are passive and do not readily interact with other materials. To overcome these issues NCC surfaces need to be modified for more efficient use in most applications. Other than that, NCC also possesses some drawbacks which are mainly associated with its tendency to form bundles or aggregates during the drying process. During the drying process, the hydrogen bond appears to draw the NCC together due to large hydrogen

forces which pose a problem in subsequent dispersion (Lu & Hsieh, 2010).This often limits the potential of NCC as reinforcement in composite material.

Another main challenge of NCC is how to achieve excellent performance by attaining homogeneous dispersion of NCC in the polymer matrix to obtain a good matrix–filler interaction. In fact, good dispersibility of the NCC in the polymer matrix is a major prerequisite in order to produce nanocomposites with good performance and sufficient properties. NCC is hydrophilic in nature but the availability of –OH groups on NCC can be further used to functionalize it in order to meet various challenging requirements.

There are a few modification approaches that have been developed for NCC to make functional NCC particles or to improve their dispersion in polymer matrices to produce nanocomposite. However, the main challenge to the functionalization of NCC is the selection of proper reagent and reaction medium. It is expected that modification will affect the nanocrystal surface alone, without changing the original morphology, and it should maintain the properties of NCC. The functionalization of NCC can be either through chemical or physical approaches. Chemical approaches usually involve the interaction of covalent bonding and the chemistries are usually done in solvent media. However, these approaches involve chemicals that are hazardous, such as azides or meta catalyst. Another drawback of this chemical approach is that the reaction conditions can be harsh, including extreme pH, high temperature, and inert gas environment. Physical approach, which are generally done in less harsh conditions than chemical may be one of the alternative to functionalize the NCC. This approach involves the adsorption of molecules on to the NCC surface via weaker chemical interactions such as electrostatic interactions, van der Waals interactions or hydrophobic interactions. Therefore, the details explanation of the methods applied for functionalization of NCC by these two approaches were discussed in the next subtopic chapter.

2.7.1 Chemical Approach

As regards chemical functionalization, derivatization is the most effective approach to change the surface properties of NCC. This includes modification of the hydrophilicity, surface charge, and density. Notably, this is still an increasingly popular

topic as revealed by the important literature that reports the various chemical modification routes applied for the functionalization of NCC(Eyley & Thielemans, 2014). Basically, the chemical approach entails a general strategy of all chemical functionalization by incorporating hydrophobic properties onto the NCC surface to promote the dispersion in non-polar organic media and/or impart better compatibility with hydrophobic polymers. In addition, this approach also introduces stable negative or positive charges on the surface of NCC, in order to obtain better electrostatic repulsion-induced dispersion. Another main advantage of chemical approach is that it can introduce either negative or positive electrostatic charges on the NCC surface, which provides better dispersion in any solvent or polymer matrix(J. George & Sabapathi, 2015). Some of the notable chemical techniques use modify NCC including grafting polymer, cationization, oxidation, silylation, and acetylation.

Grafting has been widely used in the modification of the NCC surface. Generally, grafting of polymer on the surface of NCC can be achieved by either two ways of the ''grafting onto'' or ''grafting from'' approaches. The ''grafting onto'' method involves attachment of pre-synthesized of polymer chains, deliver the reactive end groups, onto (modified) hydroxyl groups of the NCC surface. The polymer can be fully characterized before grafting, which gives an advantages in offering the possibility of controlling the properties of the resulting material. However, the steric hindrance can prevent optimal attachment during the grafting reaction due to the polymer chains which have to diffuse through the layer of the attached brushes to reach available reactive sites at the surface and hence,obtained an unfavorable reduced surface grafting density. Alternative to this, the ''grafting from'' approach was use in order to increase the grafting density of the polymer brushes on the surface and to ensure their stability in different application conditions. In ''grafting from'', polymer brushes can be grown in situ from NCC directly using the hydroxyl groups or the surface can be modified to introduce different initiator sites needed for controlled polymerization techniques.However, the drawback of this approach is the difficulty to precisely determine and characterize the molecular weight of grafted polymers.

Other than that, the NCC also can be modifiedby silylation approah using a series of alkyl dimethylchloro silanes, with the carbon backbone of the alkyl moieties ranging from a short carbon length of isopropyl to longer lengths represented by n-

butyl, n-octyl and n-dodecyl. The nanocrystal, of which the morphological integrity was preserved, became readily dispersible in solvents of low polarity (such as THF) leading to stable suspensions. However, some drawback may occur especially at high silylation, whereas, the chains in the core of the crystals became silylated, which produce high reactivity of silanes toward hydroxyl and consequently the loss of original morphology.

Most of amidation-mediated couplings were realized on carboxylic groups of pre-oxidized NCC substrates. Mostly, the covalent attachment of amine derivatives on the surface of nanocelluloses was achieved via a carbodiimide-mediated amidation reaction without alteration the morphological and crystalline attributes. Various of amine derivatives such as 4-amino-TEMPO,222 benzylamine, hexylamine, dodecylamine and Jeffamine223 were attached on the surface of NCC. Generally the method using amidation is straight forward, but in there also some case of that required multiple step procedure in order to avoid intermolecular connection.

On the other hand, esterification is a well-known method for the preparation of esters by heating a carboxylic acid in alcohol containing a small amount of catalyst, usually a strong acid. (Braun & Dorgan, 2009) studied the surface modification of NCC by esterification through modification of the accessible hydroxyl groups to produce surface-functionalized NCC in a single step. It was observed that surface esterification of NCC provides improved dispersion in organic solvents and prevents the formation of strong hydrogen bonding upon drying. In another vein, surface acetylation has also been used to modify the surface of NCC. In a particular study, Cho, Park, Yun, & Jin, (2013) performed the surface modification of NCC by surface acetylation and it was reported that this modification led to notably improvement in the NCC dispersibility in hydrophobic organic solvent.

2.7.2 Physical Approach

Besides chemical approach, NCC can also be functionalized using a simple way by physical adsorption of surfactant or polymer. This modification approach can be achieved by attaching small molecules or polymers via covalent bonds or physical interactions. As such, the surface of NCC can be modified and tuned either through physical interactions or adsorption of molecules or macromolecules onto their surfaceThese interactions with the NCC substrate are ensured through hydrophilic

affinity, electrostatic attractions, hydrogen bonds or van der Walls forces. The physical approach was reported first by Heux et al., (2000) who used surfactants of mono and di-esters of phosphoric acid (alkylphenol tails) to modify NCC. The surfactant molecules formed a thin layer at the surface of the CNCs and as a result, the forming surfactant-coated NCC dispersed well in non-polar solvents. Moreover, these surfactant-coated NCC showed very good compatibility and acted as remarkable nucleating agents wheninncorporated into the isotactic polypropylene (isoPP) matrix. Other researchers, Kim et al., (2013) and Rojas et al.,(2010)also reported the use of non-ionic surfactants to disperse NCC in polystyrene-based composite fibers. The procedure was carried out in aqueous solution, for the surface modification of NCC using quaternary ammonium salts bearing long alkyl, phenyl, glycidyl, and diallyl groups via adsorption.

Zhou et al., (2009) introduced a new way of non-covalent NCC surface functionalization based on the adsorption of saccharide-based amphiphilic block copolymers. Compared to the chemical approach, the physical approach seems to be more compromising as this approach uses a convenient operation and procedure. In addition, the physical absorption of surfactant or polymer coating is a considerably simple treatment in comparison with chemical modification. This approach is not only environmentally friendly, cheap, and easy to perform, but it upholds the mechanical integrity and degree of crystallinity of NCC.

2.8   Hyperbranched Polyester with NCC

Recently, the interest in hyperbranched polymers (HBPE) is growing rapidly as one of the novel pathways to enhance the functionalities of synthetic polymer.Hyperbranched polymer (HBPE) or dendrimers, is known as a family of macromolecules, which has a large number of branches and functional end-group (D. Wang, Jin, Zhu, & Yan, 2016).Therefore, they have a huge potential for developing new synthetic routes in various applications. The HBPE offer unique abilities which can lead to the design of novel HBPE materials for a various application such as bioimaging, drug, adsorption waste, and gene delivery, antimicrobial activity, cancer diagnosis, and sensors. Somenotable reviews have been published on the HBPE including synthesis (Zhang et al., 2016), functionalization on materials such as CNTs (A.K.M et al., 2016; Moshiul Alam, Beg, Reddy Prasad, Khan, & Mina, 2012),grapheme (Ismail, Abdullah, Zainal Abidin, & Yusoh, 2017), chitosan

(Klaykruayat, Siralertmukul, & Srikulkit, 2010), nano clay (Ganjaee Sari, Ramezanzadeh, Shahbazi, & Pakdel, 2015) silicon oxide (Ondaral, Wågberg, & Enarsson, 2006), supramolecular self-assembly and applications. Besides, by introducing the HBPE which contain an abundance of –OH terminal groups onto the surfaces of NCC using non-covalent modification is considered highly significant for diverse possible application of NCC (Demircan & Zhang, 2016).

2.9   Application of NCC in hydrogel application

Nanocrystalline cellulose offers several advantages including their wide availability of sources, low energy consumption, ease of recycling including combustion, high sound attenuation, and comparatively easy process ability due to their non-abrasive nature, allowing high filling levels and significant cost savings. Nanocrystalline cellulose (NCC) has been recognized for it diversified applications such as additives for coatings, paints, lacquers, and adhesives, switchable optical devices, pharmaceuticals and drug delivery, bone replacement and tooth repair, improved paper, packaging, and building products, reinforcement in polymer composite, additives for foods and cosmetics, and aerogels as super insulators(Leung, Lam, Chong, Hrapovic, & Luong, 2013) Composite materials consist of two main components namely a binder or matrix and reinforcement. Normally, the reinforcement is stronger and stiffer compared to the matrix, while the matrix is mainly responsible for keeping the reinforcement in place. Moreover, the binder also protects the reinforcement from the environment.

Several studies have been conducted on the application of nanocrystalline cellulose as a composite material. Specifically, strong research efforts have been focused on the use of NCC as reinforcements for polymer composites. These studies include the use of NCC as the reinforcement in polymers such as polylactic acid (PLA), poly(vinyl alcohol) (PVA), and polycaprolactone (PCL). These polymer used have both advantages and disadvantages. For example, poly(lactic acid) (PLA) is used because of its good potential for the packaging industry due to a good combination of high transparency and stiffness, excellent printability, and it can be processed using readily available production technologies (Fortunati et al., 2012). Likewise, other polymers such as Poly(vinyl alcohol) (PVA) have also been investigated based on its advantages

in barrier membrane for food packaging, pharmaceutical component, manufacturing material for artificial human organs, and biomateria(W. Li, Yue, & Liu, 2012).

Recently, there is increasing research in the development of hydrogels. Hydrogels, generally contain two words namely 'hydro' like water and 'gel combined in one. Therefore, hydrogel is defined as a three-dimension network structure of the hydrophilic polymer, containing a large amount of water and have good moisture-holding capability. This makes it suitable for applications such as wound dressings. In wound dressing application, a few requirements are needed in order to achieve the ideal outcome. Normally, the hydrogel should contain and be able to retain moisture, and it should also exhibit other properties. Specifically, it should be biocompatible, absorb fluids, have high permeation, exhibit sufficient strength, transparent, and act as a protection against microbes (Gonzalez, Ludueña, Ponce, & Alvarez, 2014).Based on these requirements, the hydrogel is one of the alternative components in different types of wound dressing. Hydrogels can be produced from either naturalpolymer (eg: starch, gelatine, chitosan, gum acacia), synthetic polymers(eg: PVA, PVP), or blend of both. Among these sources, PVA has been gaining a large interest in the development of hydrogels for wound dressing purposes. Poly(vinyl alcohol) (PVA) hydrogels are biocompatible, non-toxic, and can absorb a huge amount of exudates(Gonzalez et al., 2014).Previous studies have been done on PVA based hydrogels,and few methods have been used to produce PVA hydrogels such as electron beam irradiation(X. Yang, Zhu, Liu, Chen, & Ma, 2008), bulk mixing with crosslinking agents such as glutaraldehyde(Morales-Hurtado, Zeng, Gonzalez-Rodriguez, Ten Elshof, & van der Heide, 2015) and freeze-thawing cyclic process(Butylina et al., 2016).

Nanocrystalline cellulose(NCC), has gained considerable interest as a promising biomaterial due to its outstanding properties such as high surface area, high mechanical property, hydrophilicity, biocompatibility, and biodegradability. On the other hand, NCC exhibits good water stability which makes it suitable for mixing with water base polymer solution or emulsions. Because of its salient characteristics, NCC has been incorporated as fillers in several polymeric hydrogel matrices. Interestingly, it has been observed that the incorporation of NCC can significantly improve the mechanical performance, thermal stability, barrier, and optical properties of the hydrogel due to its improved crystallinity and better interfacial interaction.

2.10   Summary

Based on the literature, some points can be drawn as regards the preparation of NCC, the modification of NCC, and incorporation of NCC into PVA. Notably, there are varieties of potential raw materials available for NCC production. However, there is a need for proper choice of the raw material, due to a broad variety of chemical composition and structure. However, it has been observed based in this literature review that oil palm empty fruit bunch (EFB) is a potential resource material that can support the production of higher NCC yields compared to several other options available.

On the other hand, it is evident from this literature review that most of the previous studies on the production of NCC from lignocellulosic materials mostly make use of strong acid hydrolysis. Only a few reports are available on the combination of mechanical and chemical approaches. Among the available literature on a combination of chemical and mechanical approaches, there are no reports on ultrasound-assisted hydrolysis for the preparation of NCC particularly from an empty fruit bunch (EFB).On the other hand, it is observed from this literature review that the parameters that influence the combined chemical and mechanical treatment have not been fully investigated. Moreover, the optimization of these parameters has not been reported.

In another vein, it is well known that NCC possesses notable drawbacks as regards its poor dispersion due to the drying process. Therefore, various approaches have been applied to improve this and as far as concern, the modification of NCC using HPBE with –OH terminal group has not been reported. Moreover, the incorporation of HBPE modified NCC into PVA hydrogel has not been reported. All these make it necessary to conduct further studies to fill the gaps in the NCC and hydrogel applications as identified in this review.

CHAPTER 3

METHODOLOGY

3.1 Introduction

This chapter describes the raw materials, chemical reagents, and various types of apparatus used in this research. It also describes the methods used for preparation, functionalization, and incorporation of NCC and modified NCC into PVA hydrogel. The response surface methodology(RSM) for the optimization of process parameters has been mentioned. The characterization techniques for raw materials, NCC, Modified NCC, and PVA nanocomposite hydrogels have also been brief in this chapter. The followed standard methods for various testing have been mentioned accordingly.

3.2 Experimental process flow

A general overview of the experimental process flow according to the research objectives is presented in Figure 3.1. The flow covers three main objectives that have been proposed for this research. In brief, the initial part of the study involves the preparation of NCC by implementation of ultrasound into hydrolysis process. The NCC produced was then characterized through FESEM, FTIR, TGA, and XRD. On the other hand, the chemical composition of the different types of EFB fiber used such as REFB, PEFB, and Treated-PEFB was determined to analyze the cellulose, hemicelluloses, lignin, and ash content.

After this, the NCC produce from ultrasound-assisted hydrolysis was optimized using Response Surface Methodology (RSM) to maximize the NCC production yield. This optimization process involves two stages. Firstly, screening was carried out using factorial analysis through Fractional Factorial Design (FFD), to identify the best factors which contributed to the NCC production yield. This was followed by optimization of the NCC using Central Composite Design (CCD) in order to determine the optimum production conditions.

The NCC produced at the optimum condition was then modified using hyperbranched polyester. The hyperbranched polyester (HBPE) with the –OH terminal group was used to functionalize the NCC using a non-covalent approach. The surface functionalities of the modified NCC were then characterized by XRD, FTIR, and TGA..

The last part of the experimental procedure involves a study on the effect of incorporating NCC and Modified-NCC into PVA hydrogel, on the adsorption capability of the resulting hydrogel. For this part, the content of NCC was first optimized in PVA hydrogel by using the physical method (freeze-thawing method). The optimization of NCC content incorporated in the PVA hydrogel was characterized using FTIR, Gel content, swelling ratio, XRD, TGA, and compression test. Then, the NCC and Modified NCC(MNCC) were incorporated into PVA hydrogel and were characterized using FESEM, FTIR, swelling ratio, compression test, XRD, and TGA analysis. Meanwhile, the incorporation of REFB and PEFB into PVA hydrogel was also studied in comparison with NCC and MNCC. Further details about the materials used and the experimental procedures are presented in the subsequent section and sub-sections.
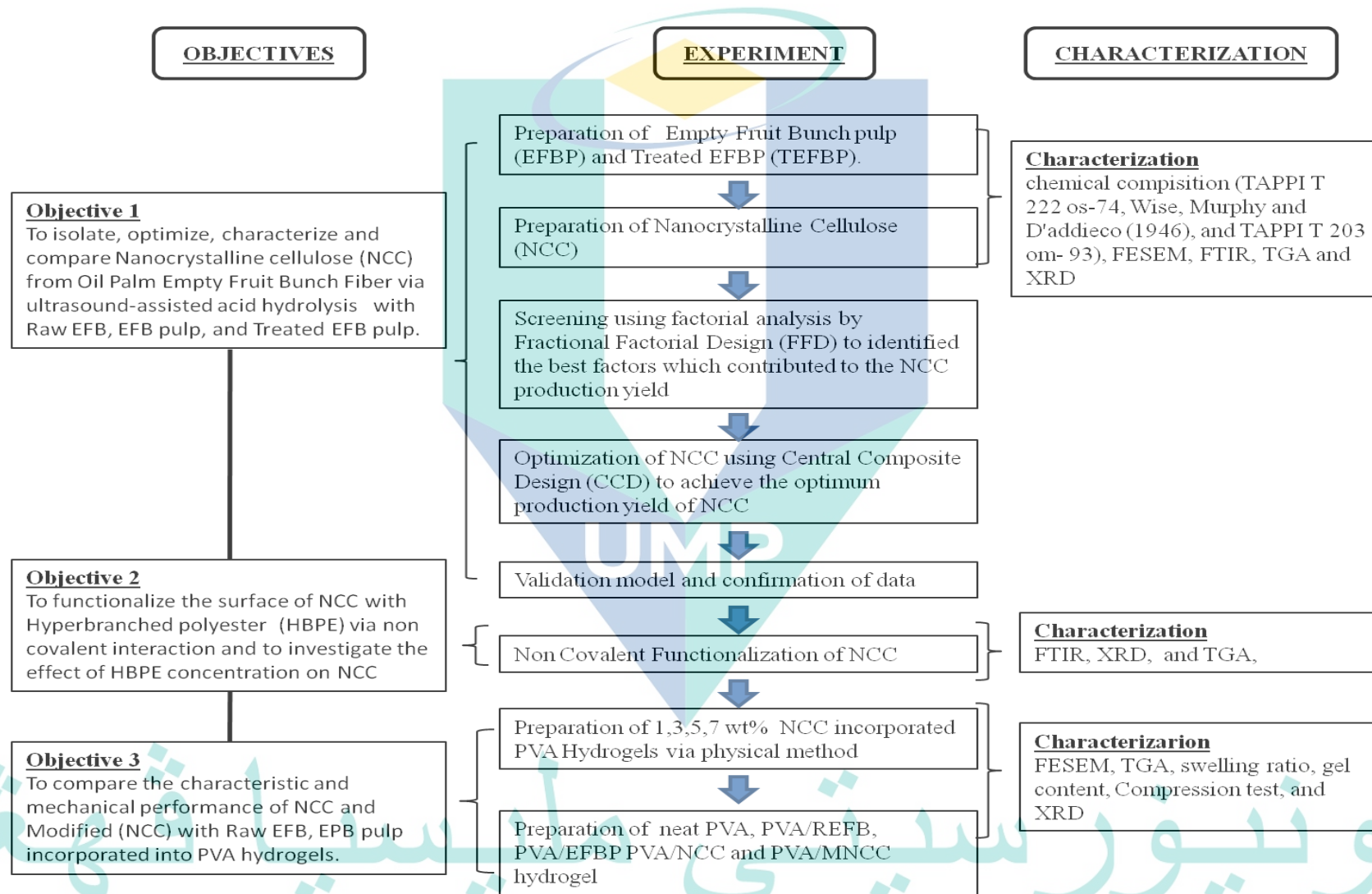
Figure 3.1   Schematic diagram of an experimental process flow according to the research objectives.

3.3   Materials

In this study, raw empty fruit bunch fibers (REFB) were used as a starting material for the experiment. The raw empty fruit bunch fibers (REFB) was collected from Malaysia Palm Oil Board (MPOB), Bandar Bangi Lama, Selangor, Malaysia. The average diameter of the REFB was 0.19mm.The raw material and specification of chemicals used are presented in Table 3.1.

Table 3.1   List of raw material and specification of the chemicals used.

Name	Manufacturer
Raw Empty Fruit Bunch (REFB), Long treated fiber	Malaysia Palm Oil Board (MPOB) UKM-Bangi
Sulfuric Acid (H_2SO_4),ACS reagent, 95.0-98.0%	Sigma-Aldrich
Dimethyl Sulfoxide (DMSO) Anhydrous, 99.9%	Sigma-Aldrich
Sodium Hydroxide (NaOH) Pellets, ≥97.0 %	Fisher Scientific, USA
Poly (Vinyl alcohol), (PVA) Mw85,000-124,000,99% hydrolyzed	Sigma-Aldrich
Polyster-16-hydroxyl-1-acetulenebis-MPA Dendron, generation 4, 96% (HBPE), 250mg	Sigma-Aldrich
Tetrahydrofuran anhydrous, ≥99.9%,inhibitor-free, 1L	Sigma-Aldrich

3.4   Preparation of Nanocrystalline Cellulose (NCC)

The preparation of nanocrystalline cellulose (NCC) was performed through a series of stages starting with the pulping of raw empty fruit bunch fiber (REFB). The fiber obtained after the pulping process is herein referred to as pulped EFB (PEFB). The PEFB was further treated to obtain TPEFBPEFB (TPEFB) which was then hydrolyzed through ultrasound-assisted hydrolysis to produce NCC.

3.4.1 Preparation of Empty Fruit Bunch pulp (PEFB)

In order to remove lignin and other unwanted substances from the REFB, it was exposed to two stages ofthe treatment process as illustrated in Figure 3.2.The first step involves a pulping treatment by water pre-hydrolysis which was then followed by soda pulping as suggested by(Rosli et al., 2003). Briefly, the pre-hydrolysis and soda pulping methods were performed in 1kg pulp digester from Forest Research Institute Malaysia, (FRIM) Kepong, KL. The liquor material ratio, cooking time, and temperature for pre-hydrolysis, as well as the soda pulping conditions employed to prepare the pulp, are presented in Table 3.2. After the cooking process, the PEFB was mechanically disintegrated in a three-bladed mixer for 1min and subsequently screened on a flat-plate screen with 0.15 mm slits. Finally, the PEFB was stored in poly bags for further analysis.
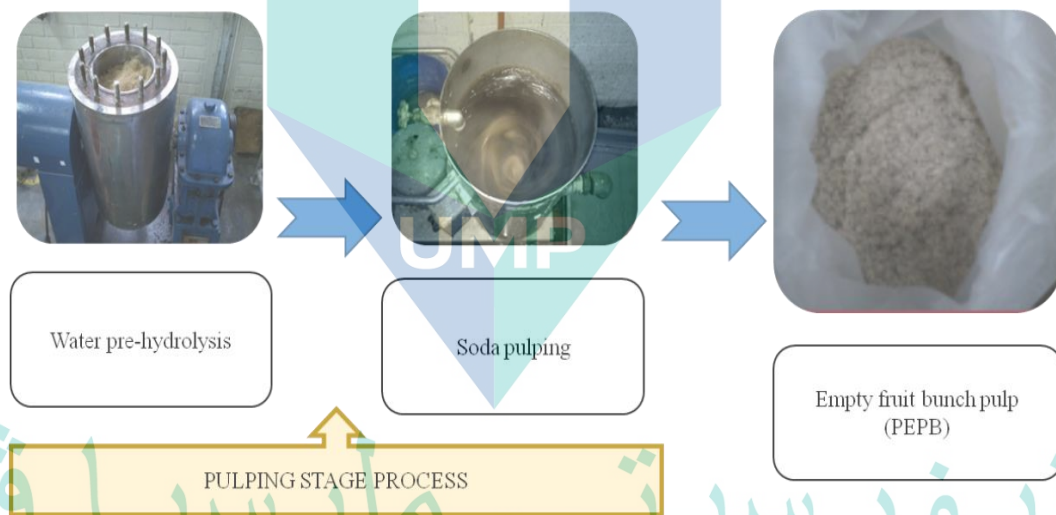
Figure 3.2   Stages involved in the pulping process.

Table 3.2   Parameters used during the pulping process

Parameter	Condition
Pre-hydrolysis stage	
liquor to material ratio	6:1
time to cooking temperature	90 min
Cooking time	60 min
temperature	170 °C.
Soda Pulping	
liquor to material ratio	10:1.
time to cooking temperature	90min
Cooking time	90min
cooking temperature	160 °C.
Alkali level:	20%

Source: Rosli et al., (2003).

3.4.2   **Preparation of Treated PEFB (TPEFB)**

After the pulping process, the PEFBwasfurther treated to remove another excessive non-cellulose material andprovide a better swelling effectof PEFB. The pre treatment of cellulose was according to (W. Li, Wang, & Liu, 2011) with slight modification. There are two stages of pre-treatment using alkaline treatment and dimethyl sulfoxide (DMSO) treatment. In brief, the mixture of PEFB and sodium hydroxide (NaOH) was heated at 80°C for 2h. The mixture was then filtered and washed with distilled water until clear wash water was obtained after which the PEFB was air-dried. The air-dried PEFB was than undergo exposed to the second stage of pre-treatment with DMSO as it was heated in a water bath at 90°C for 2h followed by filtering and washing. The TPEFBPEFB (TPEFB) was finally oven-dried at 60°C and stored for further characterization.

3.4.3   **Ultrasound-assisted hydrolysis**

Nanocrystalline Cellulose (NCC) was prepared by the combination of ultrasonic and acid hydrolysis of TPEFB as illustrated in Figure 3.3. The hydrolysis was carried out with a concentration of 64% (w/v) of H_2SO_4 solution in an ultrasound bath (Elma 37 kHz, power capacity 320 W, Germany) at temperature of 45 °C for 2 h. After hydrolysis, the milky suspension was folded for a total of 10 times of cold deionized

(DI) water to stop the reaction. The suspension was left overnight to settle down. After that, the NCC was dialyzed by using a dialysis membrane (MW cut off 12,000-14,000, 25mm) against DI water for several days until the pH of the DI water is constant. The suspension of NCC (Figure 3.4) was then centrifuged to remove the excessive acid solution and washed with DI water for several times. The obtained NCC suspension was further treated using ultrasound treatment for 30 min in order to disperse the NCC. Finally, the NCC was oven-dried at 60°C for further characterization.
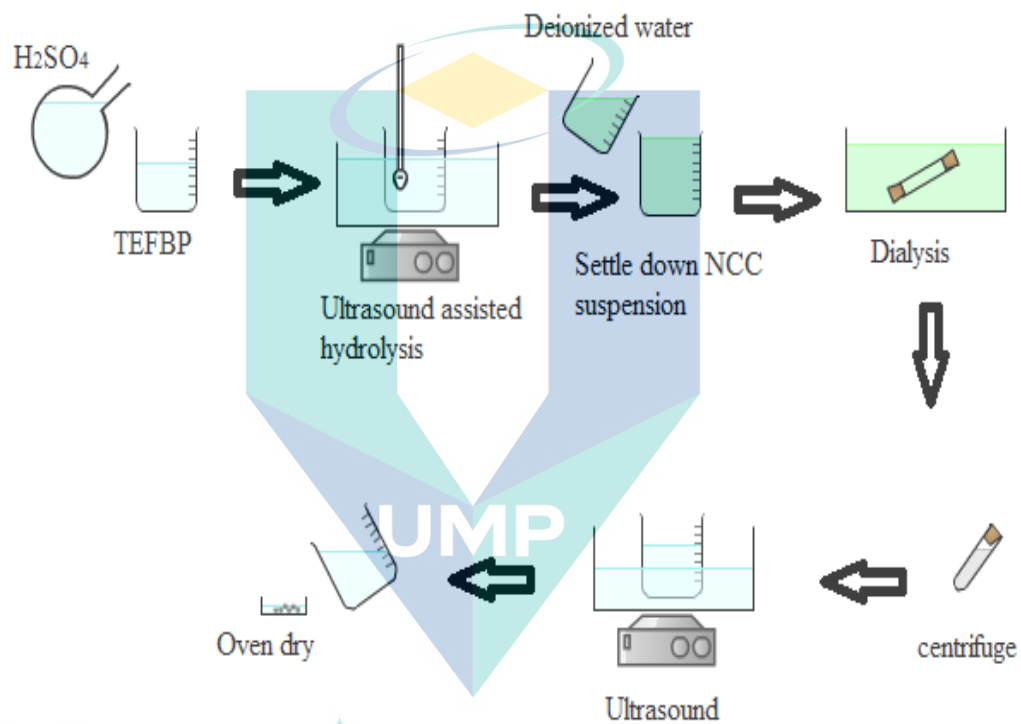
Figure 3.3   Preparation of the NCC via ultrasound-assisted hydrolysis
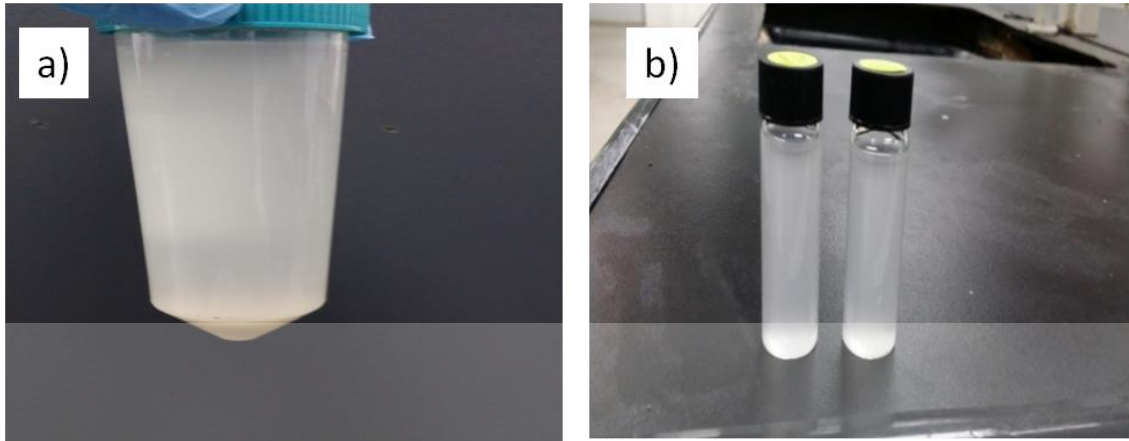
Figure 3.4   The obtained Nanocrystalline Cellulose (NCC) suspension after washing step in the centrifuge and NCC suspension and b) Nanocrystalline cellulose suspension (NCC)
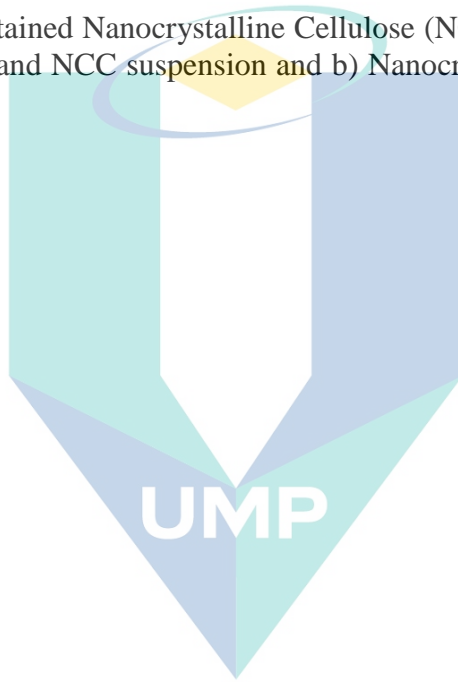
3.5 Optimization condition of NCC via ultrasound-assisted hydrolysis

The RSM was used for this study to verify the relationship between the efficiency of NCC yield (response) and four independent variables of the process parameters independent variables (acid concentration, temperature, time, and ultrasound time).The factorial design was developed with the RSM based on the full factorial design. This design is used for fitting a second-order polynomial model to the experimental runs. Then, the significant conditions were optimized using Central Composite Design(CCD) in RSM.

3.5.1 Experiment set-up for Full Factorial Design Analysis (FFD)

The screening studies through full factorial design (FFD) using Design-Expert software (Version 8.0, State-Ease) was used to determine the experimental variables and interactions that have a significant influence on the production of NCC. This experimental design consisted of 16 experiments, which were performed in triplicate for each experiment. Four range of variables influencing the yield of NCC such as acid concentration (%) time (min), temperature (°C), and ultrasound time (min) were screened by using full factorial design (FFD) as summarized in Table 3.3. On the other hand, Table 3.4 shows the range of factors involved and the coded value of the variables employed. Coded values of +1 and -1 correspond to high and low levels of variables, respectively. The outputs of the experimental design were analyzed with Design Expert 8.0 software to evaluate the effects of each factor involved. The yield of NCC was calculated based on the following equation:

$$\text{Yield} = \frac{(M_1 - M_2)V_1}{M_3 V_2} X 100 \qquad 3.1$$

Where:

M1 is weight of total mass dried NCC + Weighting bottle

M2 is Mass of weight bottle (mg)

M3 is Mass of cellulose pulp

V1 is total Volume of NCC suspension (mL)

V2 is the Volume of NCC to be dried (mL)

Figure 3.5 NCC suspension (after ultrasound-assisted hydrolysis) in dialysis tubing.

Table 3.3   Variables and their coded and actual levels used in full factorial experiments

No.	Name	Factor	Coded values of Variables		Units
			-1	1	
1	Acid Concentration	A	50	64	%
2	Temperature	B	45	60	C
3	Hydrolysis Time	C	90	180	min
4	Ultrasound Time	D	30	90	min

Table 3.4   The design of the full factorial experiments (A: Acid concentration (%), B: Hydrolysis temperature (°C), C: hydrolysis time (min) and D: Ultrasound time (min))

Standard Order	Run Order	Coded values of variables			
		A	B	C	D
1	13	-1	-1	-1	-1
2	11	+1	-1	-1	-1
3	7	-1	+1	-1	-1
4	16	+1	+1	-1	-1
5	1	-1	-1	+1	-1
6	10	+1	-1	+1	-1
7	12	-1	+1	+1	-1
8	9	+1	+1	+1	-1
9	15	-1	-1	-1	+1
10	4	+1	-1	-1	+1
11	3	-1	+1	-1	+1
12	2	+1	+1	-1	+1
13	8	-1	-1	+1	+1
14	14	+1	-1	+1	+1
15	5	-1	+1	+1	+1
16	6	+1	+1	+1	+1

3.5.2   Experiment set-up for Optimization using Central Composite Design (CCD)

Following the selection of the most significant factors through screening by factorial analysis, optimization of NCC production was then performed. The optimization aims to determine the optimum condition for the maximum yield of NCC from ultrasound-assisted acid hydrolysis. The optimization was performed by using design expert 8.0 software. The experimental table was constructed by using a central composite design (CCD) from RSM. CCD was applied to identify the relationship between the factors and the NCC response. The CCD was used to optimize the variable that has asignificant effect on the NCC production for yield improvement over the studied range as summarized in Table 3.5

Based on the initial screening result, only two independent variables were identified to have a significant effect on the NCC production yield. The outputs of the experimental design were analyzed using Design-Expert software based on the experimental runs summarized in Table 3.6.

Table 3.5 Design experimental range and levels of the variables in the central composite (CCD).

Factor	Variable	symbol	Units	Minimum	Maximum
A	Acid concentration	A	%	60	68
B	Temperature	B	°C	55	65

Table 3.6   Experimental table of central composite design.

Standard	Run	Coded values of variables	
		A	B
1	12	-1	-1
2	6	1	-1
3	2	-1	1
4	8	1	1
5	3	-1	0
6	9	1	0
7	13	0	-1
8	1	0	1
9	7	0	0
10	10	0	0
11	4	0	0
12	11	0	0
13	5	0	0

3.5.3   Validation model for NCC

The optimum condition for maximum NCC yield obtained from CCD was validated by confirmation runs performed in a 250-mL Erlenmeyer flask. Three

experiments were conducted under the proposed optimal condition and the results were compared with the predicted value in order to determine the validity of the model. This validation of a quadratic model for NCC production yield was justified by numerical features in the design expert software. The percentage errors between these values were calculated using the following equation 3.2:

$$\% \, Error = \frac{(ActualValue - PredictedValue)}{ActualValue} \times 100 \qquad 3.12$$

3.6   Functionalization of NCC

The functionalization of NCC was carried out according to A.K.M et al., (2016) with slight modification. Briefly, the different concentration of HBPE solution (0.1mmol/g, 0.3mmol/g, and 0.5mmol/g) was prepared in thetetrahydrofuran (THF) solvent, at a ratio of 1:2 for HBPE and THF. The NCC was then dispersed in the HBPE:THF solution. The suspension was stirred for another 15min until a homogeneous dispersion of NCC was observed. Then the suspension was sonicated for 30min in order to facilitate the interaction between NCC and HBPE. After that, the solution was poured into a petri dish and placed into a fume hood to eliminate the remaining THF solvent. Finally, the Modified NCC (MNCC) was oven-dried at 100 °C and stored for further analysis. The MNCC samples were denoted as 0.1 MNCC, 0.3 MNCC, and 0.5MNCC respectively based on the concentration of HBPE used. The schematic of the modification of MNCC by HBPE is presented in Figure 3.6.
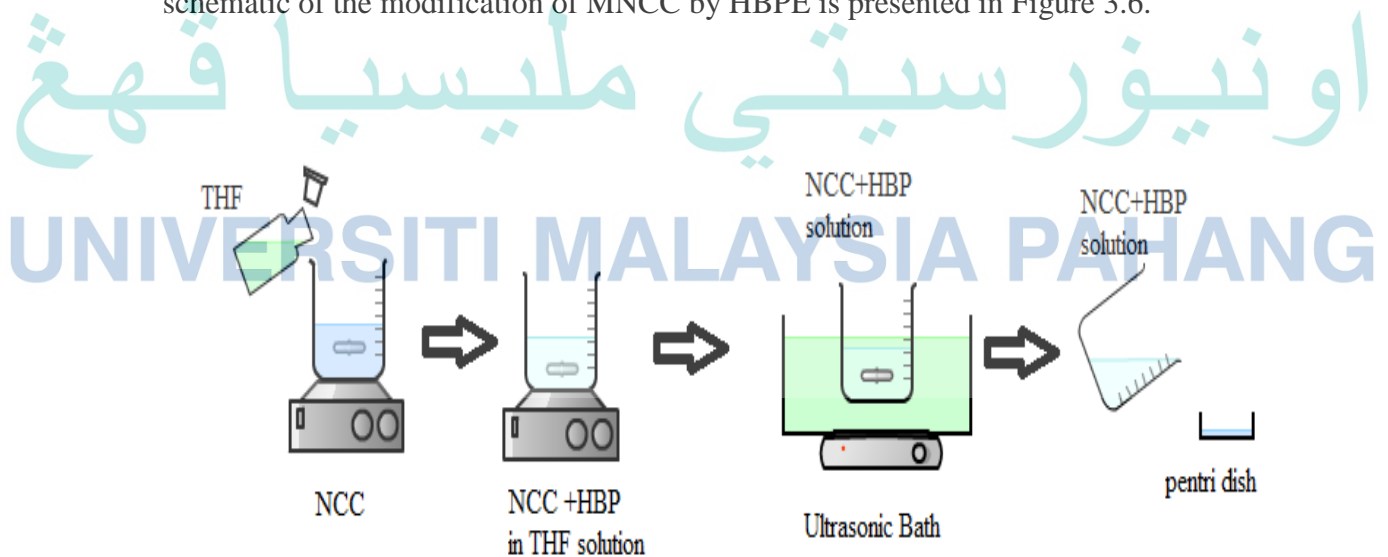
Figure 3.6   Modification NCC via non-covalent attachment of hyperbranched polyester

3.7 Fabrication of NanocompositeHydrogel

The nanocomposite hydrogel was prepared by individually incorporating the NCC and MNCC into the PVA solution using the freeze-thawing method. Briefly, the 3% of NCC and 3% ofMNCC were dispersed into DI water in an ultrasound bath for 30 min. The samples (NCC and MNCC) were then incorporated into the PVA solutionand stirred for another 30 min. The suspension of PVA and NCC (Figure 3.7) was then left overnight. After this, the suspensions were poured into a Petri dish and freeze-thawed for five cycles. Finally, the samples were keptin the freezer for further analysis. Other samples such as neat PVA, PVA/3NCC, PVA/5NCC, PVA/7NCC, PVA/REFB, and PVA/PEFB were also prepared using the same approach as illustrated in Figure 3.8.
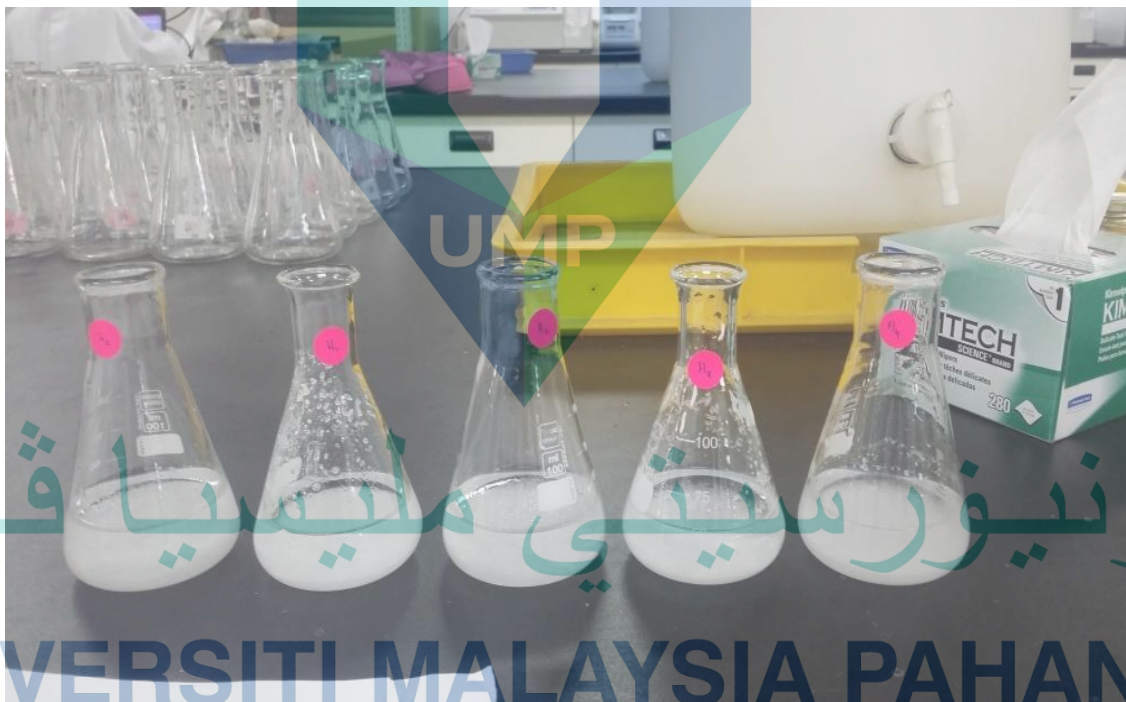
Figure 3.7   PVA/NCC suspension
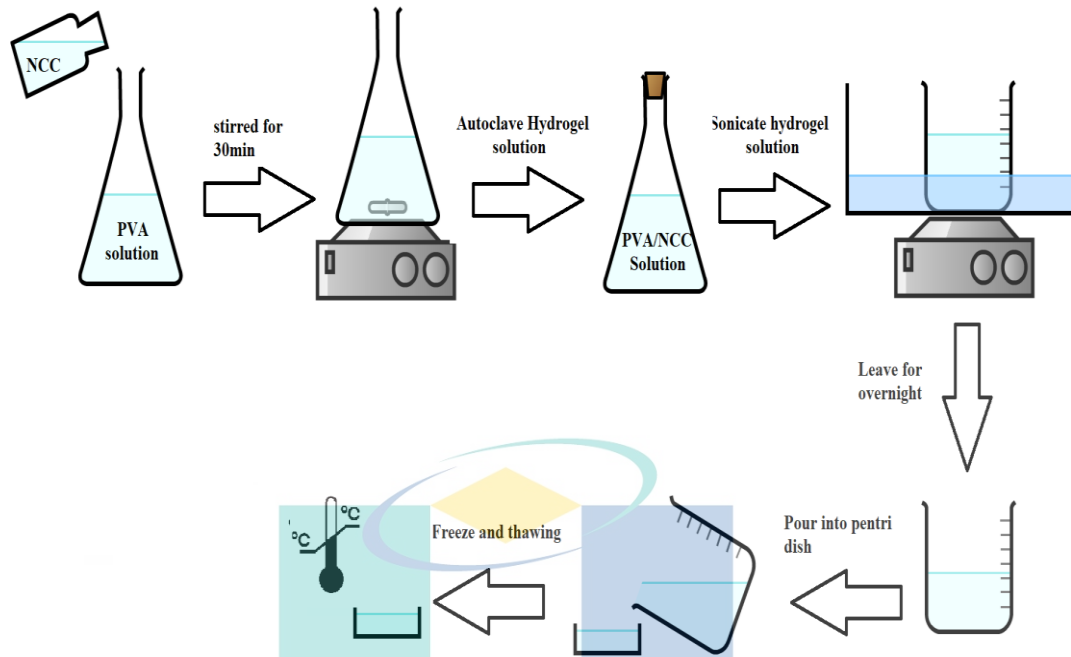
Figure 3.8   Detailed flow for the preparation of different categories of PVA-based hydrogel

3.8   Characterization Techniques

3.8.1   Chemical Composition Analysis

The composition of lignin, hollocellulose, cellulose, and ash content in REFB, PEFB, and TPEFB were analyzed based on TAPPI T 222 os-74, Wise, Murphy, and D'addieco (1946), and TAPPI T 203 om- 93 methods with slight modifications. For lignin composition, the TAPPI T 222 os-74 method was used for soluble acid lignin. The REFB sample was mixed with DI water, acetic acid (CH_3COOH), and sodium chlorite ($NaClO_2$) in a conical flask and placed in a hot ultrasound bath. The acetic acid and sodium chloride were added to the flask after every 30 min for three times. Then, the sample was filtered and washed using acetone. The obtained holocellulosewasdriedto remove the excess acetone. Finally, the dried hollocellulose was weighed and characterized. The cellulose content was determined using TAPPI T 203 om- 93 method. The hollocellulose was placed in a beaker, and 17.5% of NaOH was added to the sample and stirred for a few seconds. The addition of NaOH was repeated three times. After that, the DI water was added into the sample,and the mixture

was left for 30 min. The obtained cellulose (Figure 3.9) was washed, filtered, and oven-dried at 105 °C. Finally, the weight of cellulose after oven drying was measured.

Figure 3.9   Obtained Alfa-cellulose from samples of REFB, EFBP, and TEFBP.

3.8.2   Field Emission Scanning Electron Microscope (FESEM)

The microstructure and surface morphology of raw materials, NCC, modified NCC, and PVA hydrogel samples were investigated by using Field Emission Scanning Electron Microscope (FESEM), Zeiss Supra 55VP. The different samples such as REFB, PEFB, TPEFB, NCC, neat PVA, PVA/NCC, PVA/REFB, PVA/PEFB, and PVA/MNCC hydrogel were gold-coated prior to FESEM observation. The morphology of each sample was observed by selecting ten pictures randomly from the image at different magnifications.

3.8.3   Fourier Transform Infrared Spectroscopy (FTIR)

FTIR was used in order to understand the chemical composition of raw materials, NCC, modified NCC, and PVA hydrogel.The sample functionalities of the different samples were analyzed by Perkin Elmer Spectrum 100 FTIR Spectrometer within a spectral range of 4000–450 cm^{-1}. The spectra of the samples were recorded with a resolution of 2 cm^{-1}, taking 4 background scans for each sample.

3.8.4 X-ray Photoelectron Spectroscopy (XPS) Surface compositional analysis

XPS spectra were collected with an Axis Ultra DLD electron spectrometer (Kratos Analytical Ltd, UK) using a monochromatized Al X-ray (1486.6 eV) source operated at 150 W. Survey spectra of the samples were collected from 1100 to 0 eV at pass energy of 160 eV. Then, Kratos software was used for spectra processing.

3.8.5 X-ray Diffraction (XRD)

XRD analysis was conducted to investigate the crystalline behavior of the cellulosic materials and to monitor the changes in the crystalline structure of the starting materials to their corresponding isolated NCC.X-ray diffraction (XRD) data were collected by using a Rigaku Mini Flex II, XRD equipment operated at 30 kV and 15mA. The samples were step-wise scanned over the operational range of scattering angle (2θ) between 3 to 40°, with a step of 0.02°, using CuKα radiation of wavelength λ=1.541Å. The degree of crystallinity (Xc) was calculated using equation 3.2 as follows:

$$\text{Crystallinity}(\%) = \frac{(I_{cr} - I_{am})}{I_{cr}} \times 100 \qquad 3.2$$

Where I_{cr} and I_{am} are the peak intensities at the crystalline and amorphous regions respectively.

3.8.6 Thermogravimetric Analysis, (TGA)

TGA is a technique for measuring the change in the mass of the sample. These measurements are used to study the thermal stabilities and compositional properties of the materials. The thermal behavior of samples was investigated by using Thermogravimetryanalyzer, TGA (Pyris 1, Perkin Elmer, at HQ MPOB Bangi). A total of 10 mg of each dried sample was heated at a rate of 20°C/min over a temperature range from 30 to 700 °C under a nitrogen atmosphere.

3.8.7 Differential Scanning Calorimetry (DSC)

The DSC analysis was conducted by placing about 10 mg of the samples in the aluminum DSC crucible and sealed by analuminum lid. The samples were then heated to 400°C at a heating rate was 5°C/min under a constant supply of nitrogen.

3.8.8 Swelling Ratio (SR)

The swelling behaviour of the investigated samples was measured in water from 3 to 50 °C, using a thermostatic bath. Three different heat rates were used such as 3°C/day (from 3 to 9 °C), 24°C/day (from 24 to 36 °C), and 50°C/day (from 36 to 51 °C). The swelling ratio (SR %) for each sample was then calculated using equation 3.3 as follows:

$$SR = \frac{Ws - Wd}{Wd} X\ 100 \qquad\qquad 3.3$$

Where, Ws and Wd are the hydrogel masses in the swollen and the dry state, respectively. All measurements are performed in triplicate.

3.8.9 Gel Fraction (GF)

A slice of the tested samples was placed in an oven at 37°C until a constant weight was reached. Each sample was immersed in distilled water at room temperature for several days to eliminate unreacted species. Subsequently, the immersed sample was removed from the deionized water and dried at 37°C until a constant weight was reached. Then, the gel fraction was calculated according to Jimena S Gonzalez et al., 2014(Equation 3.4) as follows:

$$GF\% = \frac{Wf - WF}{Wi - WF} \times 100 \qquad\qquad 3.4$$

Where W_i and W_f are the weights of the dried hydrogels before and after immersion, respectively, and W_F is the weight of the filler (NCC, MNCC,REFB PEFB, and TPEFB) added in PVA hydrogel.

3.8.10 Compression test

The mechanical compression strength of hydrogel was evaluated by determining the relative change in height of hydrogel samples under the pressure. The dried hydrogel nanocomposite samples of the investigated samples such as neat PVA, PVA/3NCC, PVA/5NCC, PVA/7NCC, PVA/REFB, PVA/PEFB, and PVA/MNCC were cut into 5 mm × 10 mm (diameter × height) in dimension and incubated in distilled water for 24 h at 25°C prior tothe test. A compression test was then performed

on a CMT6503 Test Machine (Shenzhen SANS, China), with a speed of 5 mm/minaccording to ISO527-1995.
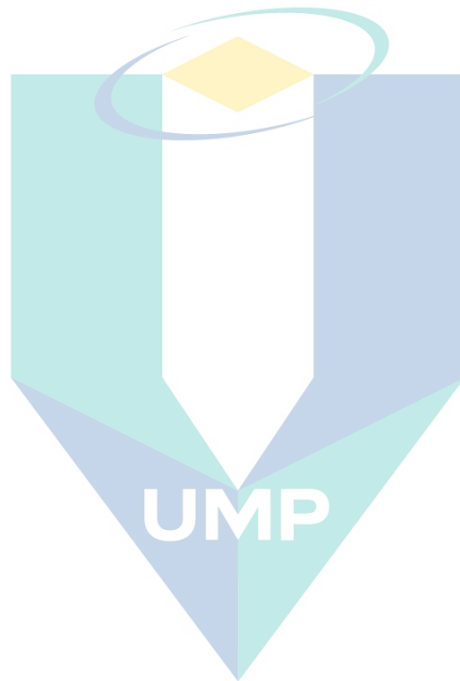
CHAPTER 4

RESULTS AND DISCUSSION

4.1   Introduction

In this chapter, the data obtained from the experimental procedures are presented in form of tables and figures. Then the presented data are discussed in line with the study objectives and based on the experiments conducted as presented in Chapter 3. Therefore, Three main subchapters were discussed and summarized as follows:

i.   This section presents the result of the obtained NCC from oil palm fiber via ultrasound assisted hydrolysis. In this part, the chemical composition such as lignin, hollocellulose, hemicellulose, cellulose, and ash content for starting materials and pre-treated fiber are studied. Other than that, the properties of NCC such as morphology, chemical structure, crystallinity,and thermal properties also have been discussed further. In the optimization part, the best condition of NCC yield was studied by screening study using full factorial design. The effect of acid concentration, hydrolysis time, hydrolysis temperature, and ultrasound time was investigated. The selected best condition parameters from the screening study then proceeded to the optimization study by Central Composite Design(CCD) using Response Surface Methodology (RSM).

ii.   Another section is the characterization of the functionalization of NCC with HBPE with OH terminal group. The variant concentrations of HBPE such as 1%, 3% and 5% were studied and the best condition of HBPE were discussed based on the chemical structure, crystallinity, thermal stability, and thermal behaviour respectively.

iii.   The last section in this chapter presents the result on the effect of NCC and MNCC into PVA hydrogel. In this section, the best concentration of NCC in PVA/NCC hydrogel composite have been studied. Whereas, the chemical structure, gel fraction, swelling ratio, crystallinity, thermal and compression properties have been discussed in detail for this part. Another comparative analysis on the performance of REFB, PEFB, NCC, and MNCC in PVA hydrogel was also studied in terms of the macroscopic appearance, morphology, chemical composition, swelling behavior, compression strength, crystallinity, and thermal properties.

Where necessary, all these discussions were presented in comparison with previous studies and relevant articles were cited.

4.2   Preparation and characterization of NCC

4.2.1   Isolation, characterization and comparative characterization of NCC.

4.2.1.1   Fiber pre-treatment and Chemical composition

Since the starting materials of this research are not pure cellulose, their main components, cellulose, hemicellulose, and lignin were determined before and after chemical processes.**Error! Reference source not found.** table 4.1 shows the c omposition of lignin, hemicellulose, cellulose, and ash content in the treated and untreated EFB such as REFB, PEFB, and TPEFB. As can be seen in table 4.1, the lignin content was significantly reduced in PEFB and TPEFB with values of about 2% and 1.05% respectively. This is obviously lower than the lignin content of REFB which is about 25%. During prehydrolysis in the pulping process, lignin and hemicellulose of REFB started to dissolve out by hot water treatment and then further degraded by sodium hydroxide during the second stage of the pulping process(Rosli et al., 2003).

On the other hand, it was possible that the small amount of lignin and hemicellulose were eliminated during the pre-treatment process of EFBP, thus resulted in a decrease in the lignin and hemicellulose proportion as well. Therefore, the percentage of cellulose component for PEFB and TPEFB was increased as the lignin and hemicellulose content was reduced significantly. The reason for this is that the

lignocellulosic complex eventually broke down and the lignin and hemicelluloses were solubilized, therefore, resulting in an increase in porosity and surface area of cellulose. Taking into account that further purification such as bleaching needs to be performed in order to remove non-cellulosic components such as. lignin and hemicelluloses. However, considering that the lignin content after pulping was low which is 2%, therefore further bleaching has been neglected. The reason is that it reached its goal due to the composition of the cellulose derived from REFB by the pulping process is suitable for the extraction of NCC (low lignin content and high cellulose content).

Table 4.1   The chemical composition of REFB, PEFB, and TPEFB.

Composition(%)	Sample		
	REFB	**EFBP**	**TEFBP**
Lignin	25.33	2.00	1.05
Hemicellulose	12.07	10.31	8.60
Cellulose	59.14	87.70	90.00
Ash	1.16	0.17	0.08

The cellulose content of the samples can be seen to follow a similar trend. Specifically, the amount of these components in PEFB is higher than in REFB and the values were further increased for TPEFB. Notably, the cellulose content of REFB is 59.14% which is in the range of cellulose content reported in the literature (Shinoj et al., 2011). However, it is interesting to note that the cellulose content was increased in PEFB and TPEFB with values of about 87.70% and 90.00%, respectively. This is believed to be due to the dissolving effect of treatment conditions on the REFB during the prehydrolysis stage as reported by Rosli et al., 2003b. Specifically, during alkaline treatment, the lignin starts to dissolve out and this would invariably increase the relative percentage of cellulose components in the resulting treated fibers. This is the reason for higher cellulose components in the treated fibers compared to the REFB.

The ash content can also be seen to be lower for the treated fibers such as PEFB, and TPEFB which can be accrued to the removal of ash and other non-cellulosic

components from the treated fibers during the pulping and pre-treatment processes. Generally, based on the composition of these fibers as presented in Table 4.1, it can be concluded that the pulping process is an effective method to remove lignin and other non-cellulosic components from EFB fiber, and can be used to prepare the cellulose from EFB fiber for the NCC production.

4.2.1.2   Morphology

FESEM has been widely used to characterize the morphological surface changes in the fibers during the entire isolation process starting from raw material to nanocellulose. To compare the morphology of the NCC and the starting materials, FESEM observation was performed on REFB, PEFB, TPEFB, and NCC samples.

Figure 4.1reveals the surface morphology of REFB, PEFB, TPEFB, and NCC. As can be seen in figure 4.1, the REFB micrograph shows a rough surface (Figure 4.1 a) due to the presence of impurities and other cementing materials on the REFB surface (Nazir, Wahjoedi, Yussof, & Abdullah, 2013). In addition, the crack surface can also be seen in the FESEM micrograph of REFB perhaps due to the resultant effects of mechanical treatment.

Figure 4.1b shows the surface morphology of PEFB. Obviously, this has a smooth surface which can be attributed to the removal of impurities, wax, hemicelluloses, and lignin. Normally, during the prehydrolysis process, the hemicelluloses would become hydrolyzed and more water-soluble thereby facilitating the accessibility of NaOH. This would then help to facilitate the removal of surface impurities, swelling of the crystalline region, and alkalization of the peripheral hydroxyl groups (Abraham et al., 2013). A few holes can also be noticed on the surface of PEFB, perhaps due to the effect of the strong chemicals used during the pulping process. The TPEFB morphology in Figure 4.1c shows no significant difference as compared to PEFB and it indicates that the pre-treatment does not alter the morphology of the fiber. Notably, the pre-treatment was applied to weaken the cellulosic bonds and provide more access sites for the acid to penetrate.

66

Interestingly, the morphology of NCC in Figure 4.1d can be seen to exhibit different forms. Specifically, it reveals a spherical shape with an average diameter in the range of 30-40 nm. Significantly, the morphology of NCC prepared here is different from those reported previously (Cao et al., 2012; Haafiz et al., 2014) which was rod-like or needle-shaped. The spherical shapes of NCC offer several advantages as an excellent stabilizer of pickering emulsion and drug delivery carrier for ecapsulation application. A few research work on spherical NCC from different resources also has been reported by Fattahi Meyabadi et al., (2014), P. Satyamurthy and N. Vigneshwaran (2013), and N. Wang et al., (2008). Therefore, the NCC morphology obtained in this study is significant and this is believed to possibly be due to the effect of mechanical treatment processes, which in this study is the ultrasonic treatment incorporated into the acid hydrolysis. The ultrasound-assisted hydrolysis might have played a major role in keeping the reactants in good contact with the treatment solution, enhancing the hydroscopicity of the cellulose, and facilitating the molecular penetration of acid into the cellulose. This would then help to increase the rate of the hydrolysis reaction (W. Li et al., 2011). Specifically, the cavitations produced from the ultrasound treatment could help to induce mechanical modification during hydrolysis thereby resulting in a smaller size of NCC.

In another vein, the morphology of NCC shows some aggregation and interconnection among the NCCs. This is perhaps due to the drying process which might have facilitated strong cohesion force among the particles as reported in similar studies (Kvien et al., 2005; N. Wang et al., 2007).There are two possible explanations for this aggregation phenomenon. First, NCC particles were aggregate due to its high surface area or strong hydrogen bonding between themselves. The second explanation lies in the existence of aggregation of NCC that may occur during FESEM sample preparation, therefore there are possibilities for NCC to be more in bundles than individual NCC. Another third explanation is that the dimensional NCC chains tend to be bundled and twisted together randomly and joined together with different bundles to produce another network configuration(Yahya, Chen, Lee, & Hassan, 2018).
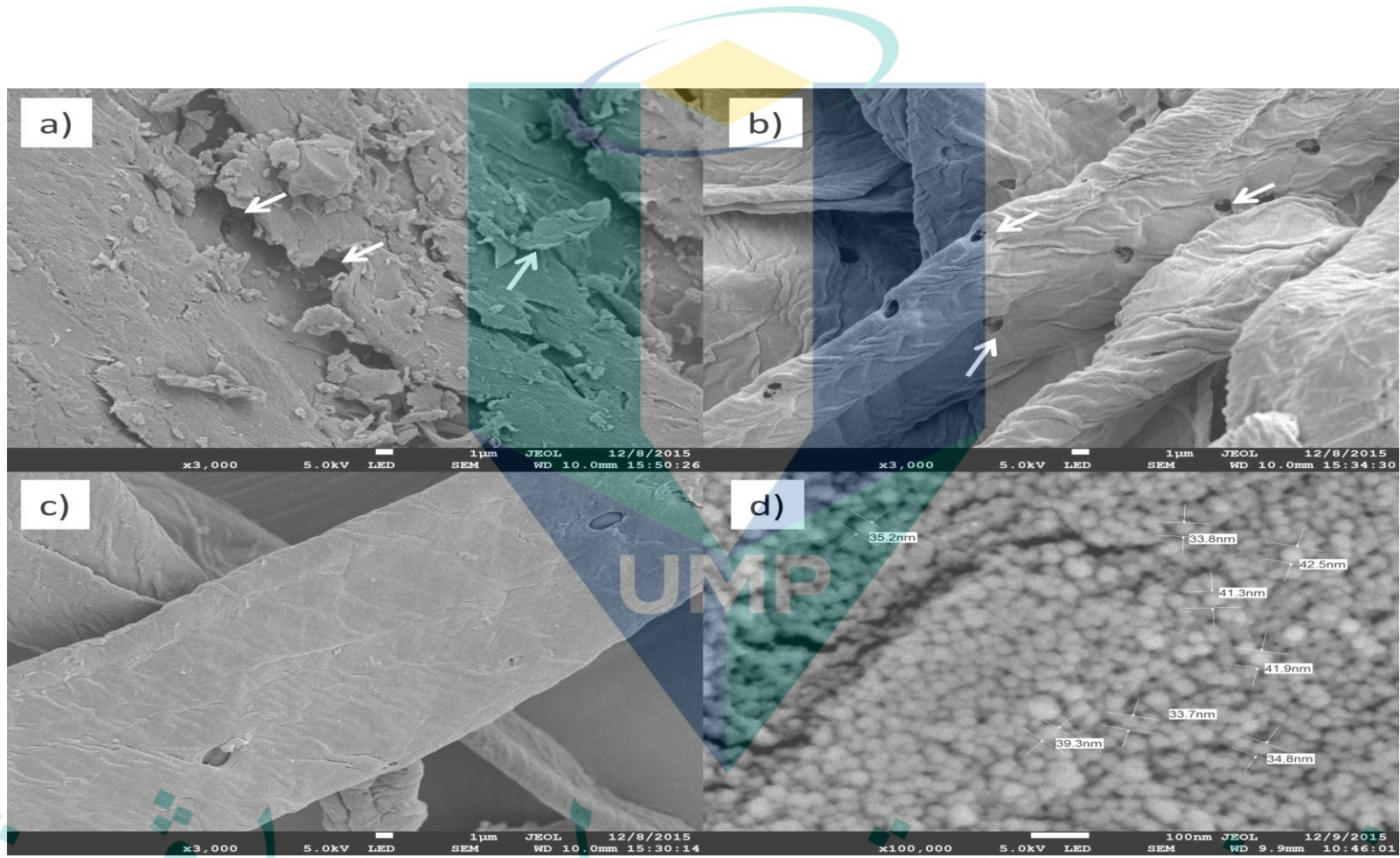
Figure 4.1   FESEM micrographs of (a) REFB, (b) PEFB, (c) TPEFB, and (d) NCC.

4.2.1.3   Chemical Structure

FTIR spectroscopy analysis is generally performed in order to investigate the structural change of the materials during the entire separation process and to confirm the resulting of the obtained cellulosic product. The FTIR spectra of the REFB, PEFB, TPEFB, and NCC are illustrated in Figure 4.2. As can be seen from figure 4.2, similar broadband is present in the spectra of REFB, PEFB, TPEFB, and NCC between 3331.86 cm^{-1} and 3337.12 cm^{-1}.This is an attribute of–OH stretching vibration. On the other hand, the absorption peak at 2899.29 cm^{-1} to 2918.44 cm^{-1} in the spectra of the different fiber types and NCC indicates the aliphatic saturated C-H stretching which is associated with methylene groups in cellulose.
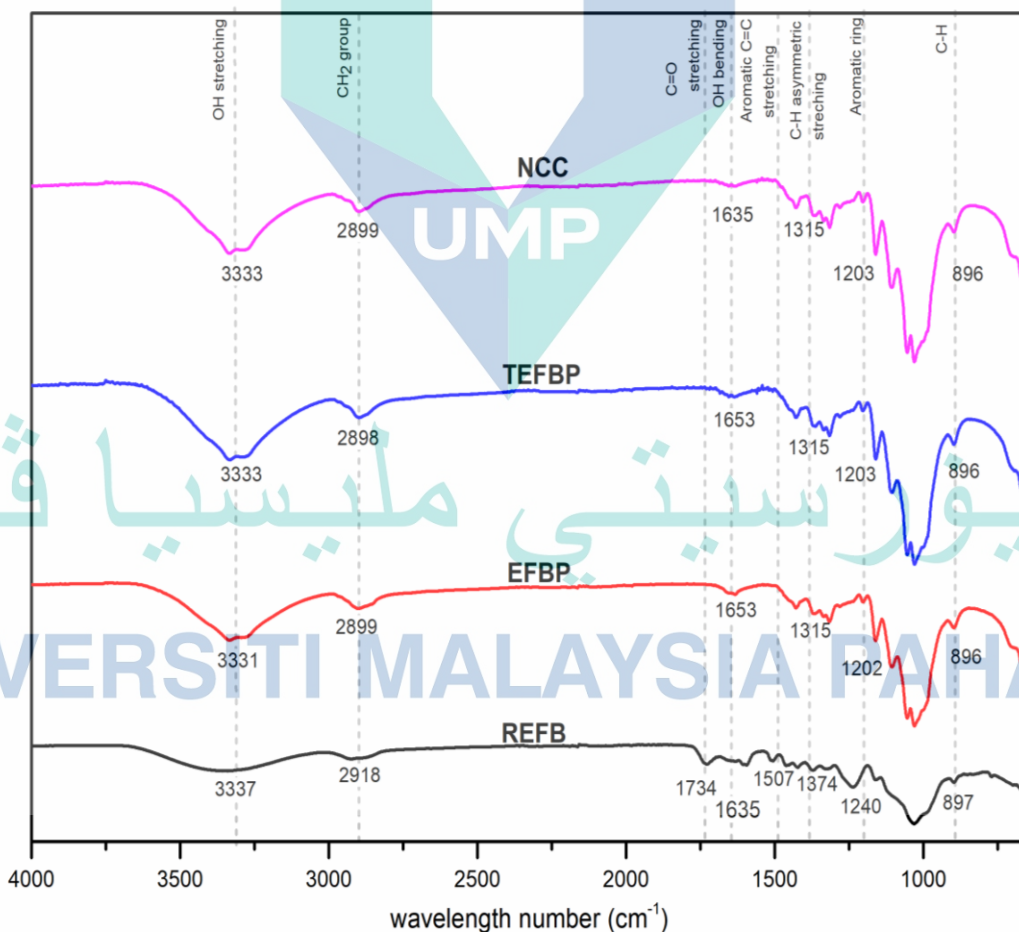
Figure 4.2   The FTIR spectra of the REFB, PEFB, TPEFB, and NCC.

It is known that the lignin is built up by oxidative coupling of the three major C6–C3 phenylpropanoid units which form a randomized structure in a tridimensional network through certain inter-unit linkages(Lamaming et al., 2015). The functional groups such as aromatic rings, carbonyls, methoxyl, and phenol hydroxyl groups all belong to lignin. The absorption band at 1734.44 cm^{-1} in REFB is attributed to the presence of the C=O bond in the aliphatic carboxylic, aryl ester, and acetyl groups in the xylan, which is a characteristic group of hemicelluloses and lignin (A., & Sain, 2008; Henrique, Silvério, Pires, Neto, & Pasquini, 2013; Sheltami, Abdullah, Ahmad, Dufresne, & Kargarzadeh, 2012). It is important to note that the peak is completely absent in PEFB, TPEFB, and NCC, indicating that the lignin and hemicelluloses had been removed by pulping and pre-treatment processes. Similarly, the band at 1507.86 cm^{-1}in the spectra of REFB is attributed to the aromatic C=C stretching from the aromatic ring of lignin.It is noteworthy that this peak disappeared after the pulping treatment as evidenced by its absence in the spectra of PEFB. This finding indicates that lignin was removed during the pulping process. On the other hand, the absorptions at 1635.78 cm^{-1}, 1653.26 cm^{-1}, 1653.27 cm^{-1}, and 1635.80 cm^{-1} in were recognized as the –OH bending mode for REFB, PEFB, TPEFB, and NCC samples which indicate the absorption of water and some of the carboxylate groups, confirming the hydrophilic nature of the cellulosic fibers (Yahya et al., 2018)

The band at 897 cm^{-1} in PEFB, TPEFB, and NCC can be attributed to the typical structure of cellulose due to the glycosidic linkages of glucose ring present in cellulose(Kaushik & Singh, 2011). Generally, based on these FTIR spectra, it can be inferred that the molecular structure of cellulose remained unchanged during the hydrolysis process. Likewise, during the ultrasonic treatment, the chemical structure of cellulose fragment was not affected by ultrasonic cavitation during the acid hydrolysis.Based on these findings, it is evident that the NCC was successfully isolated from the oil palm empty fruit bunch and the application of ultrasound during the hydrolysis does not alter the chemical structure of NCC.

4.2.1.4   Crystallinity

The crystalline behaviour of the cellulosic materials and the changes in the crystalline structure of the starting materials and NCC was investigate using XRD analysis. The comparative X-ray diffraction patterns of REFB, PEFB, TPEFB, and NCC are illustrated in Figure 4.3.As a notice, all the samples show similar XRD patterns at diffraction peaks of $2\theta = 15°$, $22°$, and $35°$representingto crystallographic planes of (1–10), (200), and (004) respectively (Yahya et al., 2018). These diffraction peaks are associated with the crystalline structure in cellulose I. It is well known that the cellulose contains both crystalline and amorphous regions. As compared to lignin and hemicelluloses, the crystalline structure in cellulose was formed by Van der Waals interaction and hydrogen bonding between adjacent molecules. In addition, the XRD result indicates that the implementation of ultrasound treatment during hydrolysis did not disrupt the crystal structure of NCC. On the other hand, the diffraction peak ($2\theta = 22°$), for NCC becomes sharper, indicating an increase in crystallinity compared to REFB, PEFB, and TPEFB which mostly appear as one broad peak.

The calculated crystallinity values for REFB, PEFB, TPEFB, and NCC are 42%, 73%, 75%, and 80%, respectively. Specifically, this observation indicating that the crystallinity increases with every progressive treatment procedure. Therefore, REFB shows lowest the crystallinity index compared to other samples. This is attributed to the presence of a large amorphous portion surrounded by hemicelluloses and lignin matrix, in the untreated fiber (J. Li, Song, Li, Shang, & Guo, 2014). Theoretically, after the ultrasound-assisted hydrolysis process, the crystallinity of NCC was increased as expected. Nonetheless, the increment in the crystallinity index of NCC as compared with their corresponding raw materials was not the same in all cases(Yahya et al., 2018).For instance, REFB which contains cellulose content (59%) rendered the lower crystallinity index than processed cellulose such as EFBP(87.7%) and TEFBP(90%) respectively. This can be explained by the presence of lignin and hemicellulose compositions in REFB, which are amorphous in nature; resulting in the lower crystallinity index. Whereas, the EFBP and TEFBP have been undertaken several chemical treatments in order to remove these amorphous portions (lignin,

71

hemicellulose, and partially amorphous cellulose) before proceeding to NCC. The removal of these components by several chemical treatments resulting in higher crystallinity.
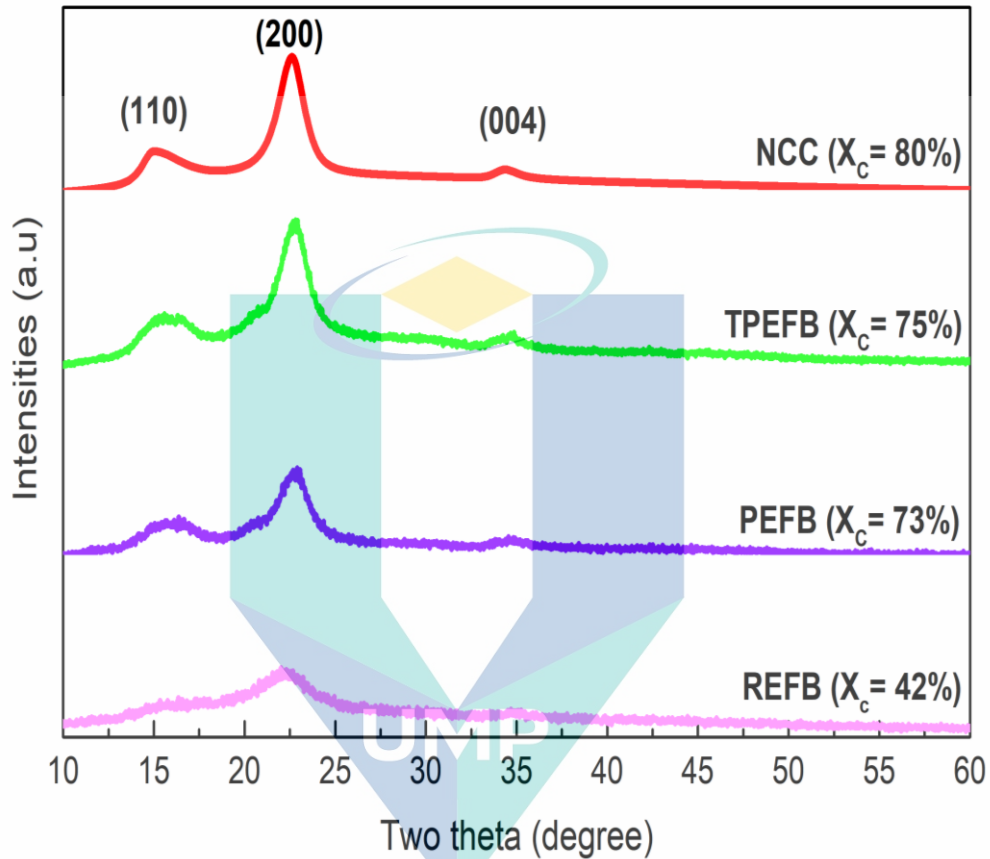
Figure 4.3   X-ray diffraction patterns of NCC, TPEFB, PEFB, and REFB.

Unexpectedly, the crystallinity obtained by NCC is slightly decreased compared to the previous reported NCC that is obtained by acid hydrolysis which yielded a crystallinity of 84% (Mohamad Haafiz, Eichhorn, Hassan, & Jawaid, 2013)This is,however, not surprising as a similar result has been reported by Rohaizu and Wanrosli, (2017) which observed a decrease in crystallinity in sono-assisted TEMPO oxidation of oil palm lignocellulosic biomass for isolation of nanocrystalline cellulose. Another low crystallinity of NCC was also observed with commercial MCC which were treated using sonication treatment(W. Li et al., 2012).The possible explanation for this is that the NCC might beover-treated during the hydrolysis treatment due to the ultrasound process. Theoretically, the presence of the cavitations process created by

ultrasound could help the penetration of acid by promoting hydrolytic cleavage of glycosidic linkages of cellulose during hydrolysis and as a result, lead to the formation of the individual crystallite. However, the ultrasound that is implementing during the hydrolysis not only improves the selectivity of acid hydrolysis but also has the potential to destroy both the amorphous and crystalline structure of cellulose. The cavitations process created by ultrasound disrupts the hydrogen bonds and the ordered packing of the cellulose fibrils, which cause the changing of crystalline structure and further destruction of crystallinity. (Rohaizu & Wanrosli, 2017b).

To summarize the finding in XRD result, the increase in the crystallinity of NCC compare to the starting material could be assumed to increase their strength, suggesting that NCC from oil palm empty fruit bunch in this research have the potential to be used for reinforcement in polymer materials especially in the mechanical properties.

4.2.1.5   Thermal stability

The determination of the thermal stability of NCC is the main factor for its potential use as the reinforcing agent in nanocomposites. It is known that the thermal stability of polymeric material is depending on the molecular interactions between the macromolecules and the sample natural characteristics. Hence, the knowledge of the degradation behaviour of NCC is a crucial part of the potential use in composite materials. The TGA and DTG curves of REFB, PEFB, TPEFB, and NCC are illustrated in figure 4.4. The reduction in weight of the samples at a temperature below 100 °C was observed for REFB, PEFB, TPEFB, and NCC are 11.06%, 10.83%, 5.54%, and 6.1%, respectively. This weight loss is attributed to the evaporation of absorbed water in the samples. The water was chemisorbed by the intermolecular hydrogen-bonded and the surface of the fibers become loosely bound moisture as apparent from the characteristic peak of FTIR spectra at $1653 cm^{-1}$. The reason behind this is that the –OH molecular structure indicates the hydrophilic nature of cellulose and shows that the water was absorbed into cellulose fiber structure (moisture water).

As illustrated in figure 4.4b, the thermal degradation of the REFB shows several stages, which indicates the presence of different components that decomposes during the heating process. Specifically, the differences in thermal behaviours can be accredited to the different chemical structure such as hemicelluloses, cellulose, and lignin content (Lamaming et al., 2015). Compared to the cellulose, hemicellulose disintegrated at a lower temperature, and this was attributed to its randomly amorphous nature and the presence of acetyl groups in its structure(Yahya et al., 2018). Another weight-loss stage was found at(200-300 °C)which related to the degradation of hemicellulose, pectin, some of the lignin, and cellulose. The major decomposition peak was also observed at the high-temperature range (300–400°C) which accounted for the cellulose pyrolysis phenomenon. During cellulose pyrolysis, several reactions are involved such as decarboxylation, dehydration, depolymerization decarbonylation, and others leading to the release of CO, H_2O, CO_2 (from decarboxylation), H_2 and CH_4 gasses. As the pulping treatment and pre-treatment were applied, the degradation temperature of PEFB and TPEFB increased to 316.92 and 354.87 °C, respectively. The increase in thermal stability of PEFB and TPEFB is believed to be due to the removal of hemicelluloses and lignin during the treatment process. This would facilitate closer packing of the cellulose crystals, thereby resulting in a right shift in the degradation temperature.
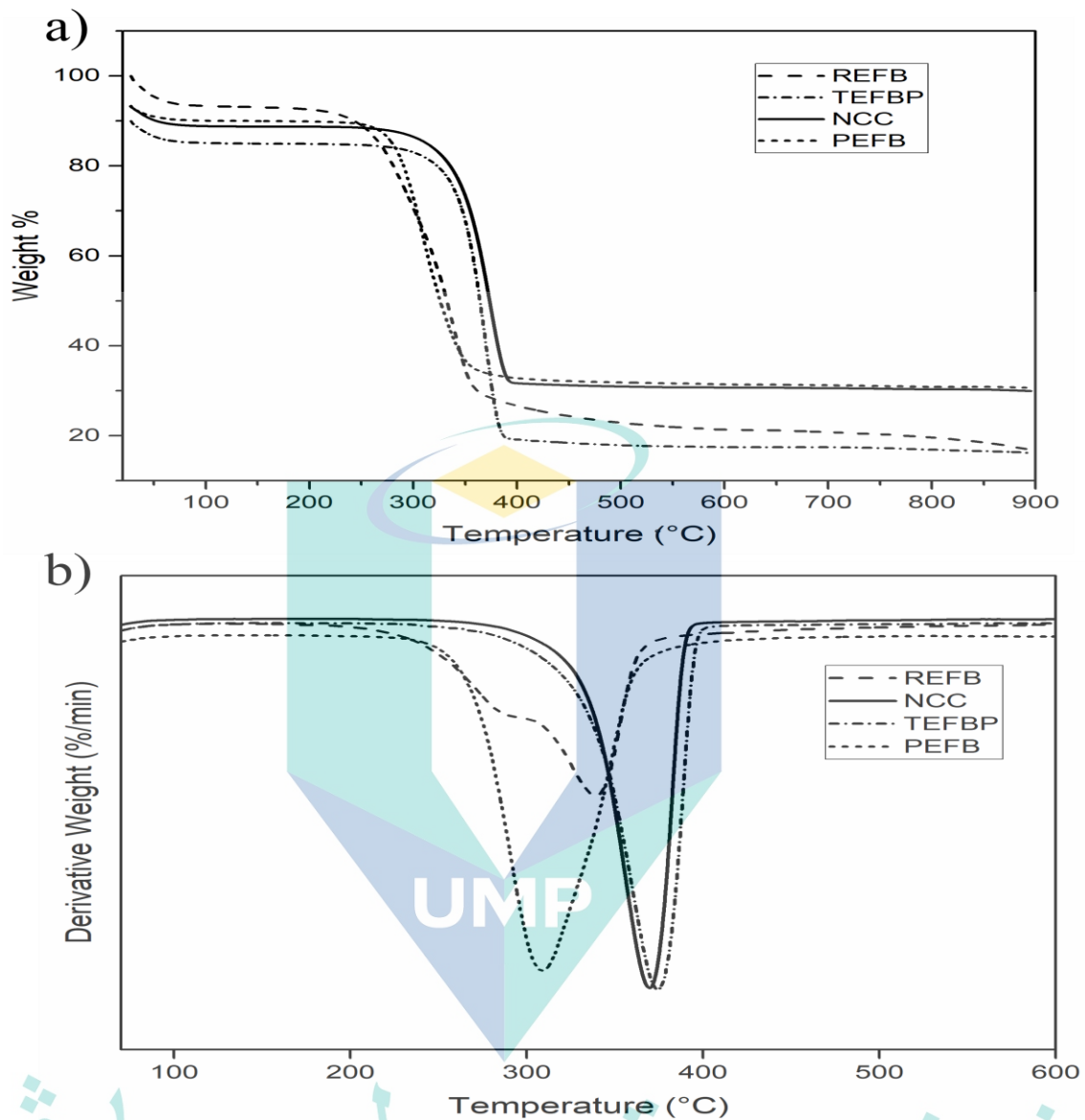
Figure 4.4   TGA (top) and DTG derivatives (bottom) of REFB, PEFB, TPEFB, and NCC

As reported by the previous study, the NCC produced by acid hydrolysis exhibits low thermal stability compared to its raw fibers (Liu et al., 2014a; Morais et al., 2013). However, in this study, the NCC obtained from acid hydrolysis assisted with ultrasound exhibits a higher thermal degradation temperature of about 362.17 °C compared to REFB fiber and PEFBPEFB. The thermal decomposition temperature of NCC is also higher (367 °C), compared to REFB (289°C) and PEFB (322°C), respectively. In fact, the thermal stability of NCC was higher compared to untreated and treated fibers. There are possible reasons for this phenomenon. First, the impurities such

as lignin, hemicelluloses, and pectin hemicelluloses of the untreated fibers can form free radicals that may initiate more active sites towards the heating process, hence accelerating the thermal degradation(C.S. et al., 2016). Second, this might be due to the increase of the intermolecular hydrogen-bonded domains after the dissolution of the amorphous components in the fiber during hydrolysis which may further enhance the thermal stability of NCC (Yahya et al., 2018). Therefore, NCC obtained by ultrasonic-assisted hydrolysis exhibited a degradation behavior that is high than REFB and EFBP. This implied that ultrasonic treatment during hydrolysis had a significant effect on the thermal decomposition of the NCC. This result is also consistent with the findings obtained from the XRD and FTIR analyses, indicating that the application of the ultrasonic process during hydrolysis did not change the cellulose chemical composition, crystal structure, and thermostability.

Table 4.2   Summary of moisture content, T_{onset}, T_{max}, and ash content for REFB, PEFB, TPEFB, and NCC.

Sample	Moisture content (%)	Degradation temperature (°C)		DTG peak (°C)		Ash content (%)
		T_{onset}		T_{max1}	$T_{max\ 2}$	
REFB	11.06	241.74		289.82	343.62	8.186
PEFB	10.83	316.92		322.64	-	6.089
TPEFB	5.54	354.87		473.09	-	3.132
NCC	6.12	362.17		367.08	-	1.056

4.2.2   Optimization Study of NCC Production

4.2.2.1   Screening of NCC production using Full Factorial Analysis

4.2.2.2   Full factorial design: responses

The design matrix and the response values for the NCC yield are presented in Table 4.3 along with the four variables (A: Acid concentration, B: Temperature, C: Hydrolysis time, and D: ultrasound time). These four variables were screened in order to identify the main factors that contribute to the production of high yield NCC. Considering the results, factors such as acid concentration and hydrolysis temperature are the most favorable conditions while hydrolysis time seems to offer only a very small contribution to the NCC yield. It is also interesting to notice that the factor, ultrasound time, does not contribute much to the percentage of NCC yield. Generally, factors such as acid concentration, temperature, and hydrolysis time have positive influences on the production yield of NCC. On the overall, the experimental design consisted of 16 experiments which were replicated 3 times for each experiment. Therefore, amongst the 16 experiments run, run numbers 2 and 9 presents the highest percentage yield of NCC yield.
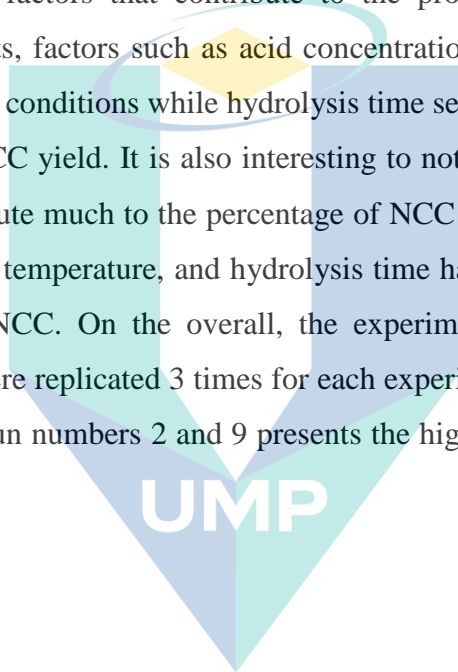
Table 4.3   Experimental design matrix of 2^4 Factorial Design of four variables for the production of nanocrystalline cellulose, NCC, with the corresponding responses.

Run	Experiemental Variable				Response
	Factor 1	Factor 2	Factor 3	Factor 4	
	A	B	C	D	
	Acid concentration (%)	Temperature (°C)	Hydrolysis time (min)	Ultrasound time (min)	NCC yield(%)
1	50	45	180	30	13.71
2	64	60	90	90	73.63
3	50	60	90	90	21.27
4	64	45	90	90	34.90
5	50	60	180	90	46.38
6	64	60	180	90	55.95
7	50	60	90	30	33.34
8	50	45	180	90	30.61
9	64	60	180	30	73.61
10	64	45	180	30	43.26
11	64	45	90	30	40.69
12	50	60	180	30	24.11
13	50	45	90	30	12.13
14	64	45	180	90	20.10
15	50	45	90	90	13.71
16	64	60	90	30	54.73

4.2.2.3 Model fitting and statistical analysis

The parameters that influenced the NCC production yield were determined by the regression model proposed. The regression model was statistically evaluated as presented in Table 4.5.In order to determine the significance of the model, the analysis of variance (ANOVA) was applied which is presented in Table 4.4. The R^2 value obtained from the ANOVA was used to indicate the closeness of the data, to the regression line. A good fitting model shows that the value of R^2 must be more than 80%. The experimental results show that the polynomial equation ($R^2 = 0.9998$) which indicates that the model fits the experimental and predicted values well. According to this result, a mathematical model in term of coded factors was proposed as follows:

$$NCC\ yield = 37.00 + 12.60A + 10.88B + 1.45C + 0.055D + 4.01AB$$
$$- 2.84AC - 3.53AD + 0.68BC + 1.37BD + 1.01ABC + 2.41ABD$$
$$- 6.48ACD - 2.38ABCD$$

Where NCC yield is considered as the response, while the terms A, B, C, and D represent the acid concentration, temperature, hydrolysis time, and ultrasound time respectively.

These factors, A, B, C, and D are the main effects, while their combinations such as AB, AC, AD, BC, BD, ABC, ABD, ACD, and ABCD are the interaction effects.The validity of the model can be evaluated by different tests. For example, the statistical significance of the regression equation can be checked using the Ficher criterion test (F-values), while the p-values may be used to determine the significance of each coefficient. According to the table, the F-value and p-value for this model are 771.41 and 0.0013 respectively. Notably, the obtained p-value shows a low value which indicates that there is only about 0.13% chance that the model F-value could occur due to noise. The effect of terms such as A, B, AB, AC, AD, BD, ABC, ABD, ACD, and ABCD was statistically significant in affecting the yield of NCC. On the other hand, the model terms such as C, D, and BC were not significant which means that the p-values are larger than 0.05.

Table 4.4   Test of significance for regression coefficient.

Source	Sum of Squares	df	Mean Squares	F Value	p-value Prob > F	
Model	5959.35	13	458.41	771.41	0.0013	significant
A-Acid Concentration	2538.14	1	2538.14	4271.17	0.0002	
B-Temperature	1892.25	1	1892.25	3184.27	0.0003	
C-Hydrolysis Time	33.76	1	33.76	56.80	0.0172	
D-ultrasound Time	0.048	1	0.048	0.081	*0.8022	
AB	256.96	1	256.96	432.41	0.0023	
AC	129.28	1	129.28	217.55	0.0046	
AD	199.37	1	199.37	335.51	0.0030	
BC	7.45	1	7.45	12.54	*0.0713	
BD	30.25	1	30.25	50.90	0.0191	
ABC	16.24	1	16.24	27.33	0.0347	
ABD	92.93	1	92.93	156.38	0.0063	
ACD	671.85	1	671.85	1130.58	0.0009	
ABCD	90.82	1	90.82	152.83	0.0065	
Residual	1.19	2	0.59			
Cor Total	5960.54	15				

$R^2 = 0.9998$, *Values of p-values greater than 0.05 indicating the model terms are not significant.

4.2.2.4   The pareto chart

The t-values of the bars are the values of the square root(R^2) of the F-values from ANOVA. Two limit lines, namely Bonferroni limit line and t-value limit line, are presented in Pareto chart as shown in Figure 4.5.
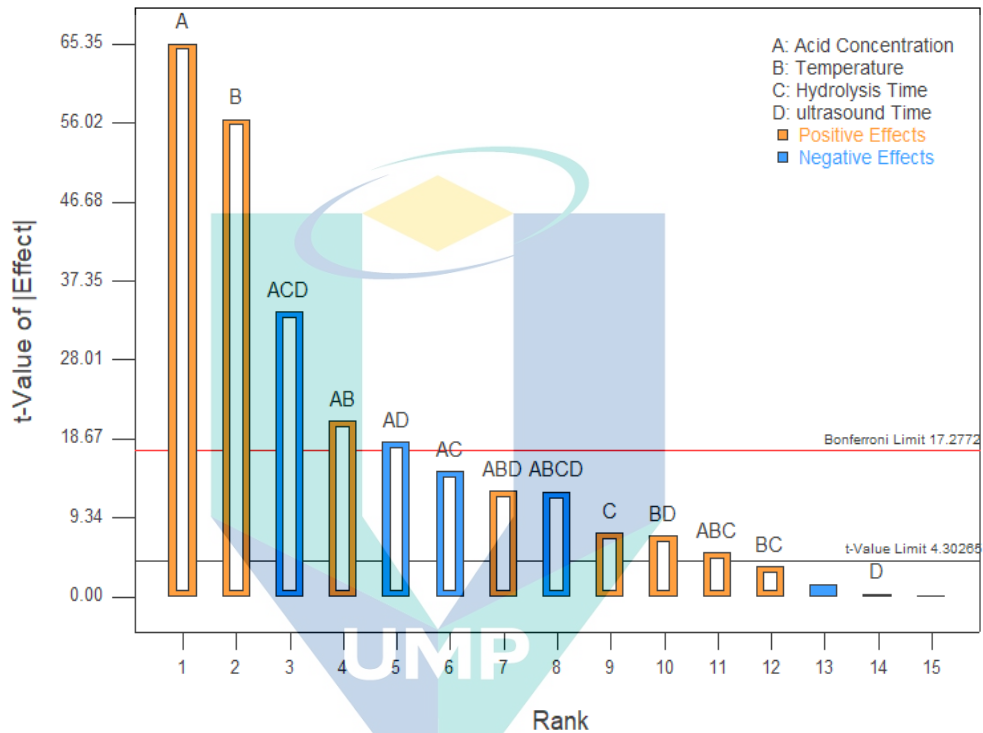
Figure 4.5   Pareto chart of the relative effect for various factors and interaction on NCC production yield.

The bars present the impact of the factors and the bars which cross the reference line (Bonferroni limit line and t-value) are statistically significant. In this Pareto chart, the value of Bonferroni limit line and t-value limit line are 17.2772 and 4.3026 respectively. As can be seen in the Pareto chart, it is evident that the factors A, B, ACD, AB, AD, AC, ABD, ABCD, C, BD, and ABC exceed the t-value limit and have significant effects for NCC production yield. Meanwhile, it is clear that main factorsA and B, and the interaction factor ACD, AB, and AD, exceeded the Bonferroni limit. Therefore, these significant factors should be taken into further consideration.

4.2.2.5   Main effects of the factors

The main effects plots of the factors (A, B, C, and D,) for the response NCC production yield, are shown in Figure 4.6. Main effects are used to analyze the relationship between the level of a factor and the change in response. While, the distance of the vertical line is directly associated with the statistical significance of a factor, and the slope of the effect implies the sign of the main effect (Ozbay & Seyda, 2018).

It can be observed in Figure 4.6 that Acid Concentration and Temperature possess the largest vertical line in main effect which indicates the high influence in NCC production yield. The acid concentration in Figure 4.6 shows that the increase of the acid concentration to 64% led to increased NCC production yield by 50%. Similar result can be seen for temperature, as an increase in the temperature to 60°C led to increase of about 50% in NCC yield. These results indicate that the acid concentration, and temperature, plays important role in the production yield of NCC. Similar observation was previously reported by Jin shi Fan, 2012 that the yield of NCC increases when the sulfuric acid concentration and temperature were increased. The reason for this perhaps the higher concentration of sulfuric acid helped to facilitate the hydrolysis of the amorphous components and crystalline segments in cellulose.

In addition, the increase in acid concentration may result into degradation of amorphous component in the presence of acid catalyst and leaving the crystalline component of cellulose intact. As for the temperature factor, the increase in temperature may enhance the reaction activity of cellulose in TPEFB thus producing more NCC yield. Moreover, the mass transfer in intra-fiber pores of TPEFB is also intensified with the rise of temperature due to the increase of the diffusion coefficient of H+ in aqueous solutions as stated in literature(Lu, Z., Fan, L., Zheng, H., Lu, Q., Liao, Y., Huang, 2013)
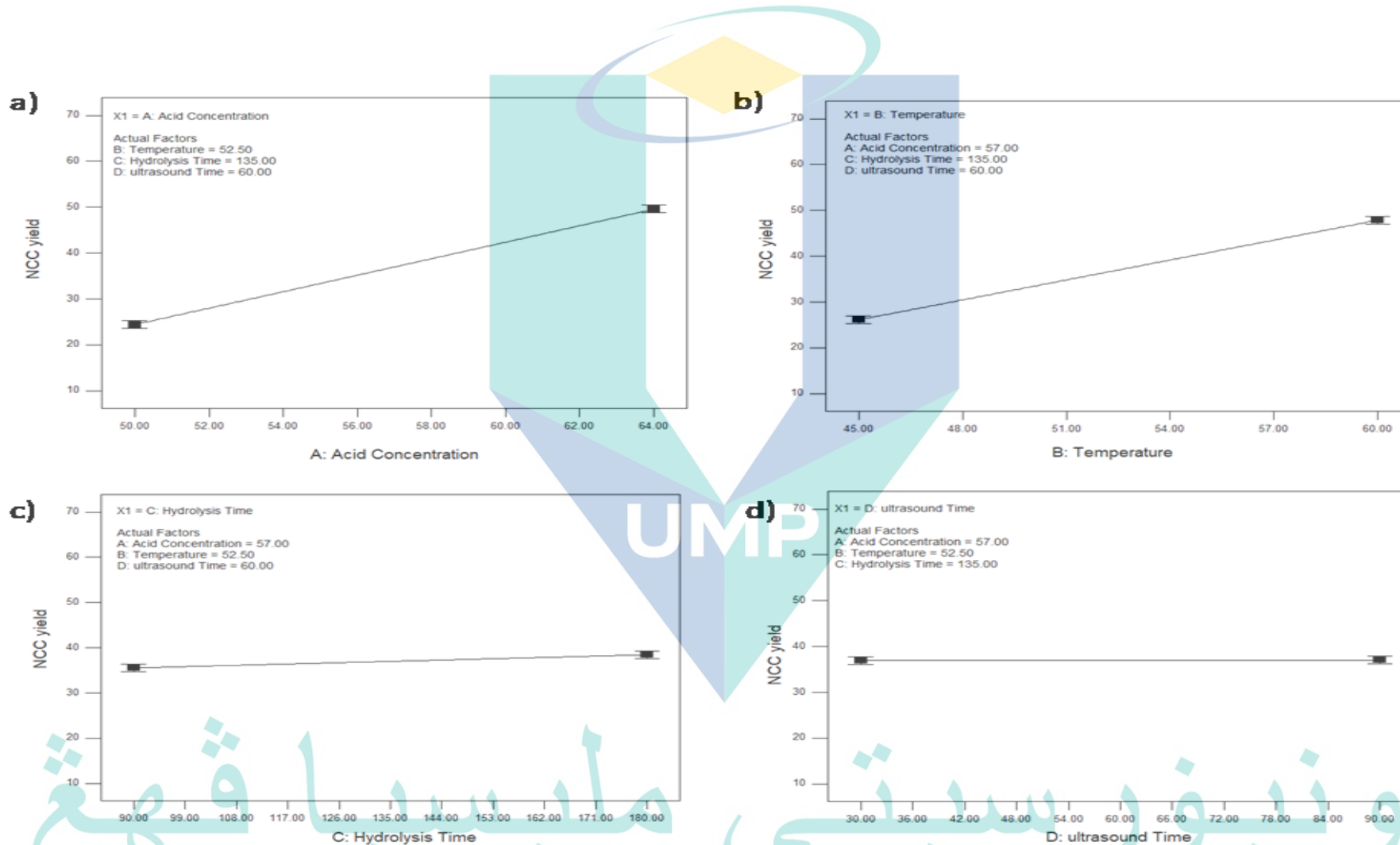
.

82

Figure 4.6   Plots of main effects of a)Acid concentration, b)Temperature, c)Hydrolysis time and d) ultrasound time on NCC yield response

Meanwhile, it was also observed that hydrolysis time shows a slightly significant effect on NCC yield. However, compared to acid hydrolysis and temperature factors, the hydrolysis time only increases the NCC yield by about 38% after 180 min. Notwithstanding, this observable increase can be accrued to the enhancement of mass transfer, which results in further improvement in the hydrolysis of cellulose.Significantly, the factor, ultrasound time, seems not to have much effect on the NCC yield. Contrary to expectations, this study did not find a significant difference between the minimum range of ultrasound time (30 min) and maximum range of ultrasound time (90 min). This indicates that variations in the ultrasound time do not have a significant effect onthe enhancementof cellulose hydrolysis.

4.2.2.6   Interaction effect of the factors

Figure 4.7 shows the interaction effect plots of a) AB b)AC, c)AD, d)BD, and e)BC on NCC yield response. The presence of interaction effects is important as it shows that two or more factors influence each other to affect the response. The interaction effect plot in an analytic model can provide a better representation as well as the knowledge of the relationship between the factors and response. The response, NCC yield lies on the y-axis, while the factors go along the x-axis. The red and black color lines indicate the minimum and maximum value of the factors respectively. The interaction effects occur when the effect of a factor depends on the values of another factor. In addition, the interaction between these factors would favor a superior expression of the process. As can be seen in Figure 4.8, the crossed lines on the interaction of AC, AD, and BD suggests that there is an interaction effect on the NCC production yield. On the other hand, the parallel lines on the interaction of AB and BC indicate that there is no interaction effect.

For the parallel lines of AB, both maximum and minimum values of temperature significantly increase with the increase of acid concentration. Furthermore, it was observed that the high yield of 62% NCC could be obtained with a high temperature of 60°C and high concentration of 64%. While the minimum temperature of 45°C with same acid concentration produced only 30% of NCC yield. From that observation, it is evident that there is a main effect emanating from Acid concentration and Temperature. Similar to the parallel lines of BC, only main effect occurred whereas, higher (50%) NCC yield can be obtained by hydrolysis time of 180 min at a temperature of 60°C. At

84

the same temperature, the minimum hydrolysis time of about 90min produced only 45% NCC yield.

For an interaction graph of AD, the crossed lines between Acid concentration and Ultrasound time for NCC yield production were stronger than the acid concentration and hydrolysis time in AC crossed line. For interaction graph of AD, the 50% NCC yield could be obtained with high acid concentration of 64% with the hydrolysis time of 180 min. However, at low acid concentration of 50% with the same concentration, low value of NCC yield of about 45% was obtained. Other than that, the interaction graph of BD shows that the ultrasound time and temperature are dependent on each other. The high value of NCC yield could be obtained by high temperature of 60°C and an ultrasound time of 90min. Nevertheless, it was observed herein that the NCC yields obtained from shorter ultrasound time are not much different.
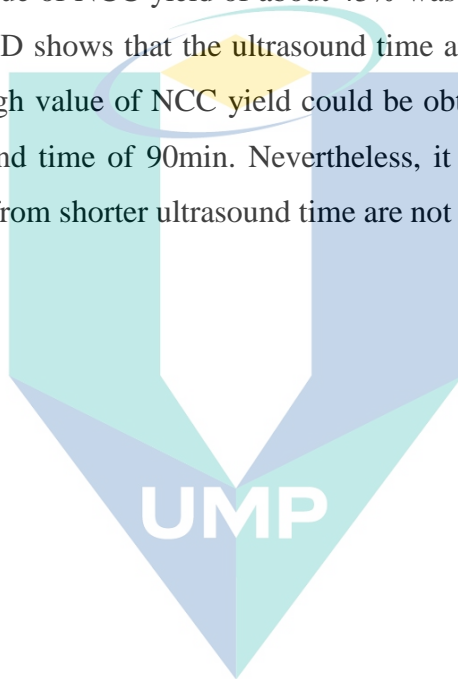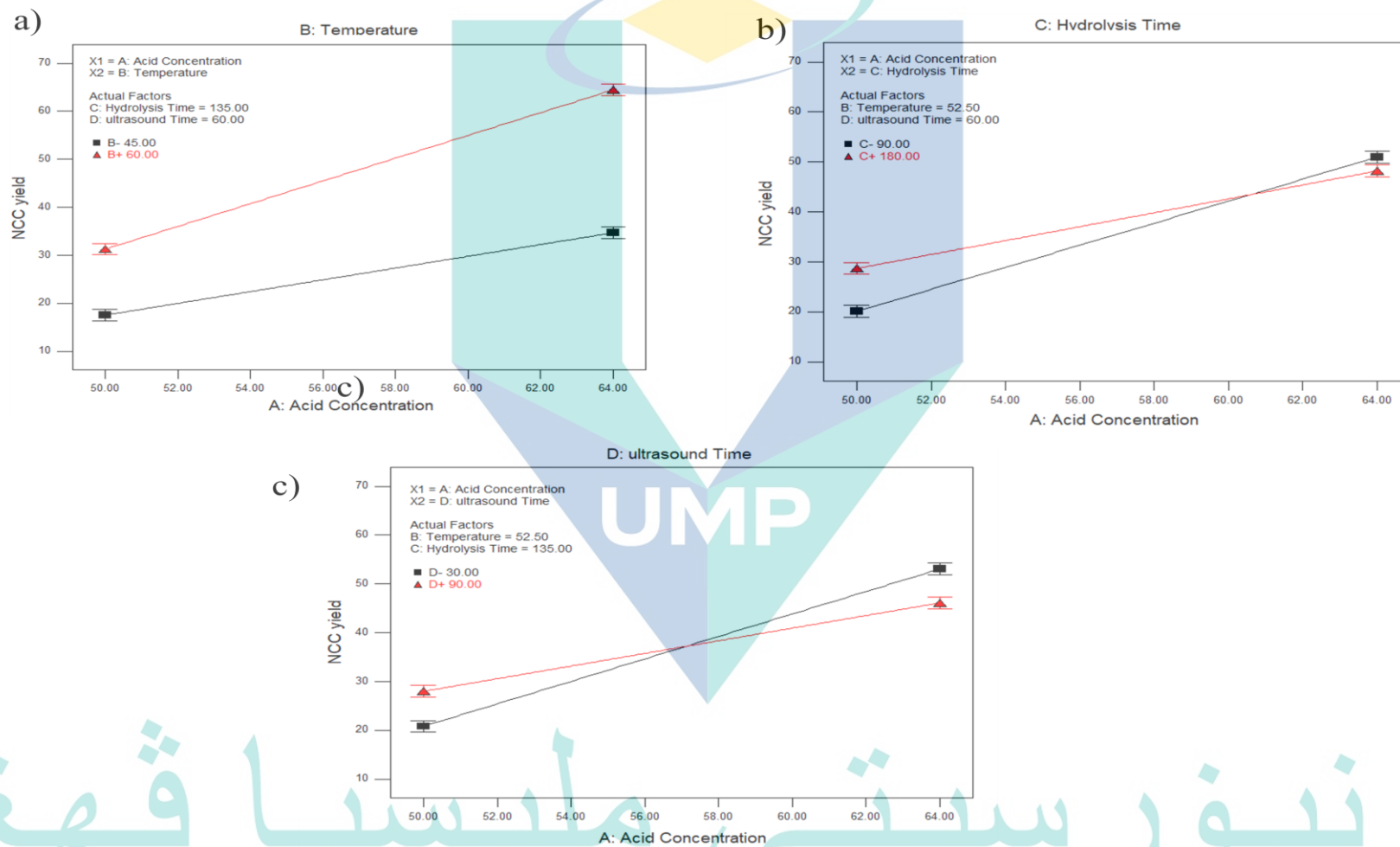
Figure 4.7   Plots of interaction effects of a)AB b)AC, c)AD, d)BD, and e)BC on NCC yield response.

4.2.3 Optimization Study of NCC Production with Central Composite Design (CCD) using Response Surface Methodology (RSM)

In optimization of NCC production yield, the factor such as Acid concentration and temperature were further investigated While, the factor that has less contribution to NCC yields such as hydrolysis time and ultrasound time were remain constant with 180min and 30min respectively. For maximizing the response (NCC production yields), the experiments were designed using the Central Composite Design (CCD) approach. The experimental yield of NCC and the standard deviations according to the factorial design are listed in Table 4.4.

4.2.3.1 Model Selection and Statistical Analysis

The process parameters for the optimization of the NCC production yield using RSM are shown in Table 4.5. The quadratic model was found to describe the relationship between acid concentration and temperature as independent (factor) variables and NCC yield as a dependent (response) variable. The cubic model was found to be aliased. The second-order polynomial model was developed to optimize the response (NCC yield) as a function of the independent variable is shown as below:

An equation in Terms of Coded Factors:

NCC yield $= 71.36862 - 7.40333A + 2.065B - 5.2975AB - 21.65552A^2 - 2.15017B^2$

Where, NCC yield is response, while the independent variable A and B are the acid concentration and temperature respectively. The terms A and B represent the main factors while AB is the interaction involved in NCC production. Apart from that, A^2 and B^2 indicate the quadratic effect.

Table 4.5   The process parameters for optimization of the NCC production yield using RSM.

Standard order	Factor		Response
	A: Acid concentration (%)	B: Temperature (°C)	NCC yield (%)
1	60.00	55.00	48.67
2	68.00	55.00	44.17
3	60.00	65.00	63.7
4	68.00	65.00	38.01
5	60.00	60.00	54.68
6	68.00	60.00	40.45
7	64.00	55.00	65.31
8	64.00	65.00	68.83
9	64.00	60.00	70.8
10	64.00	60.00	73.26
11	64.00	60.00	70.09
12	64.00	60.00	74.89
13	64.00	60.00	72.1

4.2.3.2   Analysis of variance (ANOVA)

An analysis of the variance (ANOVA) was carried out in order to determine the ''lack of fit'' and the significant effect of the independent variables on the NCC yield. The lack of fit test is a measurement of the failure of the model to represent data in the experimental region in which points were not included in the regression. The statistical significance of the regression equation can be checked by using F-values, while the p-values were used to examine the significance of each coefficient. Generally, the calculated F-value should be several times greater than the tabulated value in order to be considered as a good model. The p-values were used as a tool to evaluate the significance of the effects and the interactions among the variables. As Table 4.6 shows, the value of the F-value is 70.2460. On the other hand, the p-value for this model is < 0.0001, which indicates that there is only a 0.01% chance that the model F-value this large could occur due to noise. It is also evident from this model that the model term

affects A, AB and AA are significant in affecting the NCC production yield by having p-values (smaller than 0.05), with values of 0.0001, 0.0035, and <0.0001 respectively (Table 4.6).On the other hand, the p-values of the model term B, and BB are greater than 0.05 which indicates that they not significant.
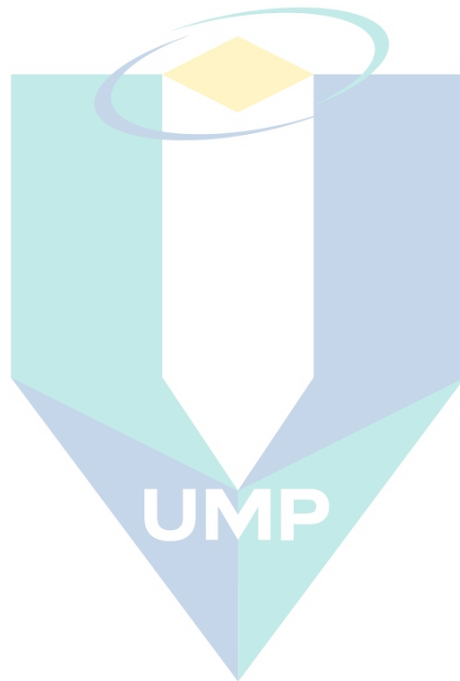
Table 4.6   Test of significance for regression coefficient

Source	Sum of Squares	df	Mean Square	F Value	p-value Prob > F	
Model	2111.3049	5	422.2609	70.2461	< 0.0001	significant
A-A	328.8560	1	328.8561	54.7075	0.0001	
B-B	25.5853	1	25.5854	4.2563	0.078	
AB	112.2540	1	112.2540	18.6742	0.0035	
A^2	1295.1855	1	1295.1856	215.4632	< 0.0001	
B^2	12.7689	1	12.7690	2.1242	0.1883	
Residual	42.0781	7	6.0112			
Lack of Fit	27.3002	3	9.1001	2.4632	0.2021	not significant
Pure Error	14.7778	4	3.6945			
Cor Total	2153.3831	12				
R-Squared	0.9805					
Pred R-Squared	0.9027					

*Values of p-values greater than 0.05 indicating the model terms are not significant.

The goodness of fit of models was estimated by the coefficient of determination (R^2), adjusted R^2, predicted R^2, coefficient of variance (CV), prediction residual error sum of squares (PRESS), and adequate precision from the ANOVA as shown in Table 4.7. It is noteworthy that the high value of R^2 indicates that the model sufficiently fits the experimental data. Furthermore, the R^2 was suggested to be more than 80% in order to have a good fitting model (Davoudpour et al., 2015). The R^2 values indicate that the fitted models accounted for a satisfactory value of 0.9805(98%), which shows a good fit between experimental and predicted values. Moreover, the Adjusted R^2 values were found to be 0.9665, which indicates that this value upholds the high significance of the model.

The coefficient of variation (CV) is the standard deviation expressed as a percentage of the mean and is determined by dividing the standard deviation by the mean value and multiplying by 100. Based on the results, the coefficients of variation for this model were found to be 4.0604% (less than10 %) which is a good fit for the selected model. As the low CV value has been obtained, it is clearly evident that a high degree of precision and good reliability of the experimental values was obtained.

The predicted R^2 in this model was found to be 0.9027 which is in reasonable agreement with the adjusted R^2. PRESS (predicted residual error sum of squares in r) value is used to provide a summary measure of the discrepancy between the data and the estimation model. The smaller the discrepancy, the better the model's estimations will be. The discrepancy is quantified in terms of the sum of squares of the residuals. The adequate precision measures the signal to noise ratio and compares the range of the predicted values at the design points to the average prediction error. The ratio greater than 4 is desirable. Thus, a ratio of 20.6773 from the results indicates an adequate signal. As such, the model can be used to navigate the design space.

Table 4.7   Statistics used to test goodness of fit of the model

p-value	< 0.0001
C.V. %	4.0605
PRESS	209.4303
R-Squared	0.9805
Adj R-Squared	0.9665
Pred R-Squared	0.9027
Adeq Precision	20.6773

4.2.3.3   Analysis of the response surface

For better graphical interpretation of the NCC production yield, the three-dimensional response surfaces are illustrated in Figure 4.8. Figure 4.8 shows a) 3D response surface and b) 2D contour plot. The 3D response and 2D contour plot demonstrates the effect of acid concentration and hydrolysis time on the NCC production yield. In general, 3D response surface plots demonstrate the effects of two variables on the response while the other variables are kept at level zero(Chen, Lee, Bee, & Hamid, 2017).

From the response surface plot shown in Figure 4.8a), NCC yield was increased until up to the optimum level and then gradually decreased with increasing hydrolysis time or temperature. The percentage of NCC production yield increases to 74% with the increase of the temperature up to 60°C. The reason may lies on more kinetically favourable during hydrolysis when more heat energy was applied and therefore, causing more removal of amorphous regions in cellulose(Chen, Lee, Bee, & Hamid, 2017). However, further increasing in temperature up to 65°C may lead into the decreasing of the NCC yield. This is probably attributed to the over-degradation of the cellulose crystalline structure by converting into glucose compounds.

Similarly, the NCC yield also increases at 74% with the increase in acid concentration up to 64%. However, when the acid concentration is more than 64%, the NCC yield decreased significantly. These results are consistent with findings reported in the literature(Fan & Li, 2012).The reason may be at higher temperature which is above 64% the cellulose were degrade into sugar molecules.

92
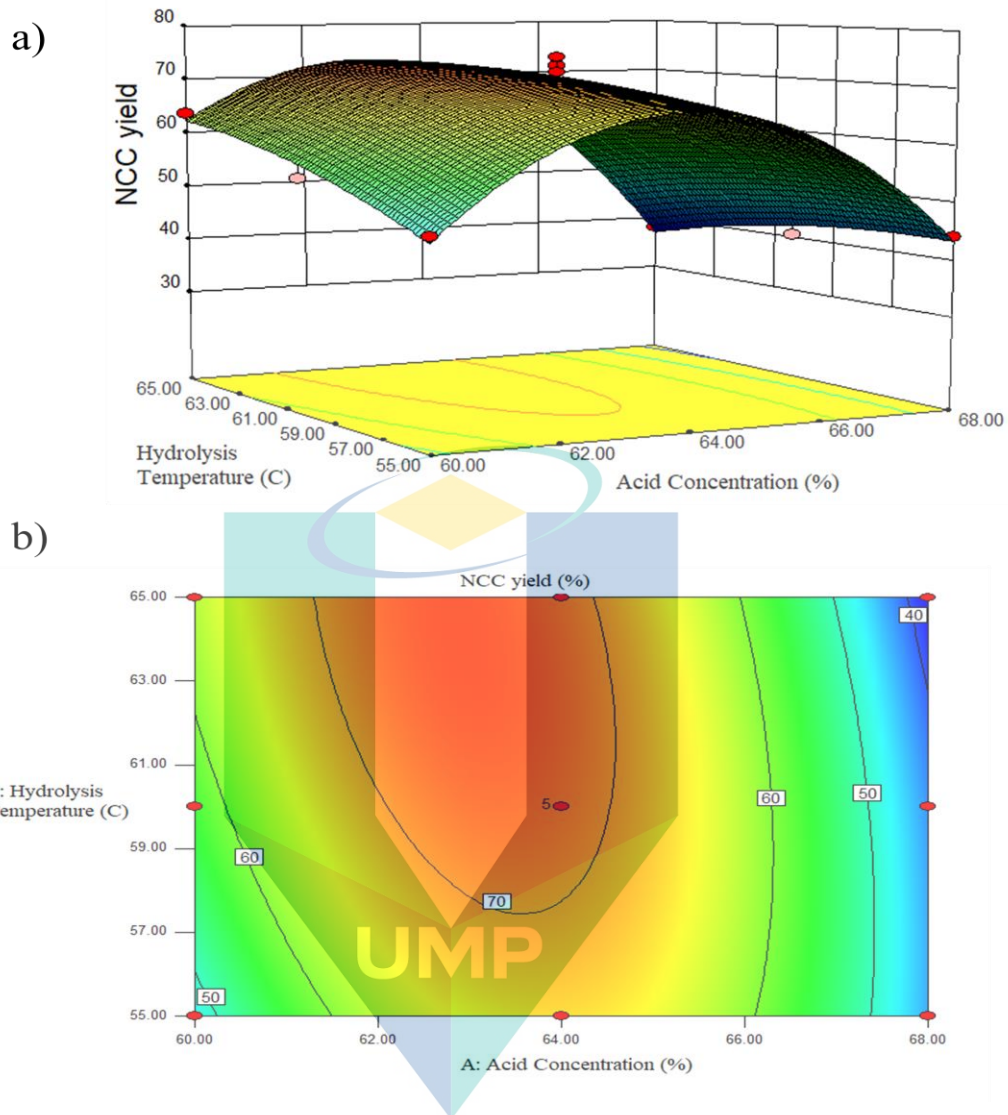
Figure 4.8   a) 3D response surface and b) contour plot.

4.2.3.4   Actual vs Predicted data

The correlation of actual conversion and values predicted by the model and normal probability plots are presented in Figure 4.9. As shown in Figure 4.9(a), the actual value and the predicted value of NCC production yield are in the range of the operating parameters, which give an indication of a well-fitted model. The normal probability plots for NCC production yield are presented in Figure 4.9(b). It is evident that a non-linear pattern of an S-shaped curve was formed which indicates the non-normality in the error term. However, this may be corrected by a transformation.
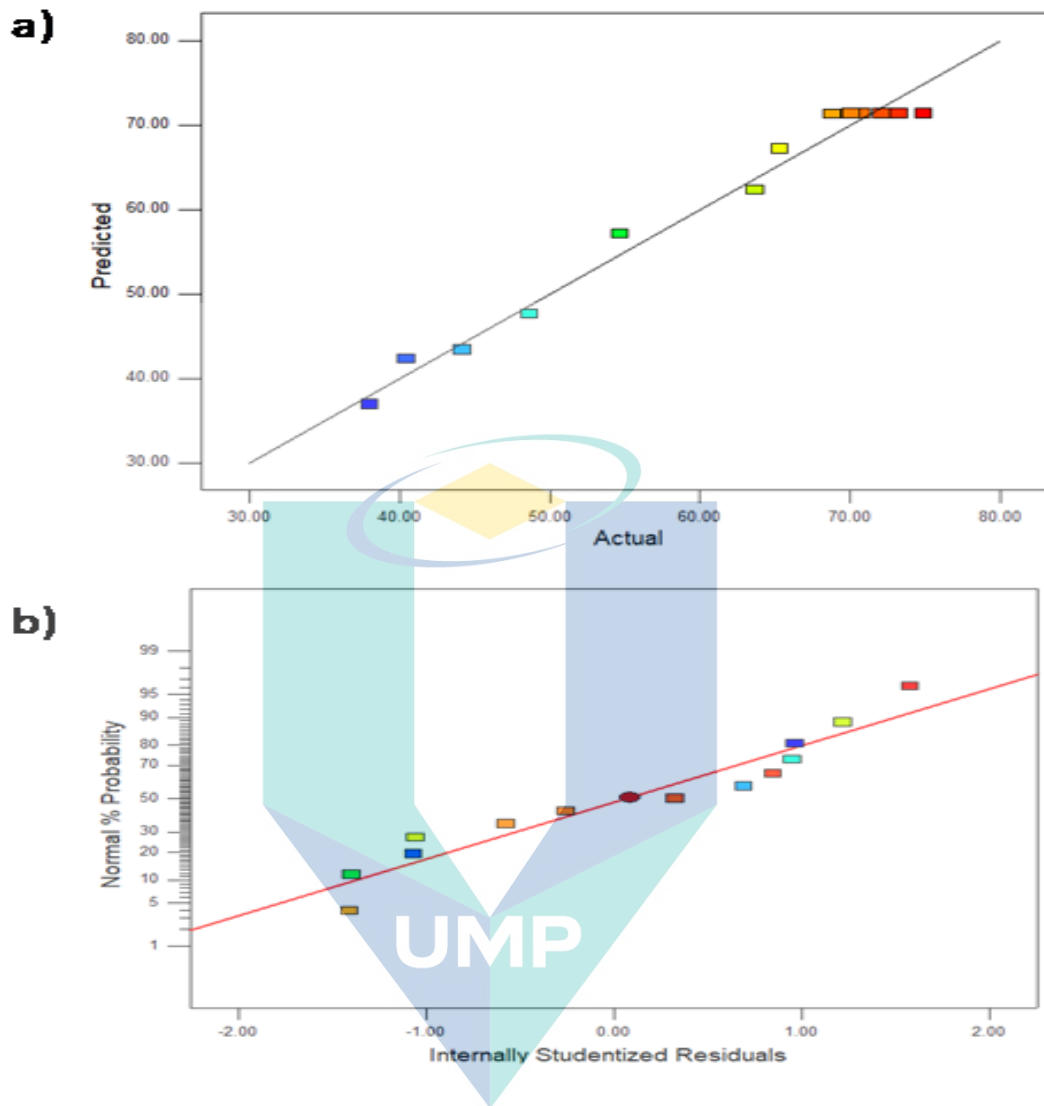
Figure 4.9   a) correlation of actual conversion and values predicted by the model and b)Normal probability plot of residuals.

4.2.3.5   Verification and Optimization of Predictive Model

In order to validate the statistical model for maximizing NCC production yield obtained by the response surface model, a validation experiment setup was performed in triplicates under optimum conditions (acid concentration and hydrolysis time). The selected parameters of acid concentration and hydrolysis time for the validation process were adjusted to 64% and 60°C respectively in order to obtain the maximum NCC production yield which is shown in Table 4.8.

Table 4.8   Optimum condition derived by RSM and adjusted Condition for
Experimental

	Factor			
A: Acid concentration	Adjusted factor A	B: Temperature		Desirability
63.92	64	60		0.954429

Table 4.9 shows the validation of Model equation (Parameter A: Acid
Concentration and B: temperature). The experimental NCC yields are 75.45%, 74.29%,
and 75.01 respectively. The percentage error for the experiments was calculated from
the predicted NCC production yield value of 73.2094%and the one obtained
experimentally. The percentage errors are 3.06 %, 1.47 % and 2.46 %, respectively.
After validation, it can be concluded that the experimental values of the NCC
production yield were reasonably close to the predicted values. Furthermore, the
predicted and the experimental results are in good agreement, with an error of less than
5% demonstrating the validity of the model.

Table 4.9   Validation of Model equation (Parameter A: Acid Concentration and B:
temperature

No	Parameter		Predicted	Experimental	Error
	A: Acid Concentration	B: Temperature			
1	64	60	73.2094	75.450	3.061
2	64	60	73.2094	74.288	1.473
3	64	60	73.2094	75.01	2.460

4.3 Modification of NCC

4.3.1 Chemical structure of MNCC

The FTIR analysis was used to investigate the chemical structures of NCC and the modified NCC (MNCC) using different concentrations of HBPE. The FTIR spectra of NCC, 0.1MNCC, 0.3MNCC, and 0.5MNCC are illustrated in Figure 4.10.
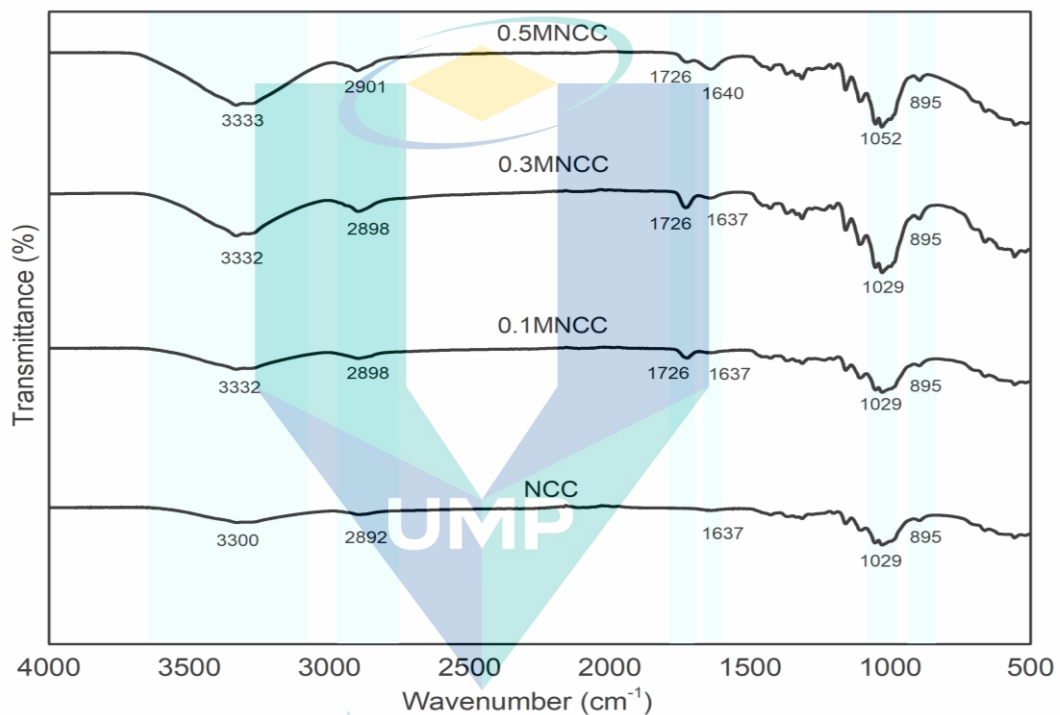
Figure 4.10   Chemical structure of NCC, 0.1MNCC, 0.3MNCC and 0.5MNCC.

The characteristic absorption peaks at 3300 cm-1, 2892 cm-1, 1637 cm-1, 1029, and 895 cm-1 in the spectra of NCC is associated with the native cellulose. Notably, there is an increase in broad absorption in the spectra of all modified NCC samples at 3333 cm-1 in. This is an indication of possible hydrogen bonding between the –OH groups present on the surface of NCC and molecules of the HBPE. This would lead to the adsorption of hydroxyl groups (Mahdavi and Shahalizade, 2015). As stated, the surface of NCC can be modified by physical interactions of Hyperbranched Polyesters via electrostatic adsorption or hydrogen-bonding interaction or Van Der Walls forces. The possible interaction mechanism of NCC and HBPE is schematically illustrated in Figure 4.11. Generally, the modification of NCC resulted in non-covalent interaction

96

between HBPE and NCC which is accrued to attractive physical interactions. The large abundance of –OH branch ends in the HBPE structure might have helped to facilitate strong H-bond interactions between the hydroxyl group of HBPE and NCC.

Another absorption peak can be seen in the spectra of neat NCC at 2892 cm^{-1}. The intensity of this peak is low but it seemed to consistently increase with increasing concentrations of HBPE. This is an indication of increasing C-H stretching. It is noteworthy that the absorption peak which appeared at 1726 cm^{-1} in the spectra of 0.1MNCC, 0.3MNCC, and 0.5MNCC is absent in the spectra of neat NCC. This peak is an attribute of C=O stretching of the ester groups, and it is an indication of the contributions from the HBPE (Dadkhah Tehrani and Basiryan, 2015). On the other hand, the peak at 1637 cm^{-1} in the spectra of all NCC and the MNCC samples is associated with adsorbed surface water.
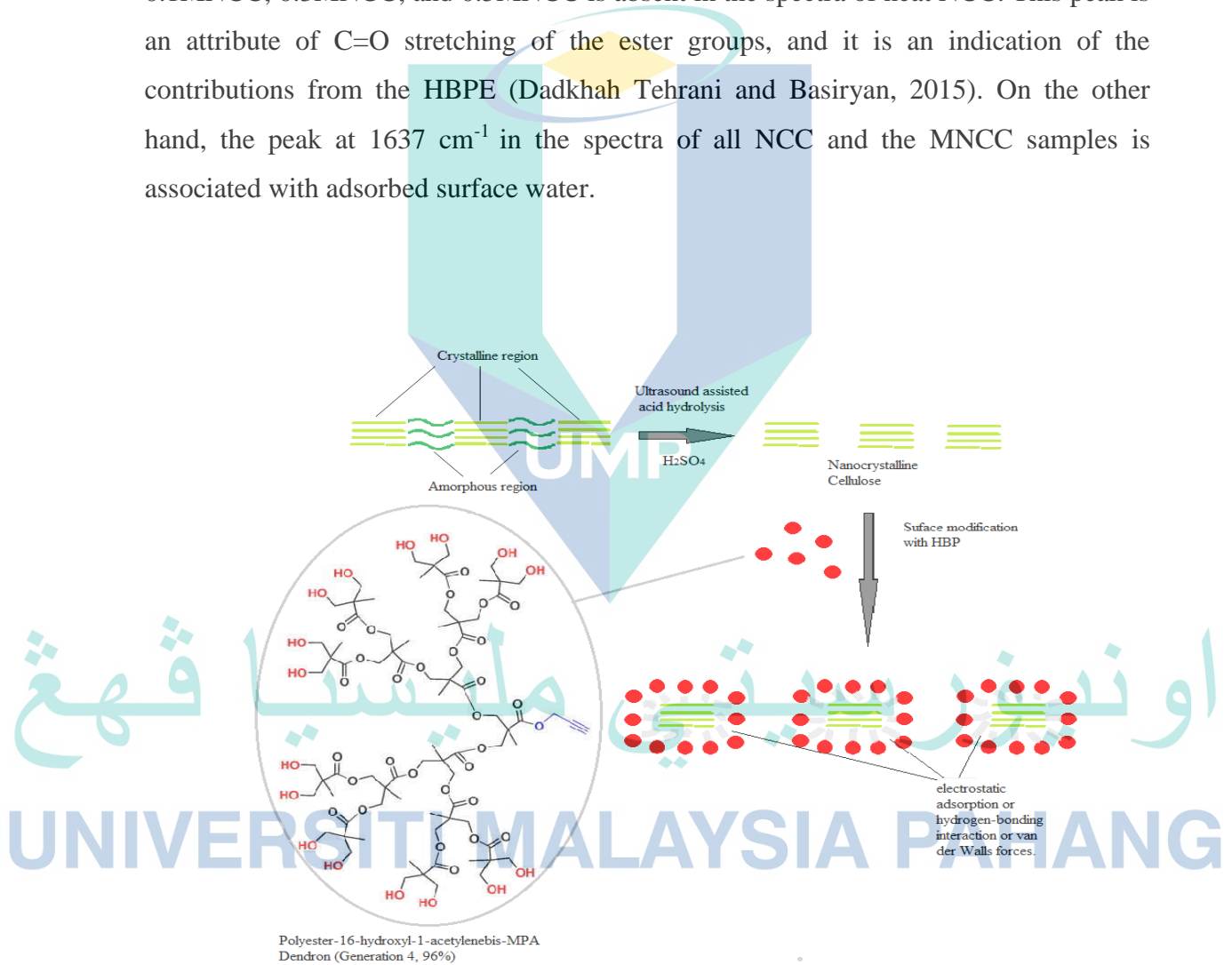
Figure 4.11   Proposed schematic attachment of HBPE on the surface of NCC.

4.3.2 Crystallinity of MNCC

The X-ray diffraction patterns of neat NCC, 0.1MNCC, 0.3MNCC, and 0.5MNCC are illustrated in Figure 4.12. It is obvious from the figure that the crystalline peaks observed in the diffraction patterns are similar for neat NCC and MNCC regardless of the concentration of HBPE used. This is an indication that the modification of NCC by Hyperbranched Polyester does not significantly alter the microstructure of NCC. Therefore, it can be inferred that the incorporation of HBPE only modified the surface of NCC, without necessarily disrupting its chemical structure. Specifically, the X-ray diffraction pattern exhibits diffraction peaks around 14.97° 22.5° and 34.24º, which are assigned to (1 0 1) and (0 0 2) planes of cellulose type I. Notably, this is similar to the cellulose nanofibers which confirms that NCC retained its crystalline even after modification using HBPE.
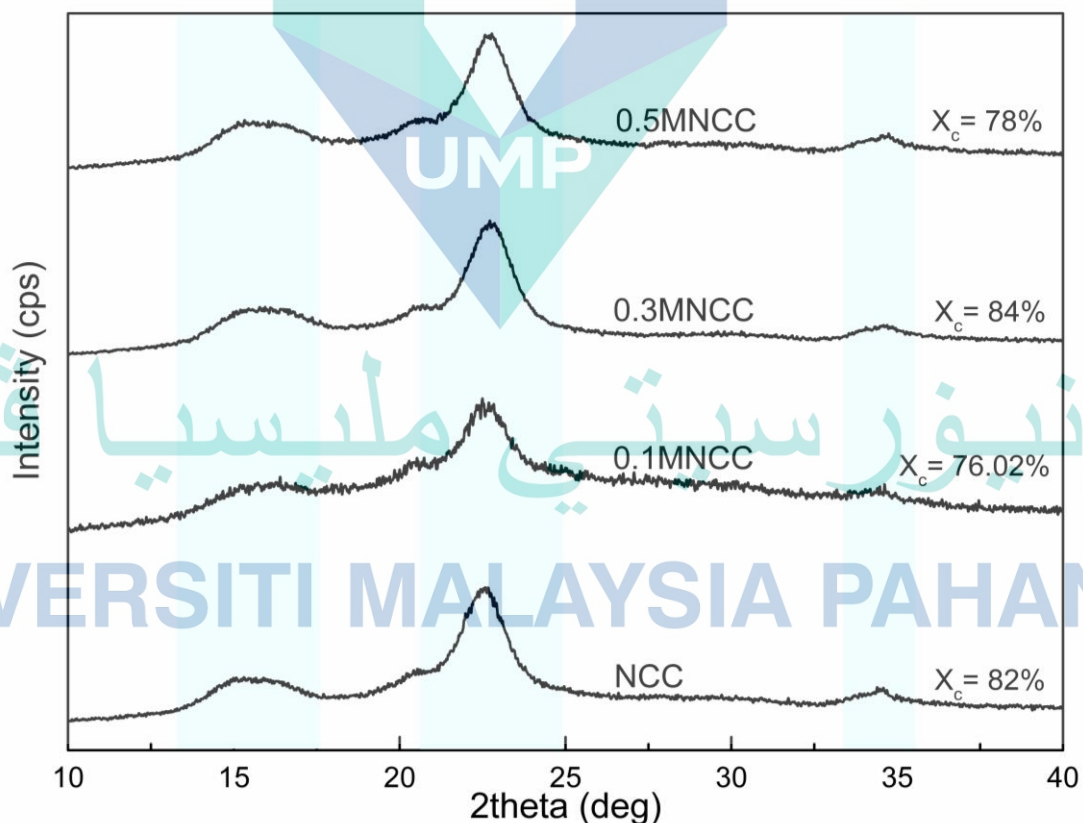
Figure 4.12   X-ray diffraction pattern of NCC, 0.1MNCC, 0.3MNCC and 0.5MNCC

It is expected that the crystallinity index will be increased after the modification of NCC. However, the result shows that only 0.3MNCC posses the highest crystallinity index with 84% compared to 0.1MNCC and 0.5MNCC with 76.02% and 78% respectively. This can be attributed to the fact that the increase in the concentration of the hyperbranched group into the NCC surface leads to an increase in the steric hindrance which directly influences the crystallization process of NCC. However, beyond the optimum concentration which in this study is 0.3%, the excessive concentration of hyperbranched HBPE led to a decrease in the crystallinity of the NCC perhaps due to possible interference with the nucleation effects of the NCC particles. Therefore, it can be inferred that 0.3% HBPE is the optimum concentration to enhance the crystallinity of NCC.

4.3.3 Thermal stability of MNCC

The thermogravimetric (TGA) and derivative thermal gravimetric (DTG) curves of NCC, 0.1MNCC, 0.3MNCC, and 0.5MNCC are illustrated in Figure 4.13. On the other hand, the moisture content, initial decomposition temperature (T_{onset}), maximum temperature (T_{max}), residue content, of NCC, 0.1MNCC, 0.3MNCC, and 0.5MNCC are summarized in the Table 4.10. Generally, the TGA curve showed a single degradation step and maximum degradation in a narrow range. The gradual loss of mass (less than 10%) at the initial heating, below 100 °C of the NCC, 0.1MNCC, 0.3MNCC and 0.5MNCC samples is attributed to the loss of adsorbed moisture.

As illustrated in Figure 4.13, all the samples started to decompose at temperatures above 300°C with an initial decomposition peak temperature (T_{onset}) of 348.36°C, 324.31°C, 341.45°C, and 331.13°C respectively for NCC, 0.1MNCC, 0.3MNCC, and 0.5MNCC respectively. Notably, NCC exhibits a high T_{onset} due to the complete removal of hemicellulose and other non-cellulosic components during the ultrasound-assisted hydrolysis process. During this process, the chemical treatments attack the amorphous region in the cellulose and increase the degree of crystallinity. Therefore, higher crystallinity values obtained by NCC resulted in greater resistance towards heat and as the result increase the maximum temperature for thermal degradation This might have helped to increase the compactness of the cellulose components, thereby increasing its thermal stability.
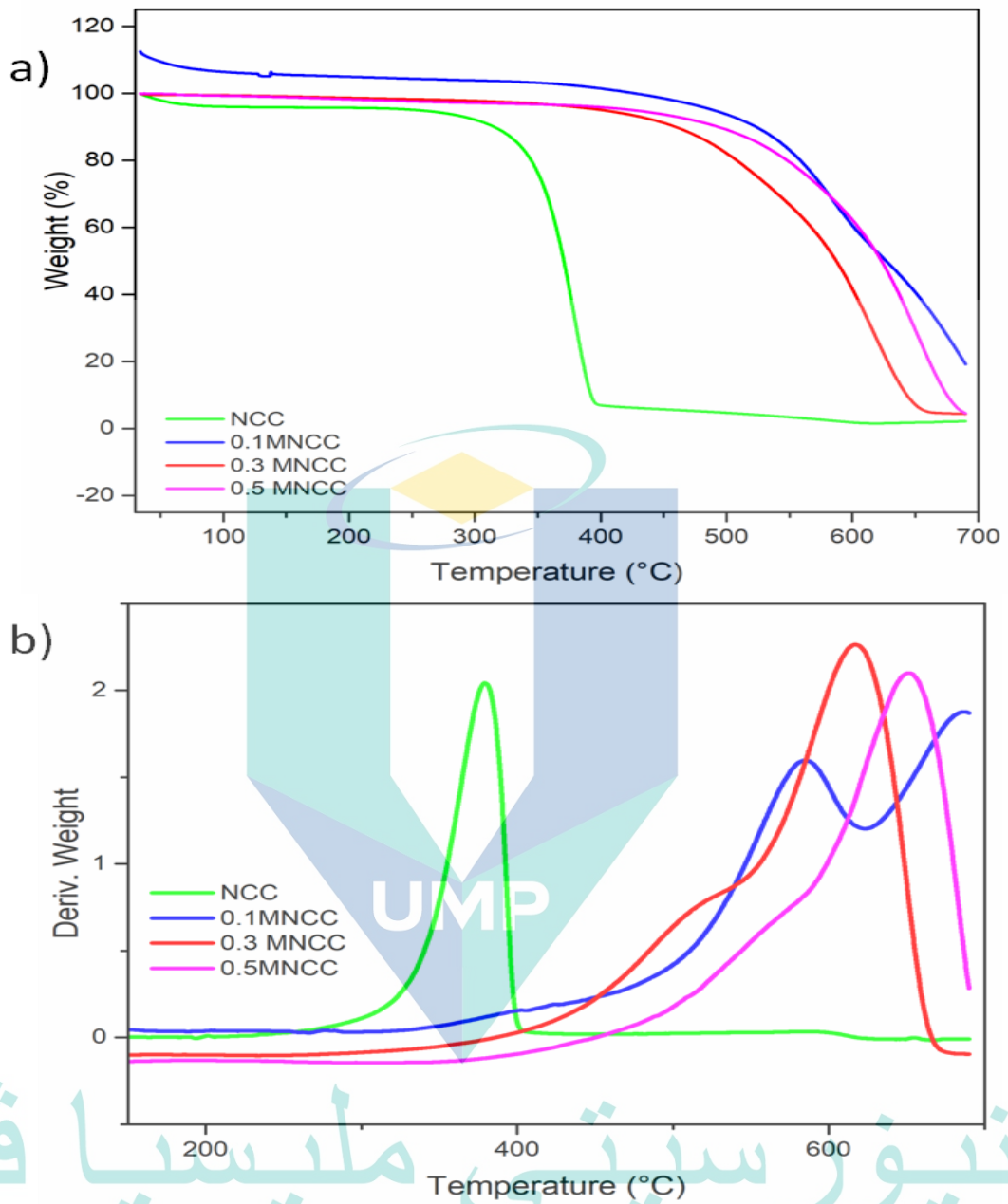
Figure 4.13   TGA and DTG thermograms of NCC, 0.1MNCC, 0.3MNCC, and 0.5MNCC.

It is noteworthy that the modification of NCC using HBPE influenced the thermal stability of MNCC. Specifically, the 0.1MNCC and 0.5MNCC samples decompose at a lower temperature, compared to neat NCC. These materials have lower thermal stability compared to the NCC due to the disruption of the cellulose crystalline structures in modified cellulose derivatives. In the case of 0.1MNCC, the low amount of HBPE might create sites for penetration of heat due to poor interaction with NCC. On the other hand, 0.5 MNCC also exhibit low thermal stability. The explanation for this might be the disruption of the hydrogen bonding of the hydroxyl units in HBPE. Therefore, this can lead to poor thermal stability due to the very low thermal stability of HBPE. The summary of the thermal properties of the samples is presented in Table 4.10. Notably, the T_{max} of 0.3MNCC appeared to be higher than the T_{max} of NCC suggests sufficient interaction between NCC and the abundance of –OH group in the terminal groups of the HBPE. This might have facilitated strong bonds such that the sample becomes more thermally stable and less susceptible to heat. The slight increase of thermal stability in modified NCC in comparison with NCC indicates the physical functionalization of HBPE on NCC by forming H-bonds.

Table 4.10   The moisture content, initial decomposition temperature (T_{onset}), degradation temperature (T_{max}), and ash content of NCC, 0.1MNCC, 0.3MNCC, and 0.5MNCC.

Sample	Moisture content (%)	Degradation temperature (°C)		Ash content (%)
		T_{onset}	T_{max}	
NCC	4.215	348.36	378.00	2.196
0.1Mod NCC	7.818	324.31	366.37	3.606
0.3MNCC	5.284	341.45	388.98	3.658
0.5MNCC	2.883	331.13	368.37	3.392

4.4 Preparation and Characterization of PVA/NCC hydrogel

4.4.1 Fourier Transforms Infrared Spectroscopy (FTIR)

The FTIR spectra of neat PVA neat, PVA/3NCC, PVA/5NCC, and PVA/7NCC hydrogels are illustrated in Figure 4.14. As can be seen in the Figure 4.14, an adsorption band associate with strong hydroxyl groups (–OH) appeared around $3290 cm^{-1}$ in the spectra of neat PVA. The hydrogen bonding between –OH groups can occur among PVA chains due to high hydrophilic forces (Jayaramudu et al., 2018). However, this band can be seen to significantly decrease in the spectra of PVA/3NCC, PVA/5NCC, and PVA 7NCC, as the NCC concentration in PVA hydrogel increased. All these changes can be explained by the interaction of hydroxyl group on the NCC with OH groups of hydrophilic polymer, therefore the OH group of NCC would be decreased in the spectrum of nanocomposites (Ng et al., 2017). Another reason may correspond to the inter molecular hydrogen-bonded between PVA and NCC during the freeze-thawing process which shows that NCC and PVA are well-interacted(Jayaramudu et al., 2018).
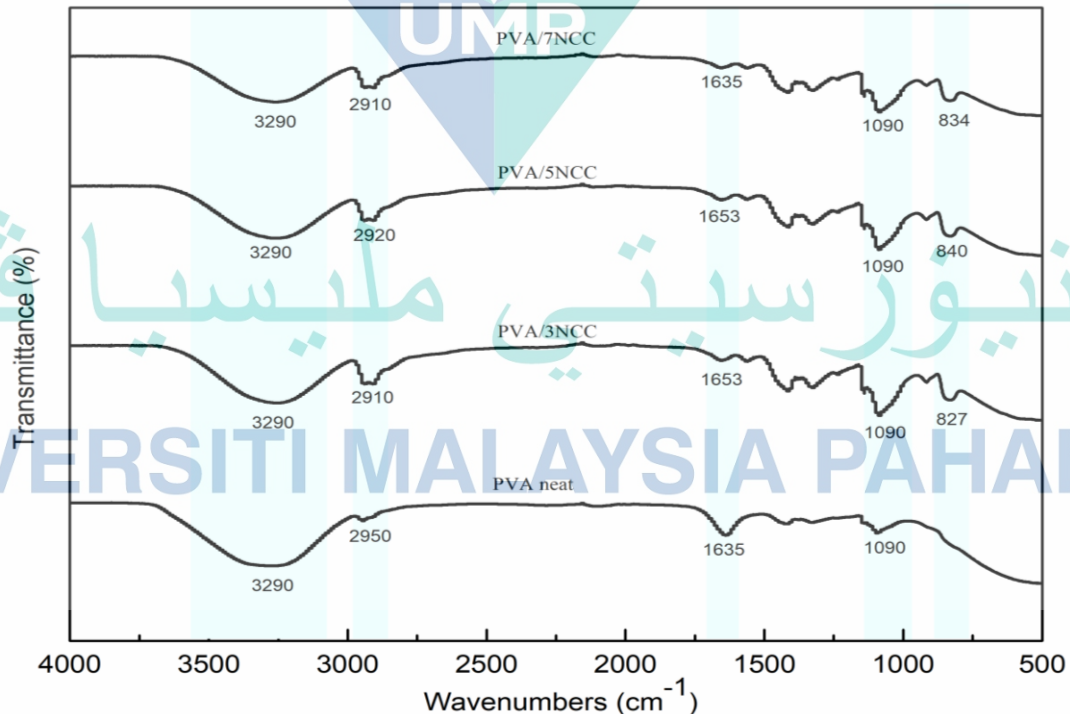

Figure 4.14   FTIR spectra of neat PVA, PVA/3NCC, PVA/5NCC, and PVA/7NCC hydrogel.

Some of the other notable peaks common to all the samples include the absorption peak at 2910cm^{-1} to 2950cm^{-1}which is attributed to the C-H stretching associated with methylene groups in cellulose. It clearly shows these the absorption peaks (2910cm^{-1} to 2950cm^{-1}) associated with freeze-thawed of PVA hydrogel (Kenawy, Kamoun, El-meligy, & Mohy, 2014).On the other hand, the peaks at 1635.78cm^{-1}, 1653.26cm^{-1}, 1653.27cm^{-1}, and 1635.80cm^{-1} represent the absorbed water and the presence of carboxylate groups(Lamaming et al., 2015).As such,this peak has been used as an indicator for PVA structure, due to its semi-crystalline synthetic biopolymer which able to form some domains (Kenawy et al., 2014). Another peak observed for all the hydrogel around 1090 cm^{-1}is attributed to CO stretching. In addition, a sharp absorption peak can be seen for PVA/3NCC, PVA/5NCC, and PVA/7NCC at a wavenumber of 827cm^{-1}, 840cm^{-1},and 834cm^{-1} respectively. This can be associated with the properties of the incorporated NCC.As there are similar peaks observed for PVA neat and PVA/NCC hydrogel, it can be concluded that there is no chemical interaction among them. It can then be inferred that PVA and NCC have a physical interaction with the forming of hydrogen bonding. The chains of PVA, and NCC were just physically entangled to form the networks.

4.4.2 Gel fraction

The gel fraction of PVA/NCC hydrogels with different concentrations of NCC is shown in Figure 4.15.It is observed that the gel fraction or cross-link density of the PVA/NCC hydrogels increases with the increase in the concentration of NCC. This can be attributed to the higher density of NCC at higher concentrations and as a result decrease in the crosslinking density of the PVA hydrogel network. This behaviour can be attributed to NCC content in PVA hydrogel might reduce the entanglement reaction and consequently, the gelation process is reduced(Kamoun, Kenawy, Tamer, El-Meligy, & Mohy Eldin, 2015).During the freezing process, PVA, and NCC were promoted to combine into the chains packing. Their molecular chains could associate more compactly to form the physically crosslinked chains packing with the increase of the freeze/thaw cycles.

104
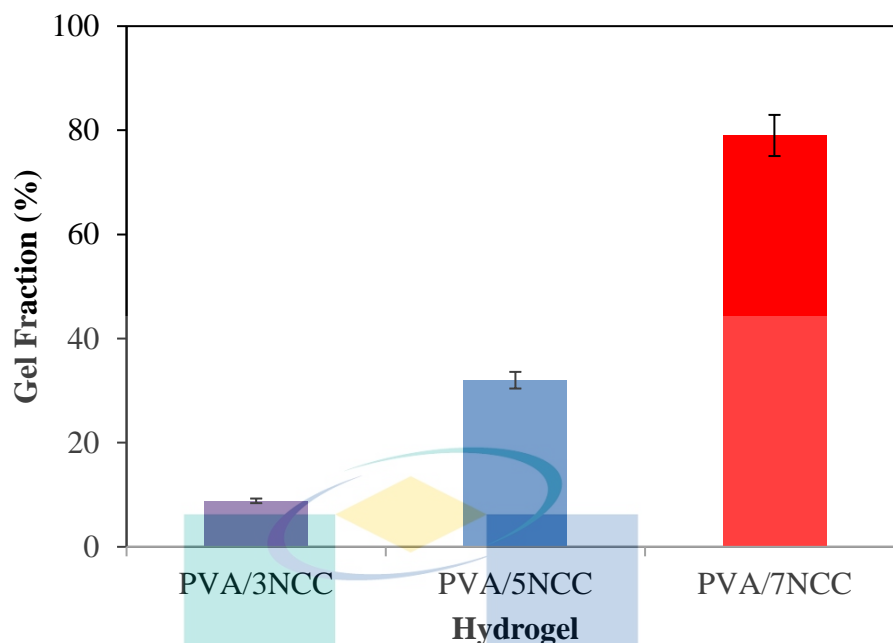
Figure 4.15 Gel Fraction of PVA/3NCC, PVA/5NCC, and PVA/7NCC hydrogel.

In essence, this observed trend of increasing gel fraction with increasing concentrations of NCC might be due to the formation of more NCC occupied in PVA hydrogel and as a result, forming more cross-linking in the blend hydrogel.

4.4.3   Equilibrium degree of swelling and equilibrium water content

Swelling is a result of the balance between two forces. The first one is the osmotic force from covalent or non-covalent bonding within the hydrogel, and the second is a dispersing force. Osmotic forces push water into the polymer network whereas dispersing forces, exerted by polymer chains, resist it. Normally, increased cross-link density enhances the dispersive force. Therefore, increasing the cross-link density within a limited scope allows free water to enter the vacant spaces of the network. However, beyond a certain limit, it decreases with increasing cross-linking. As such, swelling is an indication of cross-linking within a hydrogel. In order to investigate the incorporation of NCC in the PVA hydrogel, the NCC with concentration of 3%, 5%, and 7% were incorporated into PVA.

105
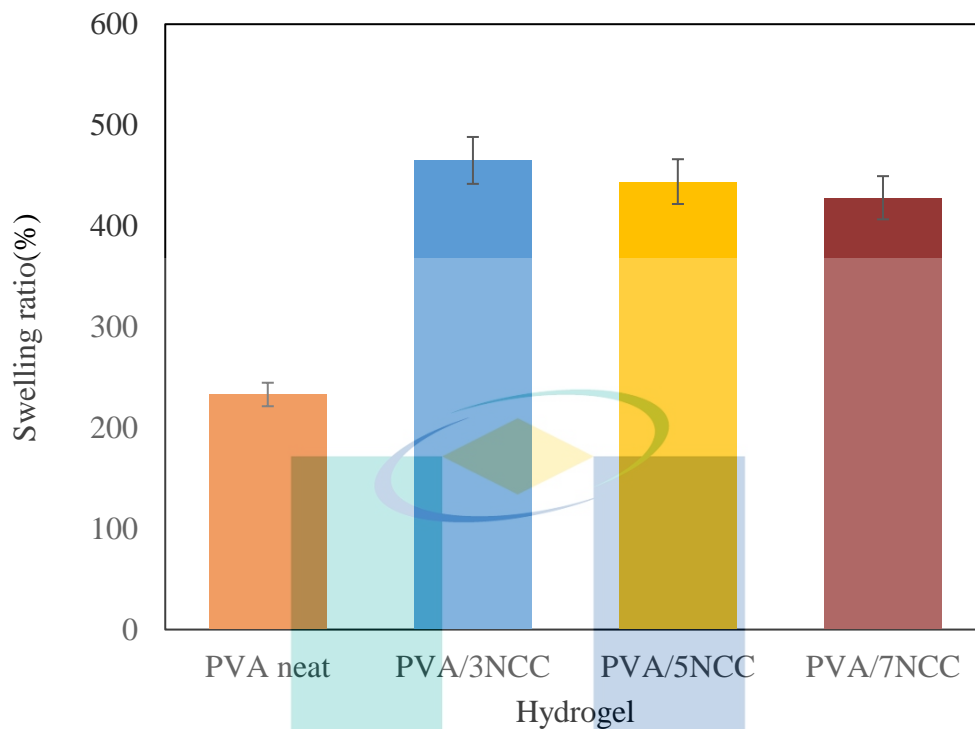
Figure 4.16   The swelling ratio of neat PVA, PVA/3NCC, PVA/5NCC, and PVA/7NCC hydrogel.

As can be seen in Figure 4.16, the swelling ratio increased with the initial incorporation of 3NCC, Therefore, it is expected that hydroxyl group of NCC are cross-linked with hydroxyl groups of PVA by hydrogen bonding, resulting in a decrease in crystallite formation. A decrease in the crystallite formation increases the free volume for water uptake. In addition, hydrophilic groups in NCC may cause the hydrogel to combine with more water molecules by forming hydrogen bonds(Khan, Zhang, & Guo, 2016). However, as the concentration of NCC was further increased in the PVA hydrogel, the swelling ratio of PVA/5NCC and PVA/7NCC were noticed to decreased with 444% and 428% respectively. Another result maybe that the maximum swelling ability increases with an increase in the NCC content in PVA hydrogel up to a certain limit of swelling, then the hydrogel structure was destructed. Another explanation can be due to the reduced space for small molecules to occupy and a longer distance for PVA chains to penetrate into the pore spaces, which leads to a smaller swelling degree.(Jimena Soledad Gonzalez & Alvarez, 2011).

Obviously, the swelling ratio of neat PVA is lower compared to the NCC incorporated PVA hydrogels. This might be due to the hydrophilic characteristic of NCC, which improved the wettability and hydrophilicity of the PVA hydrogel. It is worthy of note that although the PVA/7NCC hydrogel has the highest gel fraction as confirmed in the previous section, it possesses a lower swelling ratio compared to PVA/3 NCC and PVA/5NCC. This observation confirms with the fact that gel fraction or cross-link density is related to swelling ratio. Generally, the swelling behavior of PVA hydrogel is closely related to the cross-linkage of PVA molecules. The increased swelling capability usually accompanies a decrease of cross-linkage. However, the case could be changed, particularly when the hydrogels are reinforced by some nanofillers. However, beyond a certain limit, it can disrupt the smooth flow of water molecules into the hydrogel. Therefore, the low amount of water retained within the hydrogel might be insufficient to facilitate large swelling.

4.4.4 TGA analysis

The TGA and DTG curves of neat PVA, PVA/3NCC, PVA/5NCC, and PVA/7NCC hydrogels are illustrated in Figure 4.17. As for the neat PVA hydrogel, there degradation stages can be observed in the DTG derivative curve which corresponds to the water loss, thermal degradation of crystalline PVA, and sub-products due to the detachment of lateral groups forming water, acetic acid, and acetaldehyde (Gonzalez et al., 2014a).
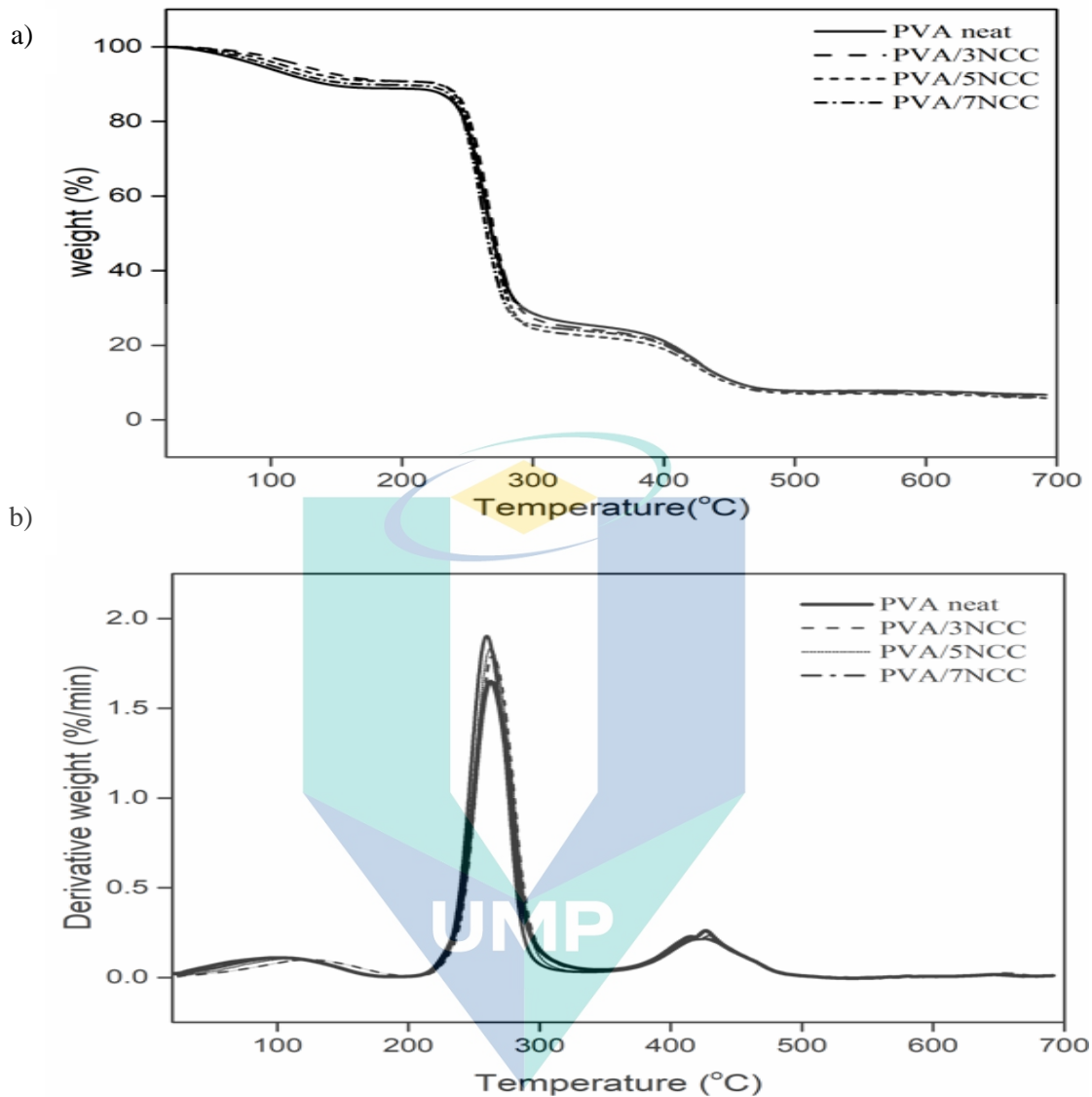
Figure 4.17   TGA (a) and DTG derivatives (b) of neat PVA, PVA/3NCC, PVA/5NCC, and PVA/7NCC hydrogel.

The incorporation of NCC into PVA hydrogel acts as a thermal barrier due to the formation of hydrogen bonds between NCC and PVA hydrogel. Based on the DTG curves, it is evident that the degradation of all hydrogel samples possesses several stages of weight-loss. This could be due to different factors such as water evaporation and hydrogel degradation. Specifically, the weight loss below 100∘C for all the hydrogel samples can be attributed to the release of adsorbed moisture from the hydrogels. Then, the second degradation stage can be associated with thermal degradation of crystalline PVA. It is noteworthy that the incorporation of NCC into the

PVA hydrogel produced a slight right shift in the degradation temperature compared to the neat PVA as summarized in Table 4.11.This suggested that the thermal stability of the PVA/NCC hydrogels was slightly improved compared to neat PVA. However, it is noteworthy that the onset of degradation temperature of the PVA/5NCC hydrogel was slightly decreased perhaps due to the influence of the thermal behavior of cellulose (W. Li et al., 2012).

Generally, the amounts of char residue of all PVA/NCC hydrogel samples are slightly lower compared to PVA neat. On the overall, the result of this thermal analysis indicates that the incorporation of NCC in PVA hydrogel offered slight influence on the thermal stability of the PVA hydrogel. Therefore, it can be inferred that the thermal stability of PVA hydrogels can be influenced by the incorporation of NCC due to the possible formation of hydrogen bonds between NCC and PVA. The formation of bonds between these polymers would invariably lead to improved thermal stability.
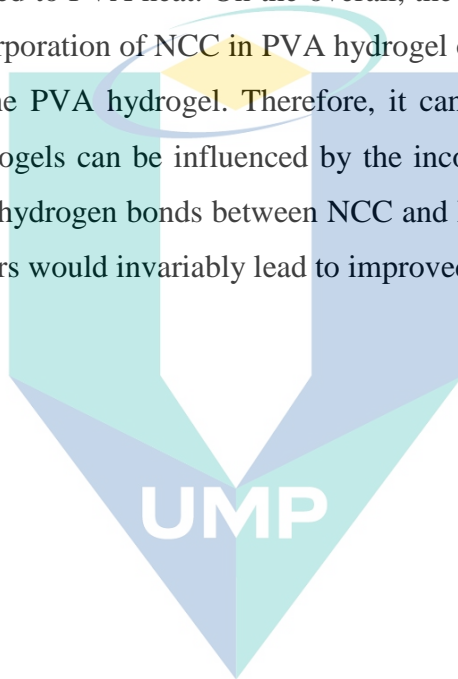
Table 4.11   Onset temperature(T_{onset}), degradation temperature (T_{max}), and ash content of PVA neat, PVA/3NCC, PVA/5NCC, and PVA/7NCC hydrogel.

Sample	First degradation		Second degradation		Third decomposition		Ash content
	T_{onset} (°C)	T_{max} (°C)	T_{onset} (°C)	T_{max} (°C)	T_{onset} (°C)	T_{max}(°C)	(%)
PVA neat	75.95	99.42	243.56	261.04	414.54	426.2	426.2
PVA/3NCC	66.73	93.81	250.75	264.93	428.18	428.36	428.36
PVA/5NCC	62.92	104.38	246.88	263.11	424.77	429.7	429.7
PVA/7NCC	60.87	118.45	254.16	260.65	459.14	433.2	433.2

4.4.5 Compression properties

In order to study the effect of NCC on the PVA hydrogel matrix, the neat PVA, and NCC incorporated PVA hydrogel samples were further subjected to a mechanical testing.The mechanical property of PVA hydrogels is important which can affect their actual applications. PVA/NCC hydrogels cannot be broken and hence the samples were more subjected to compression strength. The compressive strength of hydrogels is essential mechanical property in load-bearing applications. Figure 4.18 shows the compressive stress-strain curves of physically cross-linked neat PVA, PVA/3NCC, PVA/5NCC, and PVA/7NCC hydrogels.
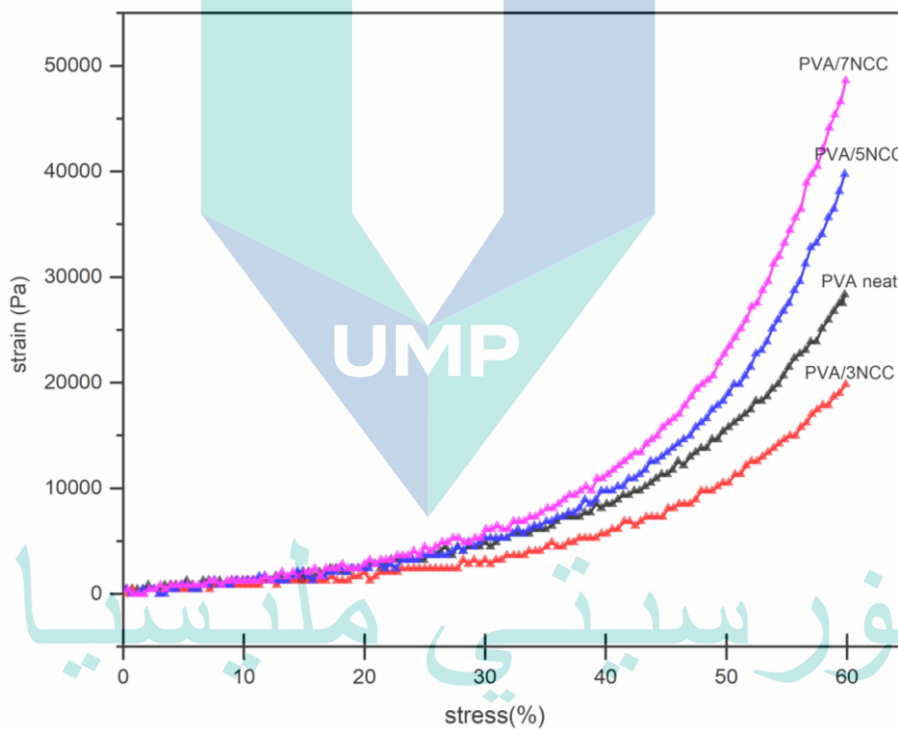
Figure 4.18   Compressive stress-strain curve of physically cross-linked neat PVA, PVA/3NCC, PVA/5NCC, and PVA/7NCC hydrogels.

As shown in the Figure 4.18, the compressive properties of all the hydrogels exhibit non-linear and viscoelastic behaviour. It is clearly seen that the addition of NCC into PVA hydrogel improved the compressive strength of the PVA hydrogel. However, the compressive strength of PVA/ 3NCC was found to be lower by 19835Pa compare to PVA neat (27521PA). This is consistent from the previous result obtained by swelling

ratio whereas the PVA/3NCC exhibit higher swelling ratio among PVA/NCC hydrogels. The reason is that the compressive strength can be further decreased by increasing the water content in PVA/NCC hydrogel. Another reason of this perhaps that the agglomeration nature of NCC form a non-uniformly distributed into PVA hydrogel which destruct the hydrogen bond interaction between hydroxyl group of NCC and PVA hydrogel and as a result, giving lower compression strengththan the PVA neat.

It is worth noting that the PVA/7NCC hydrogel presented the highest compressive stress by 50000pa which is much higher than PVA neat hydrogel. The presence of NCC formed the bonding force of hydrogen bonding on the intra- and inter-PVA polymer chains and the stability of the crystalline particles are enhanced with the increase of NCC content. Further explanation is that the improved compression property was the result of well dispersed of NCC into PVA hydrogel and the improvement in the interfacial bonding by interaction of the hydroxyl group of NCC and the free hydroxyl group in PVA molecules that are linked together to form the hydrogen bond.

Another reason may be attributed to the higher crosslink density in the PVA hydrogels at higher NCC concentration. This would result in higher stiff chains in the strong pore walls. Interestingly, this observation is consistent with what was previously reported in the literature (De France et al., 2017). Specifically, it was stated that the incorporation of NCC offered improved mechanical properties through increased modulus, crack prevention, and shape recovery. Besides, it is evident from this study that hydrogels with higher crosslink density possess higher compressive strength as well as excellent compression resistance capability compared to hydrogels with lower crosslink density.

On the other hand, the compressive strength is consistent with the result of the equilibrium swelling ratio. As discussed earlier, PVA/7NCC possesses lower swelling ratio due to the increase in NCC concentration which resulted in more compact network structure and less space in the PVA polymeric matrix to accommodate water. Therefore, the observations from these two analysis provide some support for the conceptual fact that highly crosslinked structure could increase the stiffness of the hydrogels as well prevent the release of water from the hydrogels during the compressive testing. As such, it can be inferred that the incorporation of NCC into PVA hydrogels affects the

cross-linking density and PVA hydrogel networks thereby producing a significant effect on the mechanical properties. Based on this understanding that the structural performance of PVA and PVA/NCC hydrogels can be influenced by NCC concentration, and other factors such as structural composition and mechanical properties of PVA hydrogel, and the incorporation of NCC into PVA hydrogels, NCC incorporated PVA hydrogels may be tailored to attain the properties required for various hydrogel applications.

4.4.6 Comparative characterization of REFB, PEFB, NCC, and modified (NCC) in PVA hydrogel

4.4.6.1 Macroscopic appearance

A digital image of the macroscopic appearance of neat PVA, PVA/REFB, PVA/PEFB, PVA/NCC, and PVA/MNCC hydrogels are presented in Figure 4.19. It can be seen from the Figure 4.19that the appearance of neat PVA hydrogel is opaque and white. This is due to the formation of PVA hydrogel by repetition of freeze thawing cycles. As the REFB were incorporated in the PVA hydrogel, dark spots can be seen in the PVA hydrogel which appeared milky. This is might be the present of the lignin content in Raw Efb. On the other hand, cloudy and non-uniformity can be seen in the PVA/PEFB hydrogel. This suggests that the PEFB was not macroscopically homogeneous in the PVA hydrogel matrix perhaps due to the agglomeration of PEFB in the PVA solution. In contrast, when NCC was incorporated into the PVA hydrogel, the NCC seems to be homogeneous in the PVA network and it is less transparent and cloudy perhaps due to the hydrophilic nature of NCC. Interestingly, following the incorporation of MNCC into the PVA hydrogel, there is a significant improvement in the homogeneity of the hydrogel compared to NCC incorporated hydrogel. This is due to more hydroxyl group on the Modified NCC, therefore more compatible with PVA hydrogel. This indicates that the incorporation of REFB, PEFB, NCC, and MNCC presents significant differences in the appearance, transparency, and the homogeneity of PVA hydrogel.

113
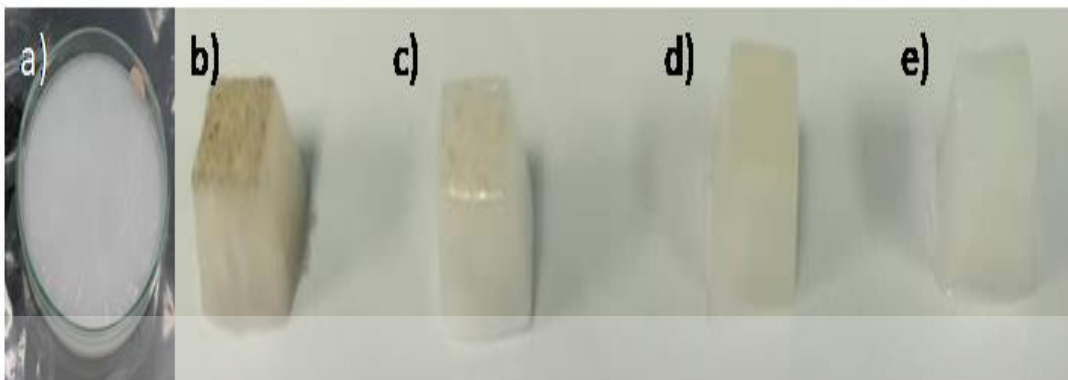
Figure 4.19   Macroscopic appearance of a) PVA neat, b)PVA/REFB, c) PVA/PEFB, d) PVA/NCC and e) PVA/MNCC hydrogel.

4.4.6.2   Morphology

In order to investigate the porous structure and the surface of the hydrogels, the neat PVA, PVA/REFB, PVA/PEFB, PVA/NCC, and PVA/MNCC hydrogels were freeze-dried in order to avoid shrinkage. Then they were observed using a FESEM imaging set-up. The FESEM imaging is often used to analyze pore morphology as well as filler dispersion in nanocomposite materials. The FESEM image of the porous structure of neat PVA, PVA/REFB, PVA/PEFB, PVA/NCC, and PVA/MNCC hydrogels are presented in Figure 4.20. On the other hand, the top surface of the neat PVA, PVA/REFB, PVA/PEFB, PVA/NCC, PVA/MNCC hydrogels are shown in Figure 4.21.

It can be observed in Figure 4.25 that all the hydrogel samples formed a macroporous honeycomb-like and the porous structure with random pore size distribution. This morphology obtained from the cross-section of the hydrogels is due to the freeze/thaw cycle, which promotes the generation of PVA crystals during the thawing and melting step. During freezing process PVA concentrates in regions, promoting the generation of PVA crystals. These crystals would be acting as crosslinking points between polymer chains. Upon repetition of thawing and melting of ice crystals, a porous matrix were generated by polymer-poor regions surrounded by polymer-rich gel. During consecutive freezing and thawing cycles, ice crystals would tend to preferentially create in the pores, increasing gel crystallinity density, and leading to a more resistant material.

114

It is worthy to note that the incorporation of REFB and PEFB in the PVA hydrogel did not introduce any significant difference in the pore structure of the resulting PVA hydrogel. This is evident in Figure 4.20b and Figure 4.20c respectively. However, an interesting morphology can be seen in Figure 4.20(d) and Figure 4.20(e) which represents the NCC and MNCC incorporated PVA hydrogels respectively. Specifically, incorporation of NCC and MNCC reduced pore structures in the PVA hydrogel. This observation is contrary to what was previously reported by Butylina et al., 2016.It was reported that there was no significant difference in pore structure with the addition of NCC into the PVA hydrogel. Therefore, a possible explanation for the result obtained in this study can be associated with the strong hydrophilic nature of NCC and MNCC due to the treatment procedures used. This might have helped to promote the formation of hydrogen bonds with the PVA matrix hydrogel during the freezing process in the freeze/thaw cycle. Invariably, this would result in a more compact and dense pore wall in the hydrogel structure(Gonzalez et al., 2014).
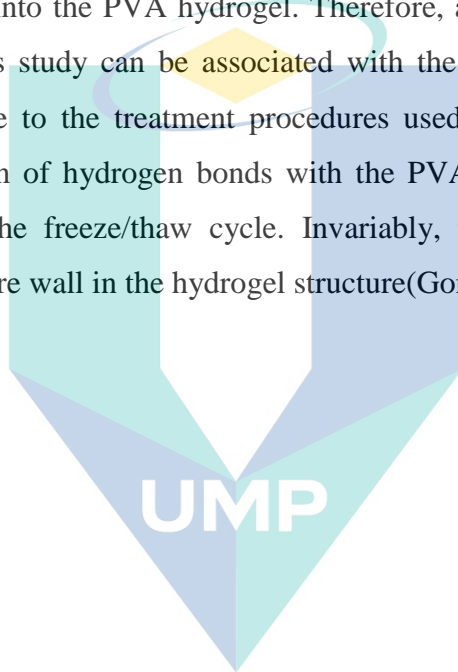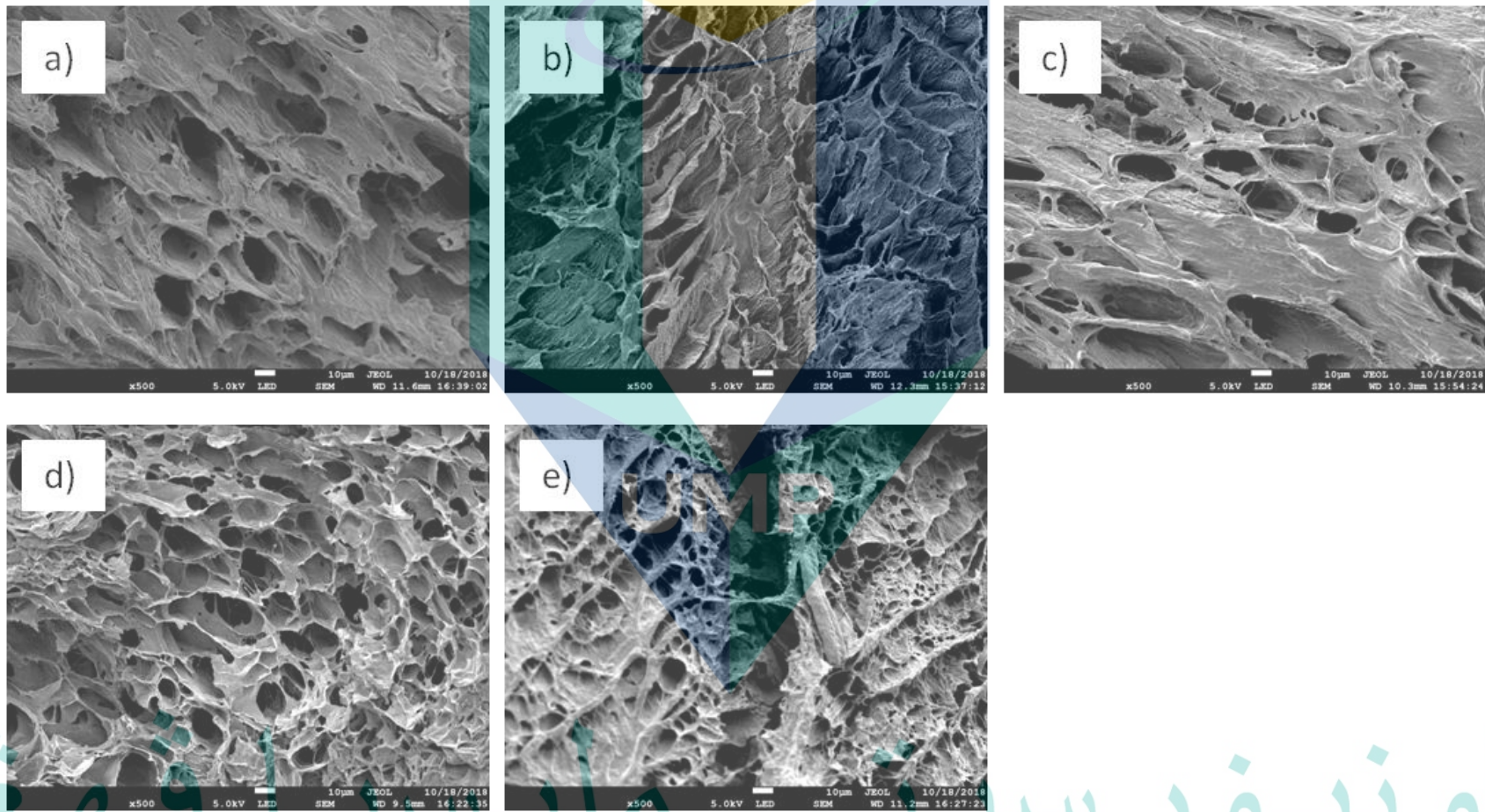
Figure 4.20   The FESEM of porous structure a)neat PVA, b) PVA/REFB, c) PVA/PEFB, d) PVA/NCC and e) PVA/MNCC hydrogels

The top surface of the neat PVA, PVA/REFB, PVA/PEFB, PVA/NCC, and PVA/MNCC hydrogels, as observed using field emission scanning electron microscopy (FESEM) is shown in Figure 4.21. As can be seen in the figure, the surface of neat PVA hydrogel appears to be rough which is characteristic of neat PVA hydrogel. However, when the REFB and PEFB are incorporated into the PVA hydrogel, a non-uniform and agglomerated distribution of REFB and PEFB can be seen as shown in Figure 4.21 (b and c). Interestingly, the NCC incorporated PVA hydrogel exhibits a uniform and less agglomerated distribution. This observation is in agreement with Gonzalez et al.,(2014).It was reported that there are tendencies for NCC to agglomerate rather than disperse inside PVA polymeric matrices. The reason may be the formation of hydrogen bonds among the NCC particles such that they might tend to form agglomeration among themselves. This phenomenon may be attributed to the nature of NCC after drying were during the drying process, capillary forces draw the adjacent NCC towards each other, causing the NCC to shrink if no other external forces are acting on it. Once the water molecules between adjacent NCC are removed, the NCC is in contact with each other, forming irreversible hydrogen bonds called interfibril hornification(Santmarti, Tammelin, & Lee, 2020).

On the other hand, the PVA hydrogel surface can be seen to exhibit a fairly uniform distribution with the incorporation of MNCC. In fact, there is no significant agglomeration on the surface of the MNCC incorporated PVA hydrogel. This is believed to be due to the highly hydrophilic structure of MNCC, compared with the NCC which might have facilitated its homogeneous dispersion in the PVA matrix.

.
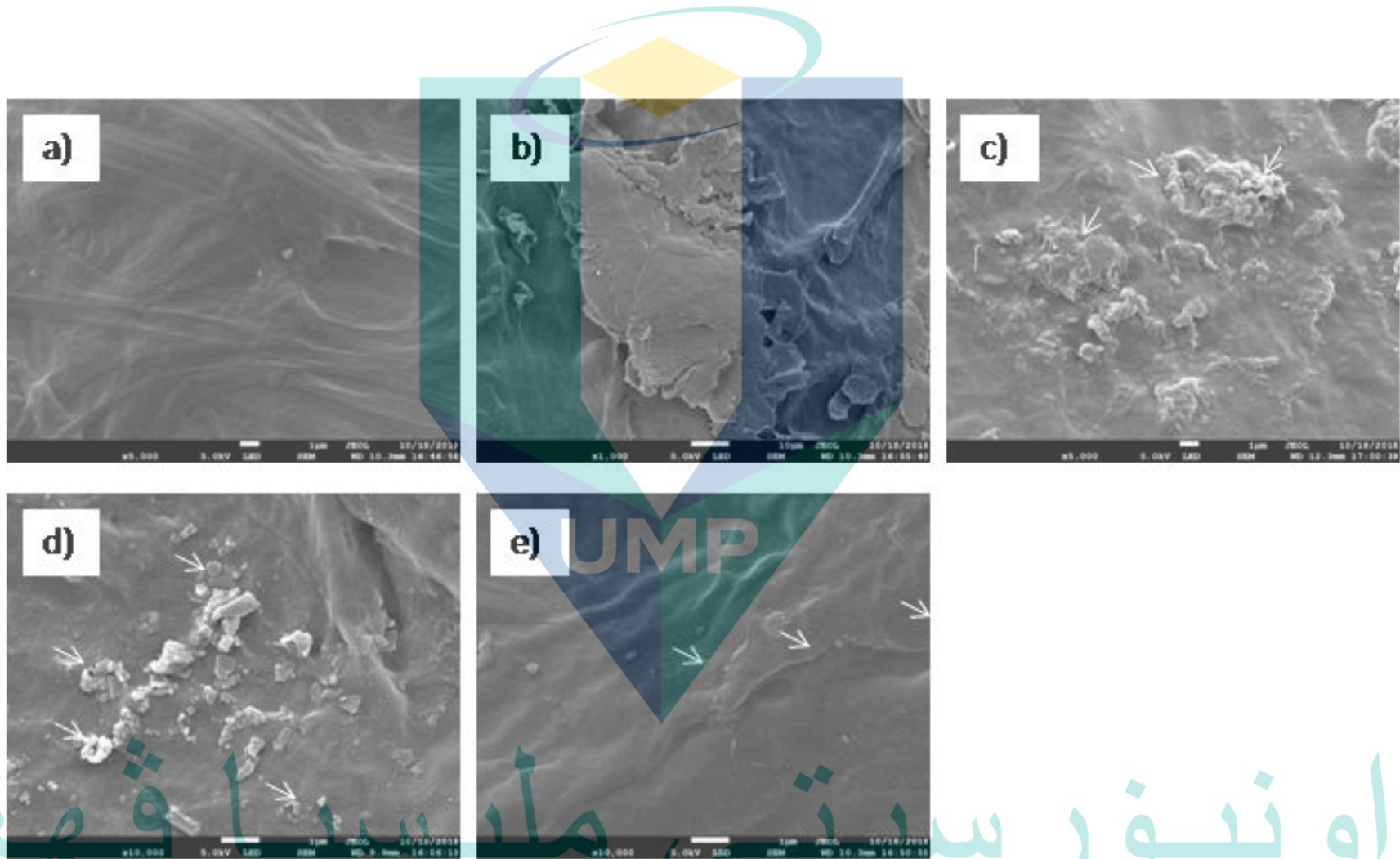
Figure 4.21   The FESEM of the top surface of a)neat PVA,b) PVA/REFB, c) PVA/PEFB, d) PVA/NCC and e) PVA/MNCC hydrogels

4.4.6.3   FTIR analysis

In order to obtain a better understanding of the structural changes in the PVA hydrogels after the incorporation of different filers, FTIR analysis was carried out. The FTIR spectra of neat PVA, PVA/REFB, PVA/PEFB, PVA/NCC, and PVA/MNCC hydrogels are illustrated in Figure 4.22.
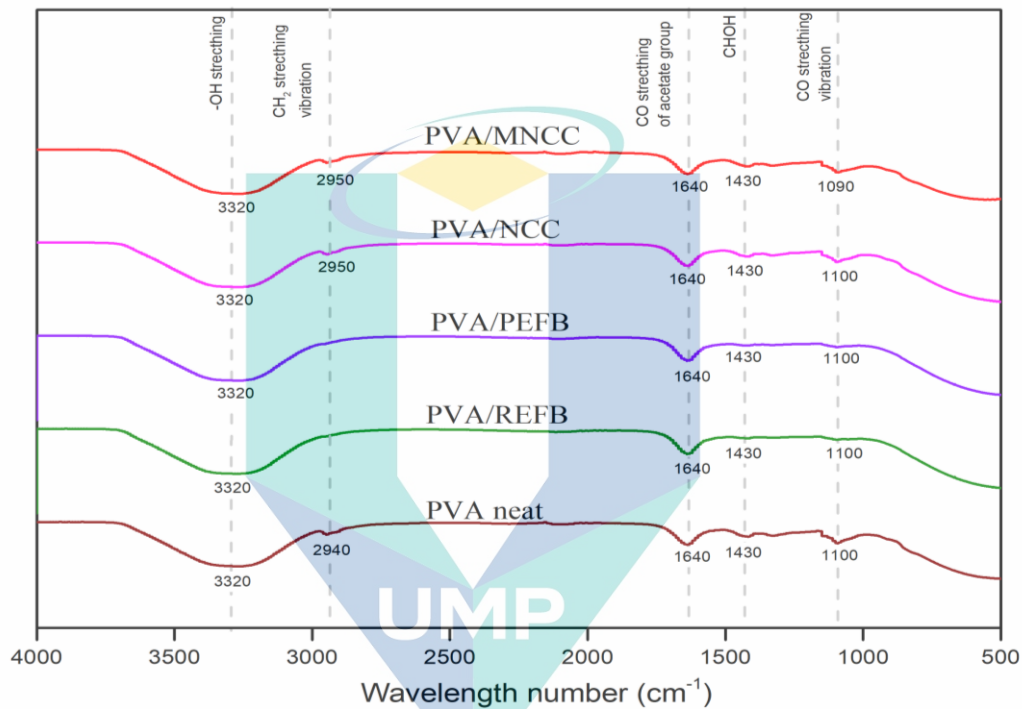
Figure 4.22   FTIR spectra of neat PVA, PVA/REFB, PVA/PEFB, PVA/NCC and PVA/MNCC hydrogels.

In the spectrum of neat PVA hydrogel, broad adsorption can be observed at 3300cm^{-1}which is an attribute of–OH stretching vibration. This can be associated with the hydroxyl group of PVA. Other than that, another adsorption peak can be seen at 2900 cm^{-1} which is associated with the stretching vibration of CH$_2$. Furthermore, a sharp adsorption peak can be seen at 1700 cm^{-1}which is assigned to the CO stretching of the acetate group of PVA. Another peak is evident at 1345 cm^{-1}which is attributed to the combination frequencies of CHOH. On the other hand, a characteristic peak present at 1141 cm^{-1}is attributed to the CO stretching vibration, which is often associated with crystalline PVA.

Generally, there are no significant changes in the spectra of PVA/REFB, PVA/PEFB, PVA/NCC, and PVA/MNCC when compared with neat PVA. This is an indication that the incorporation of REFB, PEFB, NCC, and MNCC into the PVA hydrogel did not disrupt the structural framework of the PVA hydrogel. This observation is consistent with those of Guan et al., (2014)which found that there was no difference in FTIR peak intensities when the fillers were incorporated into PVA hydrogel through freeze thawing method. A possible explanation for this might be that the hydrogen bonds were formed among REFB, PEFB, NCC, and MNCC in the PVA hydrogel by a physical reaction that occurred in the freeze/thaw process. Therefore, this suggests that there are no undesirable chemical modifications to the PVA hydrogel as a result of the incorporation of fillers.

4.4.6.4   Swelling ratio

The basic feature of the hydrogel is its ability to absorb and hold a significant amount of solvent in its network structure (Chowdhury et al., 2006).

Figure 4.23shows the equilibrium degree of swelling ratio for neat PVA, PVA/REFB, PVA/PEFB, PVA/NCC and PVA/MNCC hydrogels. As shown, the swelling water ofPVA/REFB and PVA/PEFB,decreased compared to neat PVA hydrogel. The decreased in PVA/Raw efb can be explained by the present of lignin in Raw efb which is more hydrophobic in nature. The crosslinking PVA with raw efb which is surrounded by lignin may be obstacle to adsorb more water.Surprisingly, the swelling ratio were also decreased in case for PVA/PEFB. This is contradict with the fact that the PEFB is hydrophilic in nature. This can be explained by the remaining of 2% of lignin content in

PEFB as shown in previous result of chemical composition where not all the lignin were fully removed. Therefore the remaining of lignin content in PEFB may restrict its function in adsorbing more water. Another explanation may lies on the agglomeration of PEFB as shown in Figure 4.23 where the agglomerate of PEFB may interrupt water adsorption in PVA hydrogel.

As expected, the equilibrium degree of swelling ratio for PVA/NCC and PVA/MNCC hydrogels increased compare to PVA neat hydrogel. This shows that the incorporation of NCC and MNCC improves the adsorption capability of PVA hydrogel. There are a few possible explanation for this situation. First, the improvemet in swelling ratiowith by NCC and MNCC may be due to their hydrophilic nature with large abundant of –OH groups. During the swelling process, the water need to overcome the osmotic pressure inside the PVA hydrogel. The substantial hydrophilic groups (OH) on the surface of NCC and MNCC enhance the electrostatic repulsion in the PVA hydrogel network, and as a result, the osmotic pressure difference were strengthen. As there are larger osmotic pressure difference, the water will permeates more faster into the PVA hydrogel (Li et al., 2012). This might have facilitated a higher degree of swelling. Therefore, the PVA hydrogels reinforced with NCC and MNCC fillers have a much higher swelling ratio compared to PVA neat hydrogel(Y. Zhou, Fu, Zhang, & Zhan, 2013).
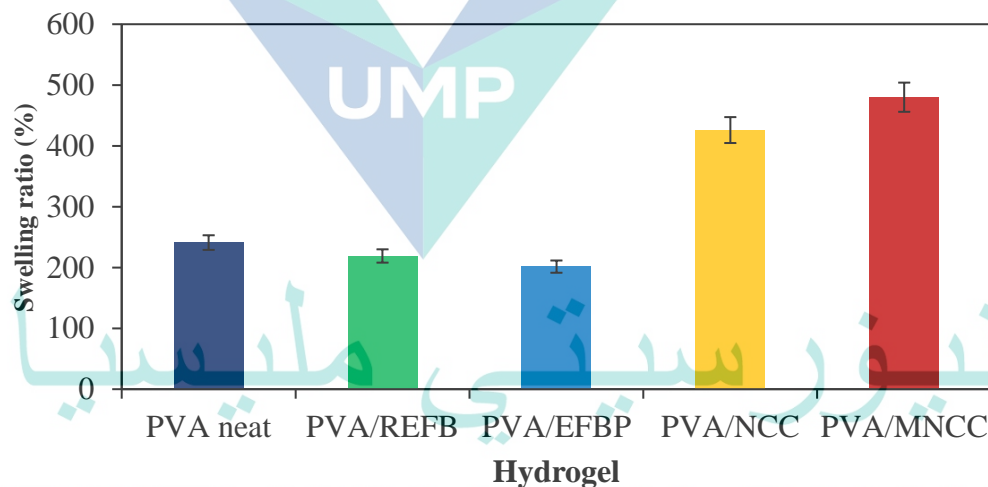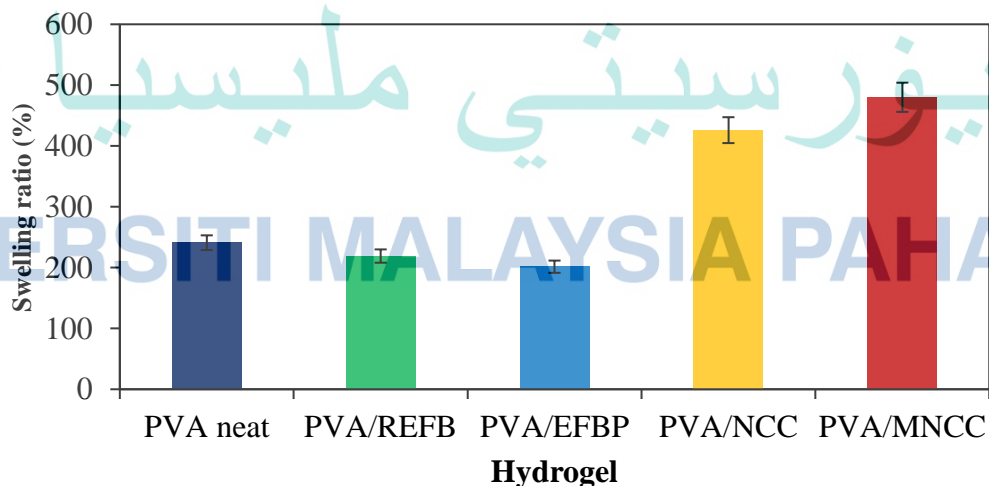

Figure 4.23   Equilibrium degree of swelling ratio for neat PVA, PVA/REFB, PVA/PEFB, PVA/NCC and PVA/MNCC hydrogels.

As expected, the the incorporated MNCC into PVA hydrogel exhibit higher swelling ratio compared to others. The reason may lies on the effect of the modification of NCC with HBP by increasing the OH group on the surface of NCC. With attachment of HBE into the NCC surface may increasing the number of hydroxyl group which is good for diffusion of water molecules into PVA hydrogel. This abundance of OH terminal group that attach on the NCC surface may attract more molecules by formig hydrogen bond and as a result more water will be adsorb into PVA hydrogel.On the overall, it can be inferred from this result that the incorporation of REFB, PEFB, NCC, and MNCC fillers presents different morphologies and swelling behaviours to composite hydrogels.

4.4.6.5   Compression strength

The compression stress-strain curves of the physically cross-linked hydrogel obtained through a compression test are shown in Figure 4.24. From the figure, it can be seen that the compressive properties of neat PVA, PVA/REFB, PVA/PEFB, PVA/NCC, and PVA/MNCC hydrogels exhibit non-linear and viscoelastic behaviour. Significantly, this is generally similar to those reported by Qiao et al., (2015). Notably, different levels of improvements in compression strength of PVA hydrogel can be seen following the incorporation of REFB, PEFB, NCC, and MNCC. According to the figure, the compression strength of the PVA hydrogels incorporated with REFB, PEFB,NCC and MNCC are higher than that the neat PVA hydrogels. This is might be due to the presence of physical crosslink of the fillers into PVA hydrogels. Generally, the incorporation of the fillers offered significant improvement in compression strength compared to the neat PVA hydrogel. This enhancement can be attributed to the denser structures of the composite hydrogels based on contributions from the fillers (Qiao et al., 2015).

From Figure 4.24, PVA/REFB hydrogel posses higher compression strength followed by PVA/MNCC, PVA/PEFB, PVA/NCC and neat PVA hydrogel. The PVA/REFB hydrogel posses higher compression strength among others might be due to the entanglement of the raw efb in PVA hydrogel network and the cross-linking of the REFB and PVA hydrogel was caused by hydrogen bond interactions. This also

consistent with the previous result of swelling ratio in section 4.4.2.5 where PVA/REFB are among lowest swelling ratio compared to other samples. In fact, the compressive strength is consistent with the equilibrium swelling ratio. Therefore, the PVA/REFB hydrogel resulting into decrease in swelling ratio and increased in the compression strength. This may attributed to a highly cross linked structure which increase the stiffness of the PVA hydrogels.

In contrast, the present of MNCC into PVA hydrogel lead to the improvement in compression strength. This is however contradicted with the previous result as it increased the swelling ratio. This possibly can be explained based on the understanding of the network structure in the PVA hydrogel, as supported from the FESEM result in section 4.4.2.1.As shown in Figure 4.21, the MNCC was well dispersed into PVA hydrogel surface and as a result, leading to reduced pore structures of PVA hydrogel(Figure 4.20). This may improved the surface area of PVA hydrogel and resulted into increase stiffness of the PVA hydrogels. Therefore, the water from the PVA hydrogels may act as incompressible fluid to resist the compression(Guan, Bian, Peng, Zhang, & Sun, 2014).Another explanation might be due to hydrogen bond by MNCC that can also serve as physical crosslink for PVA hydrogels. It is known that the MNCC possesses more hydroxyl groups that can form more intra and inter chain of hydrogen bond with PVA hydrogel and therefore exhibit more physical crosslinking points with PVA hydrogel.
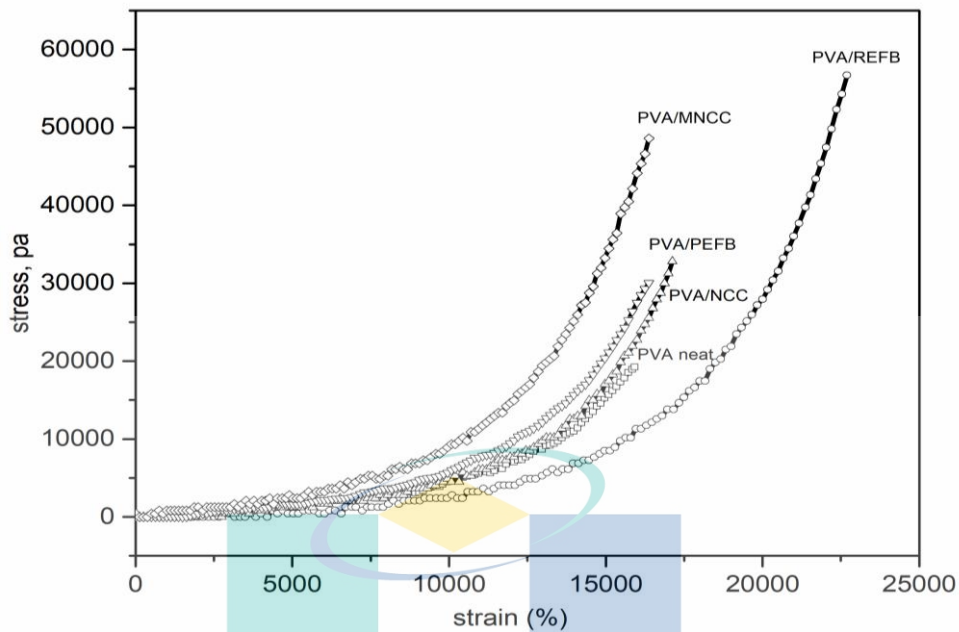
Figure 4.24   Compressionstress-strain curve of physically cross-linked neat PVA, PVA/REFB, PVA/PEFB, PVA/NCC, and PVA/MNCC hydrogels.

As compared to the fillers of REFB, Modified NCC, the incorporation of efb-Pulp was slightly improved the compression strength of PVA hydrogel. The possible explanation for this might be on the agglomeration of PEFB (as shown in Figure 4.23) that would obviously reduce the specific surface area, and the interfacial bonding strength between the PEFB and the PVA matrix. This resultant into deterioration of the mechanical properties of the PVA/PEFB composite hydrogel.

Nevertheless, the PVA/NCC shows lowest compression strength among other fillers. This indicates that the incorporation of NCC into PVA hydrogel matrix slightly improves the compression strength of PVA hydrogel. This may not surprising as the PVA/NCC hydrogel has high swelling ratios (as evident in previous section 4.4.6.4) and therefore resulting in lower compression strength. This might be explained by the mechanism of PVA hydrogel during the compression loading whereas, when the load is applied, the polymeric chains of the PVA hydrogel are reoriented; the water that occupied in the PVA hydrogel start to drain and get away from the hydrogel. As the load continues to compress the hydrogel, the orientation of the chains tends to destructed and therefore resultant in lower compression strength. Based on the compression strength, it is expected that the addition of different fillers produce improvements on the compression properties of the PVA hydrogel.

124

4.4.6.6　TGA analysis

The thermal degradation behaviour of neat PVA, PVA/REFB, PVA/PEFB, PVA/NCC, and PVA/MNCC hydrogels was studied in the temperature range of 25–700∘C under a nitrogen atmosphere. The results are illustrated in Figure 4.25　TG (a) and DTG derivatives (b) of PVA neat, PVA/REFB, PVA/PEFB, PVA/NCC, and PVA/MNCC hydrogels. On the other hand, a summary of the thermal properties of the samples is presented inTable 4.12. As shown in Figure 4.25 TG (a) and DTG derivatives (b) of PVA neat, PVA/REFB, PVA/PEFB, PVA/NCC, and PVA/MNCC hydrogels., it can be seen that all the hydrogel samples exhibited a three-step degradation process which started with the degradation below 200°C, presumably due to the elimination of the residual water trapped in the hydrogel samples.The second degradation stage which occurred at the temperature range of 243.56°C to 267.27°C is associated with the degradation of the REFB,PEFB, NCC, and MNCC fillers in the PVA hydrogel, as well as the de-polymerization of PVA hydrogel chain (Qi et al., 2015). On the other hand, the third degradation stage which occurred in the temperature range of 394.66°C to 438.04°C is mainly due to the complete volatilization of the remaining residues (Kenawy et al., 2014).This observation confirms with previous research by Kenawy et al., 2014 which reported multiple-step degradation in PVA hydrogel.

From Table 4.12, it can be seen that the degradation temperature of neat PVA, PVA/REFB, PVA/PEFB, PVA/NCC, and PVA/MNCC hydrogelsare257.71°C, 267.1°C 267.3°C, 261.88°C, and 266.08°C respectively. This is an indication that the thermal stability of PVA hydrogel was slightly improved by the incorporation of REFB, PEFB, NCC, and MNCC. The increased thermal stability of the PVA/REFB and PVA/PEFB hydrogels compared to neat PVA hydrogel might be due to the formation of the intermolecular bond between the fibers and the PVA matrix. In addition, it might be due to the stiffness imposed on the PVA matrix, by the fibers.
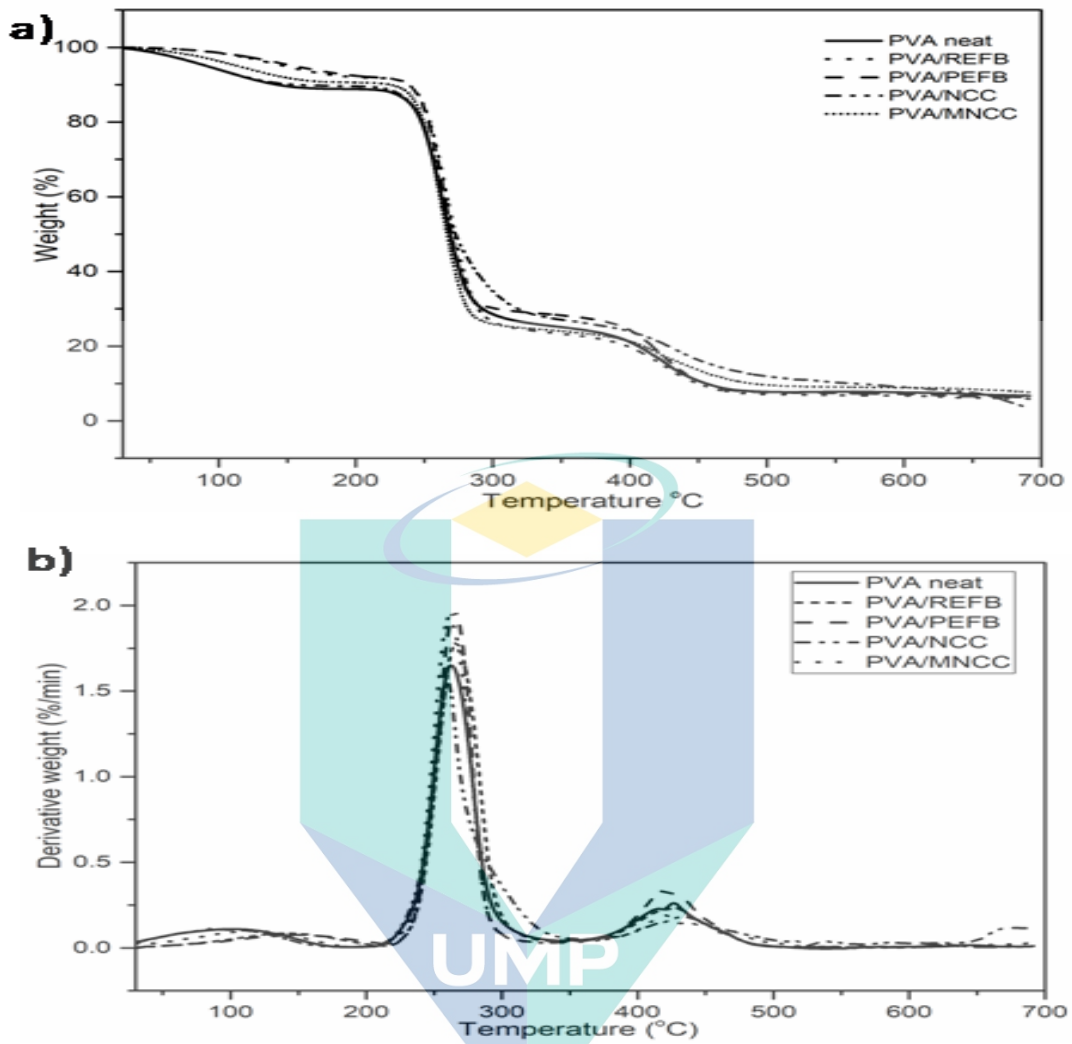
Figure 4.25   TG (a) and DTG derivatives (b) of PVA neat, PVA/REFB, PVA/PEFB, PVA/NCC, and PVA/MNCC hydrogels.

On the other hand, in the case of PVA/NCC hydrogel, the degradation temperature can be seen to be slightly lower than PVA/REFB, PVA/PEFB, and PVA/MNCC hydrogels. This might be due to the lower stiffness of NCC, which suggests that the incorporation of NCC only slightly improved the thermal stability of PVA. However, these findings do not support the previous research by W. Li et al., 2017 which stated that the incorporation of NCC resulted in very low thermal stability. The result obtained here might be due to the formation of hydrogen bonds betweenNCC andthe PVA matrix which limits the movement of the PVA chain, and as a result, produced increased thermal stability. Significantly, the PVA/MNCC hydrogel has high thermal stability compared to PVA/NCC which might be due to the abundance of hydroxyl groups attached tothe MNCC surface.This indicated that the thermal stability of PVA hydrogel was improved upon by forming PVA/MNCC hydrogel composite due to the hydroxyl groups of PVA formed hydrogen bond crosslinking with hydroxyl groups of MNCC, which limited the chain movement during thermal treatment(Qi et al., 2015). In addition, this would help to facilitate more hydrogen bonds with PVA and as a result, the degradation process will be slowed down and the decomposition takes place at a higher temperature in the presence of MNCC(Juby et al., 2012).

Generally, this result shows that the incorporation of REFB, PEFB, NCC, and MNCC into PVA hydrogel can help to enhance the thermal stability of the resulting hydrogel. However, it is noteworthy that stiffness and improved interaction will invariably facilitate the influence of fillers on the thermal stability of PVA hydrogel.

Table 4.12   Onset temperature (T_{on}), degradation temperature (Tmax) and ash contentof the neat PVA, PVA/REFB, PVA/PEFB, PVA/NCC and PVA/MNCC hydrogels.

Sample	First degradation		Second degradation		Third decomposition		Ash content
	T_{onset}(°C)	T_{max} (°C)	T_{onset} (°C)	T_{max} (°C)	T_{onset} (°C)	T_{max} (°C)	(%)
PVA neat	30.05	170.00	243.56	257.71	395.87	425.37	6.738
PVA/REFB	42.03	112.00	248.81	267.1	394.66	422.53	5.935
PVA/PEFB	45.22	158,77	249.18	267.27	395.61	416.87	6.323
PVA/NCC	88.59	158.77	244.65	261.88	404.43	432.54	3.403
PVA/MNCC	85.81	153.00	245.82	266.08	396.70	438.04	7.654

CHAPTER 5

CONCLUSION

5.1   Conclusion

This chapter presents the conclusion drawn from the results obtained and the observations made in this study. The conclusion is based on the study objectives and recommendations are provided to facilitate subsequent studies in this field. Based on the results of this research work, thereare three main conclusions:

i.   Nanocrystalline cellulose (NCC) was successfully extracted from oil palm empty fruit bunch pulp using ultrasound-assisted acid hydrolysis. Notably, the spherical morphology of NCC was revealed and the XRD analysis showed that the NCC has a higher crystallinity compared to untreated fiber and PEFBPEFB. In addition, the NCC obtained by ultrasound-assisted hydrolysis exhibits higher thermal stability. These indicate that the use of ultrasound during acid hydrolysis can help to improve the quality of the NCC produced.The optimization of process parameters for the NCC produced via ultrasound-assisted hydrolysis was conducted via two steps by screening the factor that affects the NCC production, and optimizing the selected condition for the production of NCC. The screening analysis indicated that the factor of acid hydrolysis and temperature offers the highest significant effect on the production of NCC. On the other hand, the factors of hydrolysis time and ultrasound time have a less significant effect. The acid concentration and hydrolysis temperature factors were selected in order to improve the NCC production yield. The experimental data showed that the empirical model (P < 0.0001) which describes the relationships between the factors and response is significant for the acid concentration, which indicates that this factor is very important in order to produce high NCC yield. On the other hand, the factor, hydrolysis temperature gives a p-value of 0.0078 which suggests that it is less

significant in the production of high NCC yield. The highest NCC production yield of 75% was achieved at the optimum condition of 64% (acid concentration) and 60°C (temperature). Notably, the experimental values were in good agreement with the values predicted by the model which indicates that this model was suitable to optimize NCC production yield by ultrasound-assisted hydrolysis.

ii. The surface modification of NCC was achieved by non-covalent attachment of hyperbranched polymer (HBPE) with terminal –OH. The FITR spectra of the modified NCC (MNCC) revealed the increasing of –OH groups, and new groups (C=O) which was to the modification of NCC by HBPE. In addition, the crystallinity and thermal stability also slightly increased compared to the NCC.This suggests that the modification of NCC with HBPE improved the crystallinity and thermal stability of NCC without changing the chemical structure of NCC. Notably, the experimental observations revealed that 0.3 wt% HBPE presents the best properties.

iii. The characteristics of NCC incorporated with PVA hydrogels were subjected to detailed analysis by macroscopic appearance, FTIR, gel fraction, equilibrium of swelling ratio, XRD, TGA and compression properties. The macroscopic appearance shows that the addition of NCC into PVA hydrogel changed the hydrogel appearance into a more opaque and cloudy one. FTIR spectra further confirmed the presence of NCC in PVA hydrogel with the decrease in the adsorption broad band at 3290cm−1. In addition, the swelling capacities of PVA hydrogel were elevated with the incorporation of NCC. From the investigation it is clear that the optimum concentration of NCC is 3% which have the best swelling ratio.Meanwhile, the comparative characterization of NCC and modified NCC (MNCC) incorporated into PVA hydrogel was performed. The characterization was done incomparison with the neat PVA, PVA/REFB, PVA/PEFB, PVA/NCC, and PVA/MNCC hydrogels.It was found that PVA/REFB hydrogel possesses the highest compression strength. On the other hand, the PVA/NCC and PVA/MNCC hydrogels. Likewise, the microstructural analysis revealed that the incorporation of NCC and MNCC into the PVA hydrogel reducedpore structureof PVA hydrogels. The thermal stability shows

thermal stability of PVA hydrogel was improved by the incorporation of REFB, PEFB, NCC and MNCC. From this comparative study, it can be inferred that the incorporation ofMNCC improved the adsorption capability and compression strengthof PVA hydrogel.

5.2   Recommendation for future research

Based on the results and observations from this study,the following recommendations are proposed to improve subsequent research studies:

1.   This research work explored the potential of ultrasound in hydrolysis processes for NCC production. Further studies can focus on the possible mechanisms of the function of ultrasound which made it possible to enhance the production of high-yield NCC. On the other hand, the kinetics study on the effect of ultrasound during hydrolysis should be further investigated.

2.   It is also recommended that the power intensity of the ultrasound used during hydrolysis should be varied in subsequent studies as this study is only based on the effect of low-intensity ultrasound.

3.   Although NCC has successfully produced by ultrasound-assisted hydrolysis, however, the loss of cellulose during hydrolysis still needs to be solved. So there is a need to create a route for recycling the unhydrolyzed cellulose obtained from hydrolysis in order to maximize the NCC production.

REFERENCES

A., & Sain, M. (. (2008). Isolation and characterization of nanofibers from agricultural residues – wheat straw and soy hulls. *Bioresource Technology, 99, 1664–1671.*

A.K.M, M. A., Beg, M. D. H., Yunus, R. M., Mina, M. F., Maria, K. H., & Mieno, T. (2016). Evolution of functionalized multi-walled carbon nanotubes by dendritic polymer coating and their anti-scavenging behavior during curing process. *Materials Letters*, *167*, 58–60. https://doi.org/10.1016/j.matlet.2015.12.130

Abraham, E., Deepa, B., Pothen, L. a, Cintil, J., Thomas, S., John, M. J., … Narine, S. S. (2013). Environmental friendly method for the extraction of coir fibre and isolation of nanofibre. *Carbohydrate Polymers*, *92*(2), 1477–1483. https://doi.org/10.1016/j.carbpol.2012.10.056

Amran, U. A., Zakaria, S., Chia, C. H., Fang, Z., & Masli, M. Z. (2017). Production of Liquefied Oil Palm Empty Fruit Bunch Based Polyols via Microwave Heating. *Energy and Fuels*, *31*(10), 10975–10982. https://doi.org/10.1021/acs.energyfuels.7b02098

Bai, H., Li, Z., Zhang, S., Wang, W., & Dong, W. (2018). Interpenetrating polymer networks in polyvinyl alcohol/cellulose nanocrystals hydrogels to develop absorbent materials. *Carbohydrate Polymers*, *200*(August), 468–476. https://doi.org/10.1016/j.carbpol.2018.08.041

Bai, W., Holbery, J., & Li, K. (2009). A technique for production of nanocrystalline cellulose with a narrow size distribution. *Cellulose*, *16*(3), 455–465. https://doi.org/10.1007/s10570-009-9277-1

Bian, H., Wei, L., Lin, C., Ma, Q., Dai, H., & Zhu, J. Y. (2018). Lignin Containing Cellulose Nanofibril- Reinforced Polyvinyl Alcohol Hydrogels Lignin Containing Cellulose Nanofibril-Reinforced Polyvinyl Alcohol Hydrogels. https://doi.org/10.1021/acssuschemeng.7b04172

Boujemaoui, A., Mazières, S., Malmström, E., Destarac, M., & Carlmark, A. (2016). SI-RAFT/MADIX polymerization of vinyl acetate on cellulose nanocrystals for nanocomposite applications. *Polymer*, *99*, 240–249. https://doi.org/10.1016/j.polymer.2016.07.013

Braun, B., & Dorgan, J. R. (2009). Single-step method for the isolation and surface functionalization of cellulosic nanowhiskers. *Biomacromolecules*, *10*(2), 334–341. https://doi.org/10.1021/bm8011117

Brito, B. S. L., Pereira, F. V., Putaux, J.-L., & Jean, B. (2012). Preparation, morphology and structure of cellulose nanocrystals from bamboo fibers. *Cellulose*, *19*(5), 1527–1536. https://doi.org/10.1007/s10570-012-9738-9

Butylina, S., Geng, S., & Oksman, K. (2016). Properties of as-prepared and freeze-dried hydrogels made from poly(vinyl alcohol) and cellulose nanocrystals using freeze-thaw technique. *European Polymer Journal*, *81*, 386–396. https://doi.org/10.1016/j.eurpolymj.2016.06.028

C.S., J. C., George, N., & Narayanankutty, S. K. (2016). Isolation and Characterization of Cellulose Nanofibrils From Arecanut Husk Fibre. *Carbohydrate Polymers*, *142*, 158–166. https://doi.org/10.1016/j.carbpol.2016.01.015

Cao, X., Ding, B., Yu, J., & Al-Deyab, S. S. (2012). Cellulose nanowhiskers extracted from TEMPO-oxidized jute fibers. *Carbohydrate Polymers*, *90*(2), 1075–1080. https://doi.org/10.1016/j.carbpol.2012.06.046

Chen, Y. W., Lee, H. V., Bee, S., & Hamid, A. (2017). Investigation of optimal conditions for production of highly crystalline nanocellulose with increased yield via novel Cr (III) -catalyzed hydrolysis : Response surface methodology. *Carbohydrate Polymers*, *178*(September), 57–68. https://doi.org/10.1016/j.carbpol.2017.09.029

Cho, S. Y., Park, H. H., Yun, Y. S., & Jin, H.-J. (2013). Cellulose nanowhisker-incorporated poly(lactic acid) composites for high thermal stability. *Fibers and Polymers*, *14*(6), 1001–1005. https://doi.org/10.1007/s12221-013-1001-y

Davoudpour, Y., Hossain, S., Khalil, H. P. S. A., Haafiz, M. K. M., Ishak, Z. a. M., Hassan, A., & Sarker, Z. I. (2015). Optimization of high pressure homogenization parameters for the isolation of cellulosic nanofibers using response surface methodology. *Industrial Crops and Products*, *74*, 381–387. https://doi.org/10.1016/j.indcrop.2015.05.029

De Souza Lima MM, B. R. (2004). Rodlike cellulose microcrystals: structure, properties, and applications. *Macromol Rapid Commun*, *25(7)*(771–787).

Demircan, D., & Zhang, B. (2016). Facile synthesis of novel soluble cellulose-grafted hyperbranched polymers as potential natural antimicrobial materials. *Carbohydrate Polymers*. https://doi.org/10.1016/j.carbpol.2016.11.076

Eyley, S. S., & Thielemans, W. (2014). Surface modification of cellulose nanocrystals. *Nanoscale*, *6*(14), 7764–7779. https://doi.org/10.1039/c4nr01756k

Fan, J., & Li, Y. (2012). Maximizing the yield of nanocrystalline cellulose from cotton pulp fiber, *88*, 1184–1188. https://doi.org/10.1016/j.carbpol.2012.01.081

Filson, P. B., & Dawson-Andoh, B. E. (2009). Sono-chemical preparation of cellulose nanocrystals from lignocellulose derived materials. *Bioresource Technology*, *100*(7), 2259–2264. https://doi.org/10.1016/j.biortech.2008.09.062

Fortunati, E., Armentano, I., Zhou, Q., Puglia, D., Terenzi, a., Berglund, L. a., & Kenny, J. M. (2012). Microstructure and nonisothermal cold crystallization of PLA composites based on silver nanoparticles and nanocrystalline cellulose. *Polymer Degradation and Stability*, *97*(10), 2027–2036. https://doi.org/10.1016/j.polymdegradstab.2012.03.027

Ganjaee Sari, M., Ramezanzadeh, B., Shahbazi, M., & Pakdel, A. S. (2015). Influence of nanoclay particles modification by polyester-amide hyperbranched polymer on the corrosion protective performance of the epoxy nanocomposite. *Corrosion Science*, *92*, 162–172. https://doi.org/10.1016/j.corsci.2014.11.047

George, A., Sanjay, M. R., Srisuk, R., Parameswaranpillai, J., & Siengchin, S. (2020). International Journal of Biological Macromolecules A comprehensive review on chemical properties and applications of biopolymers and their composites. *International Journal of Biological Macromolecules*, *154*, 329–338. https://doi.org/10.1016/j.ijbiomac.2020.03.120

George, J., & Sabapathi, S. N. (2015). Cellulose nanocrystals: Synthesis, functional properties, and applications. *Nanotechnology, Science and Applications*, *8*, 45–54. https://doi.org/10.2147/NSA.S64386

Gonzalez, Jimena S, Ludueña, L. N., Ponce, A., & Alvarez, V. a. (2014). Poly(vinyl alcohol)/cellulose nanowhiskers nanocomposite hydrogels for potential wound dressings. *Materials Science & Engineering. C, Materials for Biological Applications*, *34*, 54–61. https://doi.org/10.1016/j.msec.2013.10.006

Gonzalez, Jimena Soledad, & Alvarez, V. A. (2011). The effect of the annealing on the poly(vinyl alcohol) obtained by freezing–thawing. *Thermochimica Acta*, *521*(1–2), 184–190. https://doi.org/10.1016/j.tca.2011.04.022

Grishkewich, N., Mohammed, N., Tang, J., & Tam, K. C. (2017). Recent advances in the application of cellulose nanocrystals. *Current Opinion in Colloid & Interface Science*, *29*, 32–45. https://doi.org/10.1016/j.cocis.2017.01.005

Guan, Y., Bian, J., Peng, F., Zhang, X.-M., & Sun, R.-C. (2014). High strength of hemicelluloses based hydrogels by freeze/thaw technique. *Carbohydrate Polymers*, *101*, 272–280. https://doi.org/10.1016/j.carbpol.2013.08.085

Henrique, M. A., Silvério, H. A., Pires, W., Neto, F., & Pasquini, D. (2013). Valorization of an agro-industrial waste , mango seed , by the extraction and characterization of its cellulose nanocrystals. *Journal of Environmental Management*, *121*, 202–209. https://doi.org/10.1016/j.jenvman.2013.02.054

Ismail, Z., Abdullah, A. H., Zainal Abidin, A. S., & Yusoh, K. (2017). Application of graphene from exfoliation in kitchen mixer allows mechanical reinforcement of PVA/graphene film. *Applied Nanoscience*, *7*(6), 317–324. https://doi.org/10.1007/s13204-017-0574-y

Jayaramudu, T., Ko, H., Kim, H. C., Kim, J. W., Muthoka, R. M., & Kim, J. (2018). Electroactive Hydrogels Made with Polyvinyl Alcohol / Cellulose Nanocrystals, 1–11. https://doi.org/10.3390/ma11091615

Jin shi Fan, Y. hao L. (2012). Maximizing the yield of nanocrystalline cellulose from cotton pulp fiber. *Carbohydrate Polymers*, *88*, 1184–1188.

Juby, K. A., Dwivedi, C., Kumar, M., Kota, S., Misra, H. S., & Bajaj, P. N. (2012). Silver nanoparticle-loaded PVA / gum acacia hydrogel : Synthesis , characterization and antibacterial study. *Carbohydrate Polymers*, *89*(3), 906–913. https://doi.org/10.1016/j.carbpol.2012.04.033

Kamoun, E. A., Chen, X., Mohy, M. S., & Kenawy, E. S. (2015). Crosslinked poly (vinyl alcohol) hydrogels for wound dressing applications : A review of remarkably blended polymers. *Arabian Journal of Chemistry*, *8*(1), 1–14. https://doi.org/10.1016/j.arabjc.2014.07.005

Kamoun, E. A., Kenawy, E.-R. S., Tamer, T. M., El-Meligy, M. A., & Mohy Eldin, M. S. (2015). Poly (vinyl alcohol)-alginate physically crosslinked hydrogel membranes for wound dressing applications: Characterization and bio-evaluation. *Arabian Journal of Chemistry*, *8*(1), 38–47. https://doi.org/10.1016/j.arabjc.2013.12.003

Kamoun, E. A., Kenawy, E. S., Tamer, T. M., El-meligy, M. A., & Mohy, M. S. (2015). Poly (vinyl alcohol) -alginate physically crosslinked hydrogel membranes for wound dressing applications : Characterization and bio-evaluation. *Arabian Journal of Chemistry*, *8*(1), 38–47. https://doi.org/10.1016/j.arabjc.2013.12.003

Kaushik, A., & Singh, M. (2011). Isolation and characterization of cellulose nanofibrils from wheat straw using steam explosion coupled with high shear homogenization. *Carbohydrate Research*, *346*, 76–85. https://doi.org/10.1016/j.carres.2010.10.020

Kenawy, E., Kamoun, E. A., El-meligy, M. A., & Mohy, M. S. (2014). Physically crosslinked poly (vinyl alcohol) - hydroxyethyl starch blend hydrogel membranes : Synthesis and characterization for biomedical applications. *Arabian Journal of Chemistry*, *7*(3), 372–380. https://doi.org/10.1016/j.arabjc.2013.05.026

Khan, M. J., Zhang, J., & Guo, Q. (2016). Covalent/crystallite cross-linked co-network hydrogels: An efficient and simple strategy for mechanically strong and tough hydrogels. *Chemical Engineering Journal*. https://doi.org/10.1016/j.cej.2016.04.025

Klaykruayat, B., Siralertmukul, K., & Srikulkit, K. (2010). Chemical modification of chitosan with cationic hyperbranched dendritic polyamidoamine and its antimicrobial activity on cotton fabric. *Carbohydrate Polymers*, *80*(1), 197–207. https://doi.org/10.1016/j.carbpol.2009.11.013

Kumar, A., Negi, Y. S., Choudhary, V., & Bhardwaj, N. K. (2014). *Effect of modified cellulose nanocrystals on microstructural and mechanical properties of polyvinyl alcohol/ovalbumin biocomposite scaffolds*. *Materials Letters* (Vol. 129). https://doi.org/10.1016/j.matlet.2014.05.038

Lamaming, J., Hashim, R., Leh, C. P., & Sulaiman, O. (2017). Properties of cellulose nanocrystals from oil palm trunk isolated by total chlorine free method. *Carbohydrate Polymers*, *156*, 409–416. https://doi.org/10.1016/j.carbpol.2016.09.053

Lamaming, J., Hashim, R., Sulaiman, O., Leh, C. P., Sugimoto, T., & Nordin, N. A. (2015). Cellulose nanocrystals isolated from oil palm trunk. *Carbohydrate Polymers*, *127*, 202–208. https://doi.org/10.1016/j.carbpol.2015.03.043

Leung, A. C. W., Lam, E., Chong, J., Hrapovic, S., & Luong, J. H. T. (2013). Reinforced plastics and aerogels by nanocrystalline cellulose. *Journal of Nanoparticle Research*, *15*(5), 1636. https://doi.org/10.1007/s11051-013-1636-z

Li, H.-Z., Chen, S.-C., & Wang, Y.-Z. (2015). Preparation and characterization of nanocomposites of polyvinyl alcohol/cellulose nanowhiskers/chitosan. *Composites Science and Technology*, *115*, 60–65. https://doi.org/10.1016/j.compscitech.2015.05.004

Li, J., Song, Z., Li, D., Shang, S., & Guo, Y. (2014). Cotton cellulose nanofiber-reinforced high density polyethylene composites prepared with two different pretreatment methods. *Industrial Crops and Products*, *59*, 318–328. https://doi.org/10.1016/j.indcrop.2014.05.033

Li, S., Wang, Y., Ma, M., Zhu, J., Sun, R., & Xu, F. (2013). Microwave-assisted method for the synthesis of cellulose-based composites and their thermal transformation to Mn 2 O 3, *43*, 751–756.

Li, W., Wang, R., & Liu, S. (2011). Nanocrystalline Cellulose Prepared from Softwood Kraft Pulp via Ultrasonic-Assisted Acid Hydrolysis. *Bioresources.Com*, *6*(4), 4271–4281.

Li, W., Wu, Q., Zhao, X., Huang, Z., Cao, J., Li, J., & Liu, S. (2014). Enhanced thermal and mechanical properties of PVA composites formed with filamentous nanocellulose fibrils. *Carbohydrate Polymers*, *113*, 403–410. https://doi.org/10.1016/j.carbpol.2014.07.031

Li, W., Yue, J., & Liu, S. (2012). Preparation of nanocrystalline cellulose via ultrasound and its reinforcement capability for poly(vinyl alcohol) composites. *Ultrasonics Sonochemistry*, *19*(3), 479–485. https://doi.org/10.1016/j.ultsonch.2011.11.007

Liu, Y., Wang, H., Yu, G., Yu, Q., Li, B., & Mu, X. (2014a). A novel approach for the preparation of nanocrystalline 2 cellulose by using phosphotungstic acid. *Carbohydrate Polymers*. https://doi.org/10.1016/j.carbpol.2014.04.040

Liu, Y., Wang, H., Yu, G., Yu, Q., Li, B., & Mu, X. (2014b). A novel approach for the preparation of nanocrystalline cellulose by using phosphotungstic acid. *Carbohydrate Polymers*, *110*, 415–422. https://doi.org/10.1016/j.carbpol.2014.04.040

Lu, Z., Fan, L., Zheng, H., Lu, Q., Liao, Y., Huang, B. (2013). Preparation, characterization and optimization of nanocellulose whiskers by simultaneously ultrasonic wave and microwave assisted. *Bioresource Technolog*. https://doi.org/http://dx.doi.org/10.1016/j.biortech.2013.07.047

Lu, P., & Hsieh, Y. (2010). Preparation and properties of cellulose nanocrystals : Rods , spheres , and network. *Carbohydrate Polymers*, *82*(2), 329–336. https://doi.org/10.1016/j.carbpol.2010.04.073

Martínez-Sanz, M., Lopez-Rubio, A., & Lagaron, J. M. (2011). Optimization of the nanofabrication by acid hydrolysis of bacterial cellulose nanowhiskers. *Carbohydrate Polymers*, *85*(1), 228–236. https://doi.org/10.1016/j.carbpol.2011.02.021

Mohamad Haafiz, M. K., Eichhorn, S. J., Hassan, A., & Jawaid, M. (2013). Isolation and characterization of microcrystalline cellulose from oil palm biomass residue. *Carbohydrate Polymers*, *93*(2), 628–634. https://doi.org/10.1016/j.carbpol.2013.01.035

Morais, J. P. S., Rosa, M. D. F., de Souza Filho, M. D. S. M., Nascimento, L. D., do Nascimento, D. M., & Cassales, A. R. (2013). Extraction and characterization of nanocellulose structures from raw cotton linter. *Carbohydrate Polymers*, *91*(1), 229–235. https://doi.org/10.1016/j.carbpol.2012.08.010

Morales-Hurtado, M., Zeng, X., Gonzalez-Rodriguez, P., Ten Elshof, J. E., & van der Heide, E. (2015). A new water absorbable mechanical Epidermal skin equivalent: the combination of hydrophobic PDMS and hydrophilic PVA hydrogel. *Journal of the Mechanical Behavior of Biomedical Materials*, *46*, 305–317. https://doi.org/10.1016/j.jmbbm.2015.02.014

Moshiul Alam, A. K. M., Beg, M. D. H., Reddy Prasad, D. M., Khan, M. R., & Mina, M. F. (2012). Structures and performances of simultaneous ultrasound and alkali treated oil palm empty fruit bunch fiber reinforced poly(lactic acid) composites. *Composites Part A: Applied Science and Manufacturing*, *43*(11), 1921–1929. https://doi.org/10.1016/j.compositesa.2012.06.012

Naduparambath, S., T.V., J., Shaniba, V., M.P., S., Balan, A. K., & Purushothaman, E. (2018). Isolation and characterisation of cellulose nanocrystals from sago seed shells. *Carbohydrate Polymers*, *180*(April 2017), 13–20. https://doi.org/10.1016/j.carbpol.2017.09.088

Nafo, W., & Al-Mayah, A. (2020). Characterization of PVA hydrogels' hyperelastic properties by uniaxial tension and cavity expansion tests. *International Journal of Non-Linear Mechanics*, *124*, 103515. https://doi.org/https://doi.org/10.1016/j.ijnonlinmec.2020.103515

Nazir, M. S., Wahjoedi, B. A., Yussof, A. W., & Abdullah, M. A. (2013). Eco-Friendly Extraction and Characterization of Cellulose from Oil Palm Empty Fruit Bunches. *BioResources.Com*, *8*(2), 2161–2172.

Ng, H.M., Sin, L.T., Bee, S.T., … Rahmat, A. R. (2017). Review of Nanocellulose Polymer Composite Characteristics and Challenges. *Polymer-Plastics Technology and Engineering*, (56), 687-731.

Ondaral, S., Wågberg, L., & Enarsson, L.-E. (2006). The adsorption of hyperbranched polymers on silicon oxide surfaces. *Journal of Colloid and Interface Science*, *301*(1), 32–39. https://doi.org/10.1016/j.jcis.2006.04.052

Ozbay, N., & Seyda, A. (2018). Journal of Industrial and Engineering Chemistry Statistical analysis of Cu (II) and Co (II) sorption by apple pulp carbon using factorial design approach. *Journal of Industrial and Engineering Chemistry*, *57*, 275–283. https://doi.org/10.1016/j.jiec.2017.08.033

Polman, E. M. N., Gruter, G. M., Parsons, J. R., & Tietema, A. (2021). Science of the Total Environment Comparison of the aerobic biodegradation of biopolymers and the corresponding bioplastics : A review. *Science of the Total Environment*, *753*, 141953. https://doi.org/10.1016/j.scitotenv.2020.141953

Qi, X., Hu, X., Wei, W., Yu, H., Li, J., Zhang, J., & Dong, W. (2015). Investigation of Salecan/poly(vinyl alcohol) hydrogels prepared by freeze/thaw method. *Carbohydrate Polymers*, *118*, 60–69. https://doi.org/10.1016/j.carbpol.2014.11.021

Qiao, K., Zheng, Y., Guo, S., Tan, J., Chen, X., Li, J., … Wang, J. (2015a). Hydrophilic nanofiber of bacterial cellulose guided the changes in the micro-structure and mechanical properties of nf-BC/PVA composites hydrogels. *Composites Science and Technology*, *118*, 47–54. https://doi.org/10.1016/j.compscitech.2015.08.004

Qiao, K., Zheng, Y., Guo, S., Tan, J., Chen, X., Li, J., … Wang, J. (2015b). Hydrophilic nanofiber of bacterial cellulose guided the changes in the micro-structure and mechanical properties of nf-BC/PVA composites hydrogels. *Composites Science and Technology*, *118*, 47–54. https://doi.org/10.1016/j.compscitech.2015.08.004

Rescignano, N., Fortunati, E., Montesano, S., Emiliani, C., Kenny, J. M., Martino, S., & Armentano, I. (2014). PVA bio-nanocomposites: a new take-off using cellulose nanocrystals and PLGA nanoparticles. *Carbohydrate Polymers*, *99*, 47–58. https://doi.org/10.1016/j.carbpol.2013.08.061

Rohaizu, R., & Wanrosli, W. D. (2017a). Sono-assisted TEMPO oxidation of oil palm lignocellulosic biomass for isolation of nanocrystalline cellulose. *Ultrasonics Sonochemistry*, *34*, 631–639. https://doi.org/10.1016/j.ultsonch.2016.06.040

Rohaizu, R., & Wanrosli, W. D. (2017b). Sono-assisted TEMPO oxidation of oil palm lignocellulosic biomass for isolation of nanocrystalline cellulose. *Ultrasonics Sonochemistry*, *34*, 631–639. https://doi.org/10.1016/j.ultsonch.2016.06.040

Rosli, B. W. D. W., Leh, C. P., Zainuddin, Z., Tanaka, R., Division, C., & Division, F. (2003). Optimisation of Soda Pulping Variables for Preparation of Dissolving Pulps from Oil Palm Fibre, *57*, 106–114.

Ruiz et al. (2000). Processing and Characterization of new thermoset nanocomposite based on cellulose whiskers. *Compos Interfaces*, *7(2)*(117–131).

Santmarti, A., Tammelin, T., & Lee, K. Y. (2020). Prevention of interfibril hornification by replacing water in nanocellulose gel with low molecular weight liquid poly(ethylene glycol). *Carbohydrate Polymers*, *250*(July), 116870. https://doi.org/10.1016/j.carbpol.2020.116870

Sayyed, A. J., Mohite, L. V., Deshmukh, N. A., & Pinjari, D. V. (2018). Effect of ultrasound treatment on swelling behavior of cellulose in aqueous N-methyl-morpholine-N-oxide solution. *Ultrasonics Sonochemistry*, *49*, 161–168. https://doi.org/10.1016/j.ultsonch.2018.07.042

Sheltami, R. M., Abdullah, I., Ahmad, I., Dufresne, A., & Kargarzadeh, H. (2012). Extraction of cellulose nanocrystals from mengkuang leaves (Pandanus tectorius). *Carbohydrate Polymers*, *88*(2), 772–779. https://doi.org/10.1016/j.carbpol.2012.01.062

Shinoj, S., Visvanathan, R., Panigrahi, S., & Kochubabu, M. (2011). Oil palm fiber (OPF) and its composites: A review. *Industrial Crops and Products*, *33*(1), 7–22. https://doi.org/10.1016/j.indcrop.2010.09.009

Trache, D., Donnot, A., Khimeche, K., Benelmir, R., & Brosse, N. (2014). Physico-chemical properties and thermal stability of microcrystalline cellulose isolated from Alfa fibres. *Carbohydrate Polymers*, *104*, 223–230. https://doi.org/10.1016/j.carbpol.2014.01.058

Wang, D., Jin, Y., Zhu, X., & Yan, D. (2016). Synthesis and applications of stimuli-responsive hyperbranched polymers. *Progress in Polymer Science*. https://doi.org/10.1016/j.progpolymsci.2016.09.005

Wang, N., Ding, E., & Cheng, R. (2008). Preparation and liquid crystalline properties of spherical cellulose nanocrystals. *Langmuir : The ACS Journal of Surfaces and Colloids*, *24*(1), 5–8. https://doi.org/10.1021/la702923w

Wang, Y., Wei, X., Li, J., Wang, F., Wang, Q., Zhang, Y., & Kong, L. (2017). Homogeneous isolation of nanocellulose from eucalyptus pulp by high pressure homogenization. *Industrial Crops and Products*, *104*(April), 237–241. https://doi.org/10.1016/j.indcrop.2017.04.032

Wu, X., Li, W., Chen, K., Zhang, D., Xu, L., & Yang, X. (2019). A tough PVA/HA/COL composite hydrogel with simple process and excellent mechanical properties. *Materials Today Communications*, *21*, 100702. https://doi.org/https://doi.org/10.1016/j.mtcomm.2019.100702

Yahya, M., Chen, Y. W., Lee, H. V., & Hassan, W. H. W. (2018). Reuse of Selected Lignocellulosic and Processed Biomasses as Sustainable Sources for the Fabrication of Nanocellulose via Ni(II)-Catalyzed Hydrolysis Approach: A Comparative Study. *Journal of Polymers and the Environment*, *26*(7), 2825–2844. https://doi.org/10.1007/s10924-017-1167-2

Yang, X.-N., Xue, D.-D., Li, J.-Y., Liu, M., Jia, S.-R., Chu, L.-Q., … Zhong, C. (2016). Improvement of antimicrobial activity of graphene oxide/bacterial cellulose nanocomposites through the electrostatic modification. *Carbohydrate Polymers*, *136*, 1152–1160. https://doi.org/10.1016/j.carbpol.2015.10.020

Yang, X., Zhu, Z., Liu, Q., Chen, X., & Ma, M. (2008). Effects of PVA, agar contents, and irradiation doses on properties of PVA/ws-chitosan/glycerol hydrogels made by γ-irradiation followed by freeze-thawing. *Radiation Physics and Chemistry*, *77*(8), 954–960. https://doi.org/10.1016/j.radphyschem.2008.02.011

Youssef, A. M., & El-sayed, S. M. (2018). Bionanocomposites Materials for Food Packaging Applications: Concepts and Future Outlook. *Carbohydrate Polymers*, *193*(February), 19–27. https://doi.org/10.1016/j.carbpol.2018.03.088

Zhang, K., Sun, P., Liu, H., Shang, S., Song, J., & Wang, D. (2016). Extraction and comparison of carboxylated cellulose nanocrystals from bleached sugarcane bagasse pulp using two different oxidation methods. *Carbohydrate Polymers*, *138*, 237–243. https://doi.org/10.1016/j.carbpol.2015.11.038

Zhou, Y., Fu, S., Zhang, L., & Zhan, H. (2013). Superabsorbent nanocomposite hydrogels made of carboxylated cellulose nanofibrils and CMC-g-p(AA-co-AM). *Carbohydrate Polymers*, *97*(2), 429–435. https://doi.org/10.1016/j.carbpol.2013.04.088

Zhou, Y. M., Fu, S. Y., Zheng, L. M., & Zhan, H. Y. (2012). Effect of nanocellulose isolation techniques on the formation of reinforced poly (vinyl alcohol) nanocomposite films, *6*(10), 794–804. https://doi.org/10.3144/expresspolymlett.2012.85

APPENDIX A
LIST OF PUBLICATION

LIST OF PUBLICATION

1. **Zianor Azrina Z.A** , M. Dalour H. Beg , Rosli M. Y, Ridzuan Ramli , Norhafzan Junaidi and A.K.M.Moshiul Alam 2017, Spherical nanocrystalline cellulose (NCC) from oil palm empty fruit bunch pulp via ultrasound assisted hydrolysis, Journal of Carbohydrate polymer 162. pp. 115-120. ISSN 0144-8617.

2. **Zianor Azrina Z.A**, M. Dalour H. Beg, Rosli M. Y, Ridzuan Ramli and A.K.M.Moshiul Alam ,2017. Modification of NanoCrystalline Cellulose (NCC) by Hyperbranched Polymer. Indian Journal of Science & Technology (IJST).

3. **Zianor Azrina, Z. A.** and Beg, M. D. H. and R. M., Yunus and Ridzuan, Ramli (2017) Nano Crystal Cellulose Incorporated Poly Vinyl Alcohol (PVA) Hydrogel for Industrial Waste Water Treatment. Australian Journal of Basic and Applied Sciences, 11 (3 Special). pp. 137-142. ISSN 1991-8178

4. Norhafzan, Junadi and Beg, M. D. H. and R. M., Yunus and Ridzuan, Ramli and **Zianor Azrina, Z. A**. and Alam, A. K. M. Moshiul (2019) Characterization of microcrystalline cellulose isolated through mechanochemical method. Indian Journal of Fibre & Textile Research (IJFTR), 44 (4). pp. 442-449. ISSN 0975-1025